Spring 5-13-2016

Test Plan for Real-Time Modeling & Simulation of Single Pole Switching Relays

Ram Mohan Sanaboyina
University of New Orleans, New Orleans, rammohan.sanaboyina@gmail.com

Test Plan for Real-Time Modeling & Simulation of Single Pole Switching Relays

A Thesis

Submitted to Graduate Faculty of the
University Of New Orleans
in partial fulfilment of the
requirements for the degree of

Master of Science
In
Engineering
Electrical Engineering

By

Ram Mohan Sanaboyina

B.Tech. JNTU, 2006

May 2016

Acknowledgement

Firstly, I would like to express my utmost gratitude to my adviser Dr. Ittiphong Leevongwat for his full support, encouragement and always making his time available for suggestions and comments. This thesis would not have been possible without his guidance and help who in one way or another contributed and extended his valuable assistance in the preparation and completion of this study.

I am also grateful to Professor Dr. Parviz Rastgoufard for his valuable suggestions, technical support and guidance in the right direction throughout my thesis, academic research and course work during my master studies.

I would like to thank Dr. Ebrahim Amiri for taking time out from his busy schedule to serve as a member of my committee.

I would also like to thank Rastin Rastgoufard for his help in acquiring technical and software knowledge required for completing the tasks in this thesis.

I sincerely thank Mark Allen from Entergy Services, Inc. for his time and valuable guidance in developing part of this work.

I would also like to acknowledge the support from OPAL-RT personnel in helping with "HYPERSIM" modeling while conducting this research work.

Finally, I would like to acknowledge and thank my parents, my wife, my brothers and all of my friends for their encouragement and moral support to finish this research.

Contents

List of Figures

List of Tables

Abstract

A real-time simulator (RTS) with digital and analog input/output modules is used to conduct hardware-in-the-loop simulations to evaluate performance of power system equipment such as protective relays by exposing the equipment to the simulated realistic operating conditions. This work investigates the use of RTS to test relays with single-pole-switching (SPS) feature. Single-pole switching can cause misoperations due to fault arc during reclosing of the breakers. Through this investigation, a test procedure appropriate for the testing SPS relays has been developed. The test procedure includes power system modeling for real time simulation, relay test setup, and test plan. HYPERSIM real-time simulator was used to model an actual power system. Transmission lines, three-winding transformers, and induction motor were modeled with actual parameters. Models for fault arc in HYPERSIM real time simulator were developed. Test set-up for evaluating relay performance and wiring drawings for connecting relay in closed-loop to the simulator were developed.

KEY WORDS: HYPERSIM, Relay Testing, SPS, Real-Time Simulator, Independent Pole.

Chapter 1

Introduction

This chapter summarizes the background of this work and presents a literature review on protective relay testing using real-time modeling and simulation. The chapter concludes with the scope of work for the thesis.

1.1 Overview of Real Time Digital Simulators

"Real time digital simulator (RTS) applied for power systems provide power systems simulation technology for fast, reliable, accurate and cost-effective study of power systems. The RTS is a full digital electromagnetic transient power system simulator operates in real time, tests physical devices and performs studies quickly" [9]. In RTS, computer models of the power system are simulated in real-time to analyze the hardware-in-the-loop performance of the power system components under more realistic conditions [10]. The following are the major applications of RTS mentioned in [11].

- Specification study
- Verification of design

- Protective relays and power semiconductor equipments (HVDC and FACTS devices) pre-commissioning and performance analysis.

[10] The benefit of performing hardware-in-the-loop simulations of power system equipment is increased efficiency in the conduct of the tests and it is required for evaluating the performance of the equipment. The following are the situations where hardware-in-the-loop simulation is required.

1. Relays in fast re-closing & single pole auto-reclose of transmission lines.
2. Relays for out-of-step protections & distribution feeders with reclosure.
3. Relays responding to frequency excursions.
4. Power system stabilizers for excitation control system of generators.
5. Special breaker controllers.

[10] Dynamics caused in the power system due to tripping and re-close actions of relays can be captured and analyzed by hardware-in-the-loop testing of relays. Hardware-in-the-loop simulation of stabilizer determines its effectiveness on power system stability and simulations for controlled opening and closing of individual breaker poles are advantageous in reactor switching and capacitor switching respectively.

1.1.1 History of Real-Time Simulator

The early RTS [7] used digital technology utilizing power system and fault modeling capabilities of electromagnetic transient programs to implement protective relay testing simulators. This approach is flexible to the user to model the system accurately. These simulators are advantageous in meeting complex relay testing requirements, however they lack in providing meaningful interaction between

the relay and the simulator. In the later years, a new real-time simulator was developed for real time testing of protection relay to evaluate relay's performance and also to determine which relay suites best for a given application. Table 1.1 [7] summarizes application requirements that the simulator design required to meet for testing relays.

Table 1.1: Application Requirements for Relay Testing [7]

Applications	Requirements
Parallel Lines	Three terminal simulator configuration and coupled RL branches modeling
Series compensated long lines	Modeling of distributed and frequncy dependent parameter lines
MOV and arrester protection	Modeling for short line representation
Close-in and Far-end faults	PI circuit modeling for short line representation
Single-pole auto reclosing	Real-time interaction, modeling of circuit breakers and switches
Different fault cases	Selection of fault type, resistace, incidence angle and location
Influence of relaying transformers	Accurate modeling of CCVT and CT transient response
Timing sequence of circuit breakers	Modeling of circuit breaker timing logic

The following are the commercially available RTS in today's market [9]:

- RTDS developed by RTDS technologies Inc.
- HYPERSIM developed by Hydro-Quebec.
- eMEGAsim developed by OPAL-RT Technologies Inc.

1.2 A Review of Real Time Digital Simulator for Relay Testing

Many research papers [10]-[12], published on testing relays using RTS, evaluating the performance of relays and determining best protection principles. A numerical distance relay incorporated with new positive sequence directional element was tested with RTDS for verifying the operation of directional element incorporated in the relay in [13]. In [14], Numerical Distance relay performance was validated by developing models of a Chinese 500kV dynamic network and conducting tests using

the RTDS. The results of these digital simulations are compared with dynamic simulation results for validation of high performance relays. Line protection relays and transformer protection relays were tested and evaluated using the RTS, $ARENE^{TM}$ for fault cases applied on the protected line between the two series capacitor banks in [15]. In [10], Test setup for hardware-in-the-loop testing of a feeder relay, a power system stabilizer, and a circuit breaker controller were described. In [16], tests on the existing line relays were carried out to obtain settings for the relays for all the possible operating conditions and to determine deficiency in the performance of the relay.

The work published in [17] compared the performance of different line protection systems on Hydro-Quebec series compensated network to determine the best protection principles. A distance relay and a PCM current differential relay tested using the RTDS for verifying the scenarios in which relay fails to operate as desired in [18]. Relay configured for over-current scenario was tested and analyzed for closed loop performance using RTDS in [19]. In this publication, effect of CT saturation on closed loop performance of relays was also analyzed. Performance of Numerical Distance Relay using RTDS was evaluated in paper [20]. Different scenarios including fault types, positions, inception angles and fault resistances were used for evaluating relay transient performance. An actual relay was tested using automatic testing procedure and manual testing procedure in [21]. This publication identified which approach is best suited for testing and analyzing the performance of relays for a particular fault scenario of interest.

M. Kezunovicl and M. McKenna in [7] tested RTS for accuracy of producing and speed of calculating fault transients. A full and reduced models of series capacitor power system network were developed. A single phase to ground fault was applied and the relay was tested for accuracy and speed for both the models. EMTP and RTS waveforms were compared for the same fault event to determine the accuracy of simulation. Time step required to carry out simulations in real-time evaluated the speed of computation.

Most of the relays tested with RTS use lumped parameter line models for transmission lines in the power system networks. In publications [7] and [17], distributed frequency dependent line model was used for transmission lines in the power system network. In papers [7], [17], [13] and [15], the test system modeled and simulated for testing relays includes a series capacitor. Effect of CT and CVT on the performance of relays was analyzed in [14] and [20]. Load was modeled as constant impedance and motor load in [17] and as an inductive motor load in [14]. In majority of the research publications, sources were modeled as constant voltage sources behind impedance's. In [14], source was modeled as generator. Effect of shunt compensation on the performance of relays was analyzed in papers [17], [13] and [14]. In [17], power system network used for studying the performance of line protection system consists of equivalents for voltage levels below 315kV. Network simulation in [17], include transformer saturation and the power system network in [13] has three-winding transformer model.

1.3 Overview of Single Pole Switching

Single pole switching (SPS), which is a combination of single-pole tripping (SPT) and single-pole reclosing (SPR) is a feasible approach to the operation of power systems. According to [22], SPS application on transmission lines is a useful and feasible means to improve power system reliability. In [23] SPT is defined as "Opening of faulted phase due to single line to ground fault" and SPR as "re-closing of the faulted phase following a single pole trip". SPS applications on transmission line open a single pole of the transmission line breakers in the event of fault keeping the other two poles intact. The two ends of the transmission line are metallically connected via other two poles allowing transfer of power and reduce the possibility of loosing synchronism [24]. SPS application improves power system stability and in [25] it was shown that the stability is maintained due to flow of synchronizing power which reduces the rate of rotor angle drift between the synchronous

machines. In [26], it was shown that SPS application on transmission lines for all temporary single-line-to-ground faults, automatic generator shedding and automatic load shedding conditions were prevented and voltage stability margins were also improved during single pole open period due to flow of smaller amount of reactive power from the system.

Majority of faults occurring on HV transmission lines are single line to ground faults, SPAR takes advantage of this fact. Table 1.2 [8] shows the statistics of percent of different types of faults occur on HV transmission lines.

Table 1.2: Relative Number of Different Types of Faults on HV transmission lines [8]

Fault type	Percent
LG	70
LL	15
LLG	10
3L	5
Total	100

The spacing between conductors on EHV/UHV lines is more, therefore the percentage of multi-phase faults is less. Table 1.3 [8] shows the statistics of percent of different types of faults that occur on a 525 kV transmission lines.

Table 1.3: Relative Number of Different Types of Faults on 525 kV transmission lines [8]

Fault type	Percent
LG	93
LL	4
LLG	2
3L	1
Total	100

The following are the benefits of SPS application on transmission lines listed in [23]:

- Transient state stability improvement.
- System reliability improvement and availability of system with one or two transmission lines.
- Switching over voltages reduction.
- Shaft torsion oscillations reduction.

In spite of benefits associated with SPS schemes [26], some utilities still do not apply this technology for the following reasons:

- Additional expense for breakers.
- Added complexity in the protection scheme.
- Presence of secondary arc.
- Added stress to the generating units.

The dynamic interaction between a fault arc and the power system is extremely important to determine the instant of successful reclosure of a faulted system [5]. The success of SPS application depends on a number of parameters such as secondary arc current, recovery voltage across the arc path, arc location and meteorological conditions.

[26] A single line to ground fault results in the formation of primary arc between the faulted phase and ground. The fault is isolated by the line protection system by tripping the single pole of the breaker in SPS applications, there by extinguishing the primary arc. The two ends of the transmission line are metallically connected by the other two healthy phases during the single pole open period. Voltage is induced in the open phase conductor due to capacitive and inductive coupling between the healthy phase conductors and open phase conductor. As the air is already ionized from the primary arc, the induced voltage creates secondary arc.

For successful reclosure, it is essential to detect extinction of secondary arc. In case of 500kV lines, special compensation schemes become necessary to limit the secondary arc current and recovery voltage to ensure successful high speed re-closing. The published literature [27] says that the behavior of secondary arc current can be studied through simulation or by means of recording naturally occurring or staged faults. Naturally occurring faults are unpredictable and staged fault tests are expensive and complex to perform. Real time simulation with a RTS can overcome many of these problems.

1.4 A Review on Single Pole Switching Studies

Research on single pole switching focuses on advantages of having SPS schemes, challenges with SPS applications. [8], [22], and [27] - [28] presented findings on SPS applications on power systems.

According to published literature [29] majority of faults occurring on a 132kV line were single phase to ground faults and successful single pole tripping and re-closing was recorded for most of the cases. Also [29] discusses the advantages of having single pole tripping over multi-pole tripping in that better system stability and minimization of overall system disturbances during fault clearing operations. In [30] Reactor compensation makes the extinction of secondary arc possible by reducing the phase to ground fault current in the open phase of the line. The degree of compensation required to limit the secondary arc current to a level that can be extinguished depends on the length of the line. Greater the length of the line greater the degree of compensation. Affects of shunt reactor compensation on successful reclosure, secondary arc extinction and stability of the power system during SPS operation on 500 kV system were verified by conducting staged fault tests in [31]. Transient stability limit and critical clearing time are compared for single pole switching and three pole switching in paper [32]. The problems with implementing single pole switching (SPS) schemes were addressed in papers [28], [33] and [34]. The major problem addressed is tripping of

one pole of circuit breakers at both ends of a transmission line for clearing single line to ground fault produces high negative sequence current in nearby generators.

Single pole opening induces voltage across secondary arc path after the extinction of primary arc. The induced voltage is called as Recovery Voltage. [35] [36] [37] discuss this recovery voltage. In [35], the transient recovery voltages of a transposed transmission system with neutral reactor and un-transposed system during single-pole switching operation were compared. In [36], maximum possible transient recovery voltage for a transmission system during SPS operation was determined by varying fault application time, position and duration of faults. In [37], it was shown that magnitude of secondary arc current and recovery voltage determines the success of re-close operation on 765 kV system. [38] and [39] discuss the methods to minimize the secondary arc current.

In [27],[40],[41],[42] and [43], modeling and simulation of primary and secondary arc using various modeling softwares were published. Realistic arc models were developed and incorporated in EMTP in [42] based on mathematical models developed by A.T. Johns, R.K. Aggarwal and Y.H. Song [40]. [42] investigated single phase re-closing using arc model on single and double circuit transmission line to determine the characteristics of secondary arc current for single phase to ground faults. Realistic arc models are developed using FORTRAN statements and incorporated in ATPDraw in [43] based on mathematical models developed by M. Kizilcay, G. Ban, I. Prikler, P. Handl [41]. [43] validated primary and secondary arc models and implemented on a power system to verify the settings for SPAR protection scheme. Arc models developed and simulated in real time in [27] to determine the response of relays with secondary arc detection and to identify the extinction of secondary arc.

1.5 Scope of Work

The work done in this thesis is continuation of work published in [12] and [44]. [12] focused on evaluating performance of various digital line protection relays using a closed-loop real-time power system digital simulator called ""HYPERSIM"" to determine the best suited protection scheme for a series capacitor line. An equivalent test system was modeled in HYPERSIM and distance relays of two different manufacturers and a differential relay were connected in closed loop with the real-time simulator at each end of the line. Different fault scenarios were performed and relays were tested to verify their expected performance. Distance relays were found to have deficiencies and differential relay successfully cleared all internal faults. The test results concluded that for series capacitor lines dual primary differential relays with back up distance and over-current elements to be used with Zone 1 distance elements turned off. The study continued in [44] by replacing the existing relays with two dual primary differential relays in loop with the real-time simulator and tested with the same scenarios for evaluating the performance of these new relays. The tests performed on the system concluded that the relays did not operate as intended in a few scenarios.

This thesis is part of an investigation of Single Pole Switching (SPS) in commercial protective relays used in electrical system protection scheme. The main objective of this work is to create a test plan to evaluate the performance of two different digital line differential protection relays that are configured to control IPO breakers modeled in real-time simulator. The second objective of this work is to design a test setup, including necessary signals appropriate for capturing the performance of SPS operation.

The following tasks were performed to achieve the two objectives:

- A portion of a power system which is two-bus deep from the protected series capacitor line is modeled using a real time digital simulator called HYPERSIM. The power network used

comprises of the study area with detailed parameters for accurate line models, motor load models, two-winding and three-winding transformer models, series capacitor with surge arrester and shunt capacitor components. The rest of the power network is equivalenced in ASPEN to voltage sources, transformers and π lines.

- Investigation on implementation of fault arc models in HYPERSIM real time simulator is also carried out in this thesis. Arc models would help capture the effect of the remaining active phases when only single phase is tripped in SPS operation.

- Systematic study is performed to select the worst case switch timings for the faults that result in the worst fault currents. The selected faults are performed on a line with series capacitor connected at one end and high capacity motor connected at the other end. Close-in faults (close to series capacitor bus), faults at middle of line, and remote faults (close to motor bus) are applied automatically at different incidence angles for each scenario in order to determine the worst case switch time.

- Test setup includes the design of line differential relays protection schematics to include breaker trips, breaker status, breaker close and breaker fail logic's for testing the protection scheme of series capacitor line. AUTOCAD is used to design the protection schematics.

Chapter 2

Mathematical Formulation

The previous chapter has already given some idea on relay testing and single pole switching applications. Reminding once again, the main objective of this work is to come up with a power system model suitable for testing relays in hardware-in-the-loop for single pole switching applications. In view of this, this chapter discusses mathematical modeling of power system components in the model developed in this thesis and background of power system components modeling in HYPERSIM real time simulator software. Background of mathematical models and HYPERSIM models of power system components used in this thesis are illustrated in section 2.1 to section 2.4.

2.1 Transmission Lines [1]

A Transmission line is characterized by four distributed parameters: series resistance, series inductance, shunt conductance, and shunt capacitance. Magnetic and electric effects around the conductor are represented by series inductance and shunt capacitance and leakage current along insulator strings and ionized pathways in the air is represented by shunt conductance. In this thesis, transmission lines are modeled as distributed parameter lines. Let us look into the mathematical equations representing the distributed line model.

2.1.1 Mathematical Model of Transmission Line

The per phase circuit diagram of a transmission line is shown in Figure 2.1. l be the length of the transmission line, V_1, I_1 be the sending end bus voltage and current, V_2, I_2 be the receiving end bus voltage and current, z be the series impedance per meter, and y be the shunt admittance per meter to neutral. z, y are represented by equations Equation 2.1 and Equation 2.2.

$$z = r + j\omega l \tag{2.1}$$

$$y = g + j\omega c \tag{2.2}$$

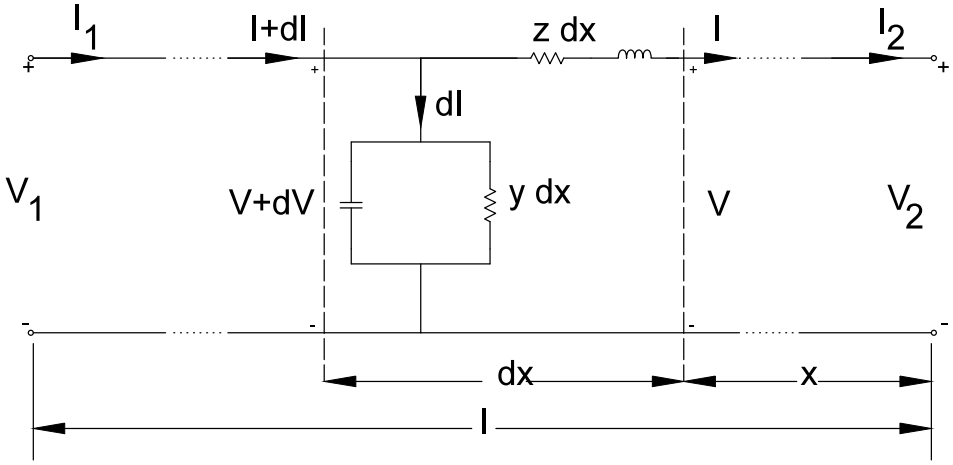

Figure 2.1: Distributed Transmission Line [1]

The relation between sending end and receiving end of transmission line is represented by Equation 2.3 and Equation 2.4.

$$V_1 = V_2 \cosh \gamma l + Z_c I_2 \sinh \gamma l \tag{2.3}$$

$$I_1 = I_2 \cosh \gamma l + \frac{V_2}{Z_c} \sinh \gamma l \tag{2.4}$$

where

$$\gamma \triangleq \sqrt{yz} \tag{2.5}$$

is called the propagation constant.

Rewriting Equation 2.3 and Equation 2.4 as Equation 2.6 and Equation 2.7 respectively.

$$V_1 = AV_2 + BI_2 \tag{2.6}$$

$$I_1 = CI_2 + DV_2 \tag{2.7}$$

where

$$A = \cosh \gamma l \tag{2.8}$$

$$B = Z_c \sinh \gamma l \tag{2.9}$$

$$C = \cosh \gamma l \tag{2.10}$$

$$D = \frac{V_2}{Z_c} \sinh \gamma l \tag{2.11}$$

Rearranging Equation 2.6 and Equation 2.7 in matrix form, we get Equation 2.12

$$\begin{bmatrix} V_1 \\ I_1 \end{bmatrix} = \begin{bmatrix} A & B \\ C & D \end{bmatrix} \begin{bmatrix} V_2 \\ I_2 \end{bmatrix} \tag{2.12}$$

$$T = \begin{bmatrix} A & B \\ C & D \end{bmatrix} \tag{2.13}$$

where T is called transmission matrix.

2.1.2 HYPERSIM Model of Transmission Line [2]

The equivalent circuit representing a single mode of a transmission line is shown in Figure 2.2.

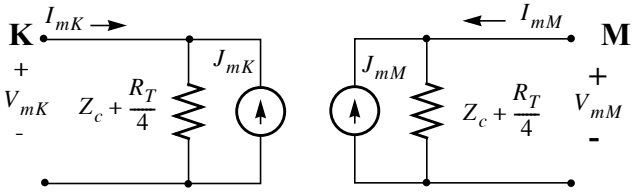

Figure 2.2: Equivalent circuit of One Mode of a Transmission Line [2]

A single mode line model is represented at each terminal (sending end and receiving end) as an equivalent circuit composed of a current source in parallel with a resistor. The current source at terminal K is given by Equation 2.14.

$$J_{mK} = \left(\frac{1-h}{2}\right)\left(\frac{V_{mK}(t-\tau)}{R_{eq}} + hI_{mK}(t-\tau)\right) + \left(\frac{1+h}{2}\right)\left(\frac{V_{mM}(t-\tau)}{R_{eq}} + hI_{mM}(t-\tau)\right) \quad (2.14)$$

where

$$R_{eq} = Z_c + \frac{R_T}{4} \quad (2.15)$$

$$h = \frac{Z_c - R_T/4}{Z_c + R_T/4} \quad (2.16)$$

Z_c is the line characteristic impedance.

τ is the transmission delay along the line.

R_T is the line loss.

We can also have a similar expression for J_{mM}, the current source at terminal M.

2.2 Mathematical Model of Three-Winding Transformers [3]

The section 2.1 summarized mathematical model and HYPERSIM model for representing transmission lines and in this section, mathematical model and equations representing three-winding transformers shall be discussed. A single phase equivalent circuit of a three-winding transformer with all the physical quantities is shown in Figure 2.3. The subscript p, s and t represent to primary, secondary and tertiary quantities respectively. The transformer is represented by three equivalent impedance's connected in star to a fictitious point unrelated to system neutral. The effect of magnetizing reactance is neglected in this equivalent circuit. The difference between the ratio of actual turns and base voltages is represented by off nominal turns ratio (ONR) and values of equivalent impedance's (Z_p, Z_s and Z_t) are obtained by performing short circuit test on the three-winding transformer.

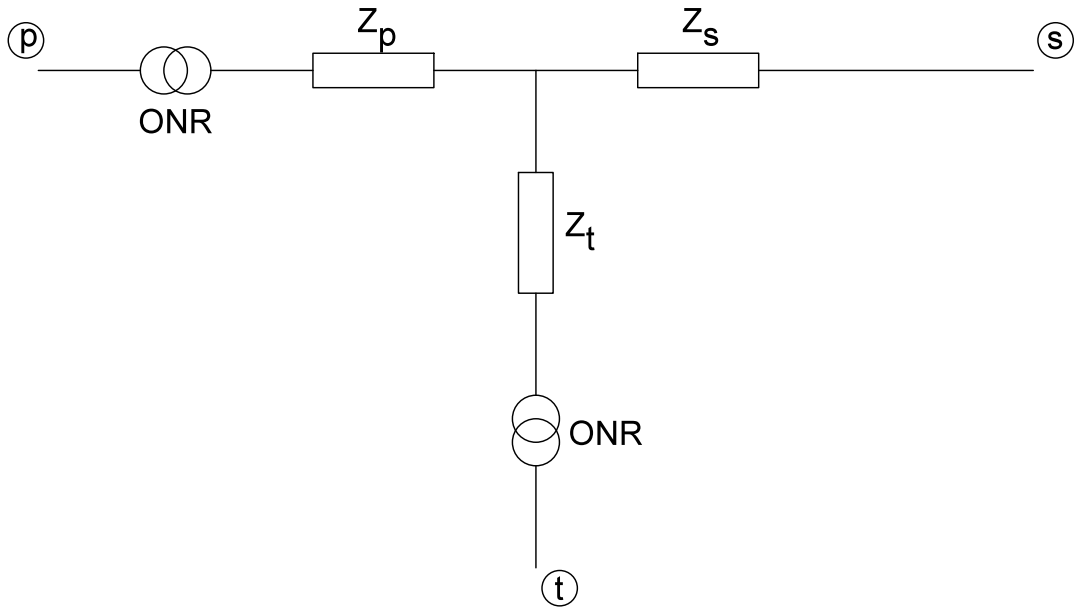

Figure 2.3: Equivalent Circuit of Three-Winding Transformer [3]

From the short circuit test, parameters Z_{ps}, Z_{pt}, and Z_{st} are obtained. Equation 2.17 to Equation 2.19 represent expressions for Z_{ps}, Z_{pt}, and Z_{st}.

$$Z_{ps} = Z_p + Z_s \tag{2.17}$$

$$Z_{pt} = Z_p + Z_t \tag{2.18}$$

$$Z_{st} = Z_s + Z_t \tag{2.19}$$

Rearranging and solving Equation 2.17 to Equation 2.19 yields Equation 2.20 to Equation 2.22

$$Z_p = \frac{1}{2}[Z_{ps} + Z_{pt} - Z_{st}] \tag{2.20}$$

$$Z_s = \frac{1}{2}[Z_{ps} + Z_{st} - Z_{pt}] \tag{2.21}$$

$$Z_t = \frac{1}{2}[Z_{pt} + Z_{st} - Z_{ps}] \tag{2.22}$$

Where

Z_{ps} = Leakage impedance measured in primary with secondary shorted and tertiary open.

Z_{pt} = Leakage impedance measured in primary with tertiary shorted and secondary open.

Z_{st} = Leakage impedance measured in secondary with tertiary shorted and secondary open.

2.3 Mathematical Model of Induction Motors [4]

In section 2.2, mathematical model for three-winding transformer was reviewed and in this section, mathematical model for three-phase induction motor shall be reviewed.

Idle running and blocked-rotor tests made on induction motor provides equivalent circuit parameters. Equivalent circuit of a three-phase induction motor is shown in Figure 2.4.

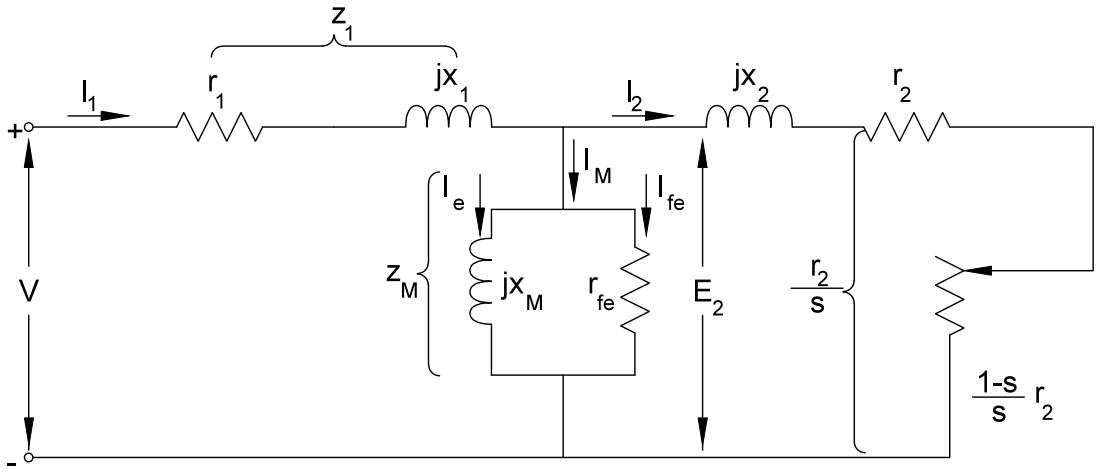

Figure 2.4: Equivalent Circuit for Three-Phase Induction Motor [4]

2.3.1 No-Load Test

Equivalent circuits of three-phase induction motor under no-load conditions are shown in Figure 2.5 and Figure 2.6.

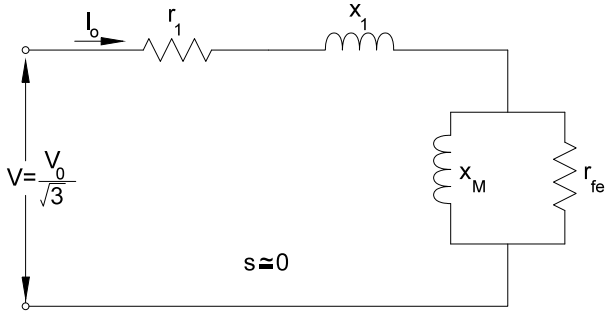

Figure 2.5: No-Load Test Equivalent Circuit-1 for Three-Phase Induction Motor [4]

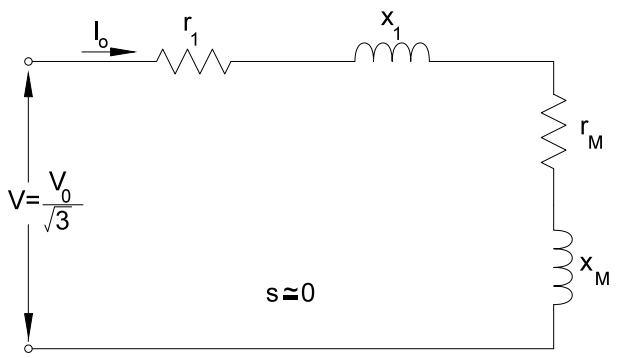

Figure 2.6: No-Load Test Equivalent circuit-2 for Three-Phase Induction Motor [4]

Let

V_0 = Rated line-to-line voltage.

I_0 = Line current

P_0 = Power input.

r_1 = Stator resistance in ohms per phase.

From Figure 2.6,

$$V = \frac{V_0}{\sqrt{3}} \tag{2.23}$$

$$z_0 = \frac{V}{I_0} \tag{2.24}$$

$$P_0 = 3I_0^2 r_0 \tag{2.25}$$

where

$$r_0 = r_1 + r_M \tag{2.26}$$

$$x_0 \simeq x_1 + x_M \tag{2.27}$$

$$x_0 = \sqrt{z_0^2 - r_0^2} \tag{2.28}$$

2.3.2 Locked-Rotor Test

The parameters x_1, x_2 and r_2 are obtained from the locked-rotor test. Equivalent circuit under locked-rotor condition is given in Figure 2.7. Simplified equivalent circuit applied to locked rotor conditions by making s=1 is given in Figure 2.8

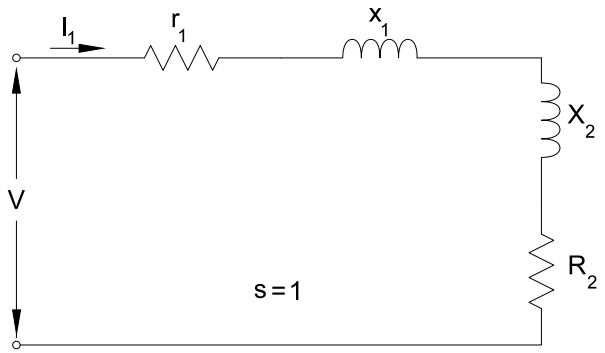

Figure 2.7: Locked-Rotor Test Equivalent Circuit for Three-Phase Induction Motor [4]

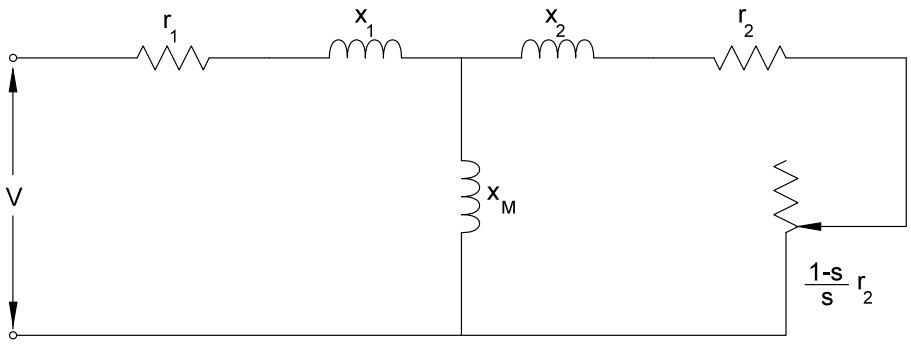

Figure 2.8: Simplified Equivalent Circuit for Three-Phase Induction Motor Under Load [4]

Let

V_L = line-to-line voltage.

I_L = Line current

P_L = Power input.

Impedance of the motor is given in Equation 2.29, equivalent resistance and reactance expressions are given in Equation 2.30 and Equation 2.31 respectively.

$$z_L = \frac{V_L}{\sqrt{3} I_L} \tag{2.29}$$

$$r_L = r_1 + R_2 = \frac{P_L}{3 I_L^2} \tag{2.30}$$

$$x_L = x_1 + X_2 = \sqrt{z_L^2 - r_L^2} \tag{2.31}$$

Proportions of induction motor leakage reactances depends on the classification of motor. When the classification of the motor is not known it is assumed that x_1=x_2=$0.5x_L$.

From Figure 2.7 and Figure 2.8,

$$R_2 + jX_2 = \frac{(r_2 + jx_2)jx_M}{r_2 + j(x_2 + x_M)} \tag{2.32}$$

Rearranging Equation 2.32 and equating real parts yields Equation 2.33,

$$R_2 = \frac{r_2 x_M^2}{r_2^2 + (x_2 + x_M)^2} \tag{2.33}$$

Since $r_2 \ll (x_2 + x_M)$, Equation 2.33 can be approximated to Equation 2.34.

$$R_2 \simeq \frac{r_2 x_M^2}{(x_2 + x_M)^2} \tag{2.34}$$

And the rotor resistance referred to stator is given in Equation 2.35.

$$r_2 = (r_L - r_1)\left(\frac{x_2 + x_M}{x_M}\right)^2 \tag{2.35}$$

2.4 HYPERSIM Models for Power System Components in Substation [2]

In section 2.2 and section 2.3, the mathematical equations and circuits pertaining to transformers and induction machines (Machines & Motor) were discussed. In this section, HYPERSIM modeling of power system components in a substation shall be reviewed.

A substation comprises of passive elements (Resistor, Inductor and Capacitor), Circuit breakers, Generation equipment represented as voltage and current sources with control system, Machines and Motors considered as sources with control systems. Control systems are modeled using the block diagram principle whose inputs are node voltages and currents and outputs are used to control sources and switches. All power elements are interconnected via nodes working at power system level voltages and currents. These power elements are simulated simultaneously using a single equation called the node equation.

$$YV = I \tag{2.36}$$

where $\mathbf{Y}$ is the substation admittance matrix, $\mathbf{V}$ is vector of node voltages and $\mathbf{I}$ is vector of node currents.

The following sections illustrate mathematical background of modeling power system components in a substation in HYPERSIM Real-Time Simulator software.

2.4.1 RLC Element Model

HYPERSIM, as EMTP uses trapezoidal integration technique in modeling lumped components. General equation for trapezoidal integration technique is given in Equation 2.37

$$y(t) = \int_0^t x(t)dt \tag{2.37}$$

Equation 2.37 is evaluated as

$$y(t) = y(t-T) + \frac{T}{2}[x(t) + x(t-T)] \tag{2.38}$$

where T is the calculation time step.

Applying the rule, the derivative part $\frac{dy(t)}{dt}$ approximated as a difference equation on Equation 2.38 yields Equation 2.39.

$$\frac{y(t) - y(t-T)}{T} = \frac{1}{2}[x(t) + x(t-T)] \tag{2.39}$$

In the following sections, voltage across an inductor and current through a capacitor are illustrated by using trapezoidal integration technique.

Inductor Branch

Voltage across the inductor connected between nodes k and m as shown in Figure 2.9 is defined by Equation 2.40.

$$v = L\frac{di}{dt} \tag{2.40}$$

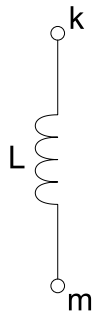

Figure 2.9: Inductor Branch [2]

After applying trapezoidal integration technique on Equation 2.40 yields Equation 2.41.

$$i_{km}(t) = \frac{v_k(t) - v_m(t)}{R_eq} + i_{hist}(t - T) \tag{2.41}$$

Where

$$R_{eq} = \frac{2L}{T} \tag{2.42}$$

$$i_{hist}(t - T) = i_{km}(t - T) + \frac{v_k(t - T) - v_m(t - T)}{R_eq} \tag{2.43}$$

Equivalent circuit of L branch using the trapezoidal rule is shown in Figure 2.10.

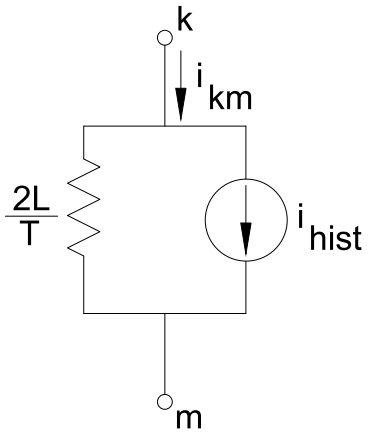

Figure 2.10: Equivalents of Inductor Branch using the Trapezoidal Rule [2]

Capacitor Branch

An expression similar to current passing through inductor branch can also be derived for current passing capacitor branch.

Current through the capacitor connected between nodes k and m as shown in Figure 2.11 is given by Equation 2.44.

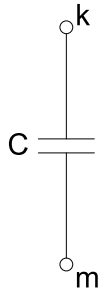

Figure 2.11: Capacitor Branch [2]

$$i = C\frac{dv}{dt} \tag{2.44}$$

After applying trapezoidal integration technique on Equation 2.44 yields Equation 2.45.

$$i_{km}(t) = \frac{[v_k(t) - v_m(t)]}{R_{eq}} + i_{hist} \tag{2.45}$$

Where

$$R_{eq} = \frac{T}{2C} \tag{2.46}$$

$$i_{hist} = -i_{km}(t-T) - \frac{2C}{T}[v_k(t-T) - v_m(t-T)] \tag{2.47}$$

Equivalent circuit of capacitor branch using the trapezoidal rule is shown in Figure 2.12.

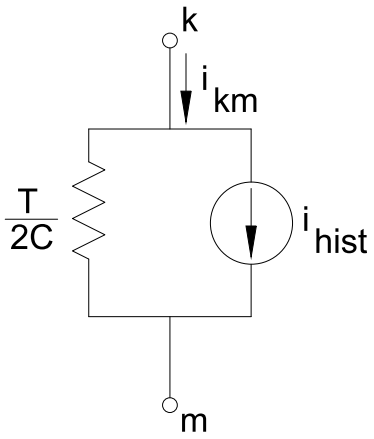

Figure 2.12: Equivalent of Capacitor Branch using the Trapezoidal Rule [2]

Note 1: According to Equation 2.41 and Equation 2.45, an inductor and a capacitor branch is equivalent to a resistor R_{eq} in parallel to a current source i_{hist} whose values depends only on the values of voltages and current of the previous time step.

2.5 Mathematical Model of Fault Arcs [5]

The section 2.1 to section 2.4 reviewed mathematical background of power system components and their HYPERSIM Real-Time Simulator models. The previous chapter has already provided some idea of fault arc scenarios during single pole switching applications. This section illustrates mathematical equations required for modeling primary and secondary fault arcs in HYPERSIM.

2.5.1 Primary Arc Model

The solution of the Equation 2.48 presented by Kizilcay [45] gives dynamic primary arc conductance.

$$\frac{dg_p}{dt} = \frac{1}{T_p}(G_p - g_p) \tag{2.48}$$

where g_p is the primary arc conductance and G_p is the stationary primary arc conductance evaluated by Equation 2.49

$$G_p = \frac{|i|}{V_p L_p} \tag{2.49}$$

where "i" is the fault current, V_p is the arc voltage gradient whose average value for the currents in range of 1.4kA to 24kA is given in Equation 2.50 and L_p the arc length.

$$V_p = 15V/cm \tag{2.50}$$

The time constant T_p in Equation 2.48 is empirically obtained by fitting with the experimental volt-ampere cyclograms.

$$T_p = \frac{\alpha I_p}{L_p} \tag{2.51}$$

With $\alpha = 2.85 \times 10^{-5}$, I_p is the peak value of arc current under bolted fault conditions.

2.5.2 Secondary Arc Model

The dynamic behavior of secondary arc conductance is governed by Equation 2.52.

$$\frac{dg_s}{dt} = \frac{1}{T_s}(G_s - g_s) \tag{2.52}$$

and the expression for G_s is given in Equation 2.53

$$G_s = \frac{|i|}{V_s \times l_s(t_r)} \tag{2.53}$$

Expression for the constant voltage gradient can be approximated by Equation 2.54 for the currents in the range of 1A to 55A.

$$V_s = 75 I_s^{-0.4} \tag{2.54}$$

Secondary arc length for low wind velocities is a function of time spent from the initiation of secondary arc (t_r), i.e. the moment at which breaker trips. An empirical expression is given in Equation 2.55.

$$L_s(t_r)/L_{s0} = \begin{cases} 10.t_r, & t_r > 0.1s \\ 1, & t_r \leq 0.1s \end{cases} \tag{2.55}$$

Where L_{s0} is initial arc length equal to the primary arc length.

An empirical expression is given in Equation 2.56 for time constant T_s in Equation 2.52. The equation is determined according to the rate of rise of the secondary arc voltage.

$$T_s = \frac{\beta I_s^{1.4}}{I_s(t_r)} \tag{2.56}$$

Where $\beta = 2.51 \times 10^{-3}$. An empirical expression to represent the arc re-ignition voltage is given in Equation 2.57.

$$V_r(t_r) = \left[5 + \frac{1620 \times T_e}{2.15 + I_s}\right] \times (t_r - T_e) \times h(t_r - T_e) \times I_s(t_r)[kV] \tag{2.57}$$

Chapter 3

HYPERSIM Modeling and Relay Design

This chapter explains HYPERSIM environment, methodology to build power system model suitable for closed loop simulations and relay testing in HYPERSIM environment and illustrates protective relay scheme for series capacitor line.

Figure 3.1 illustrates the objective of this work. Closed loop simulations with relay hardware-in-the-loop for analyzing its performance necessitates power system model and relay set-up. Power system components shown in Figure 3.1 are modeled to develop test system for performing simulations and analysis. Each power system component is modeled in HYPERSIM according to the application requirements for relay testing shown in Table 1.1. Relay set-up includes design of protective scheme and determination of signals required for line differential relays and over current relays. The protective relay scheme designed in this thesis for the series capacitor line is capable of testing two different line differential relays connected at each end of the line. Power system model together with relay set-up simulate fault conditions, trip, status, close and breaker fail conditions for the relay hardware and breaker models in HYPERSIM.

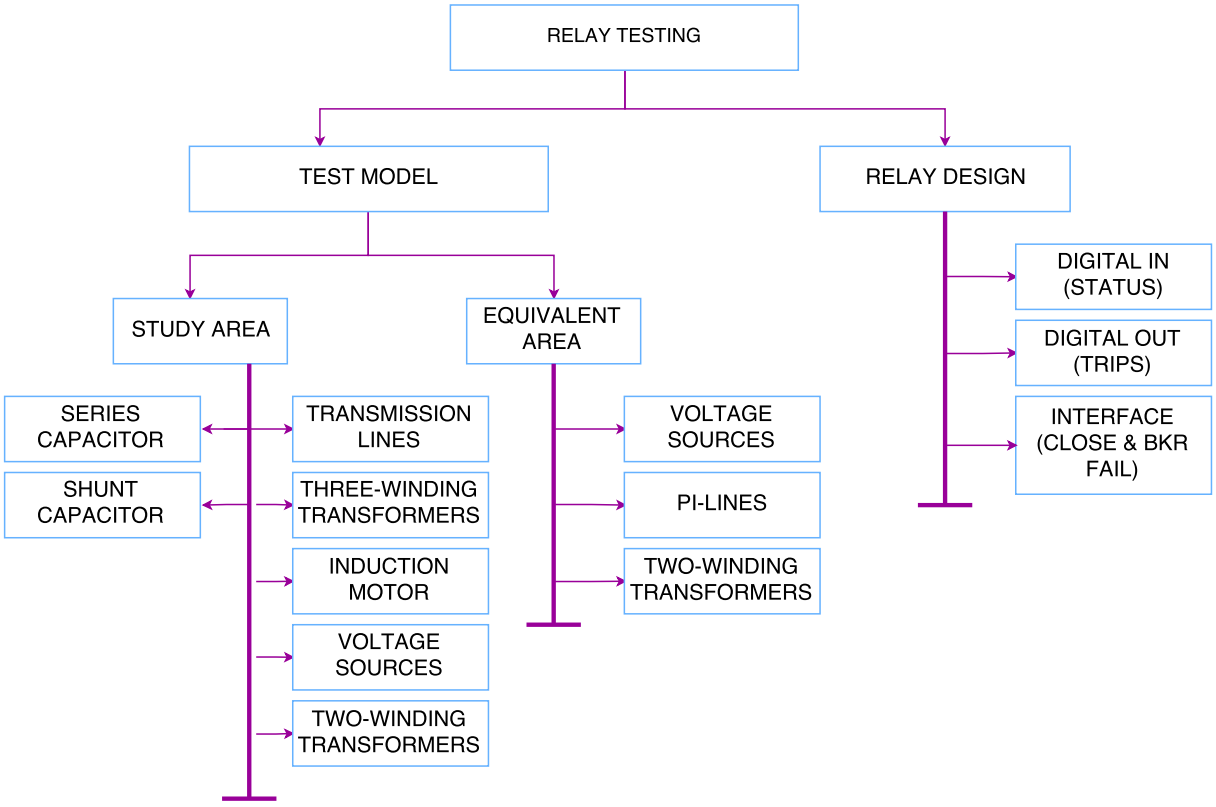

Figure 3.1: Methodology

3.1 HYPERSIM Hardware & Software Environment [6]

In this section, the environment in which power system model built will be discussed. "HYPERSIM is primarily a software that runs over a Real-Time OS base of Linux for performing hardware-in-the-loop simulations. Simulation can be off line simulation executed in differed time on a parallel computer or on a multiple core type (PC, SGI or OPAL-RT) or Real time simulation achieved on SGI or OPAL-RT computer type (1 sec of simulation = 1 sec on a clock)".

3.1.1 HYPERSIM Hardware Environment

Hardware topology of HYPERSIM includes the following:

- REAL-TIME (LINUX) dedicated simulator for simulating at real time using parallel processing.

- HOST PC (LINUX) for modeling and control of the simulation running on the REAL-TIME simulator.

3.1.2 HYPERSIM Software Environment

Software topology of HYPERSIM includes the following:

- HYPERSIM: "HYPERSIM is the primary software of the suite used as modeling tool for the simulation. It controls both offline and Real-Time simulations".

- ScopeView: "Scopeview is the visualization software of the simulation. It is a graphic tool that let the user to view everything during the simulation. Also, it allows advanced studies directly from the data collected".

- HyperView: "Hyperview is the communication server between HYPERSIM, ScopeView and TestView. It also offers advanced features such as load flow calculations, a line programming tool and a transformer programming tool".

- TestView: "Testview is the test automation center that let the user configure the system to run multiple test without human intervention and generate the final report".

3.2 Power System Model

In this section, modeling of major power system elements in HYPERSIM will be discussed. Figure 3.2 illustrates series of steps involved in developing power system model for simulation and analysis.

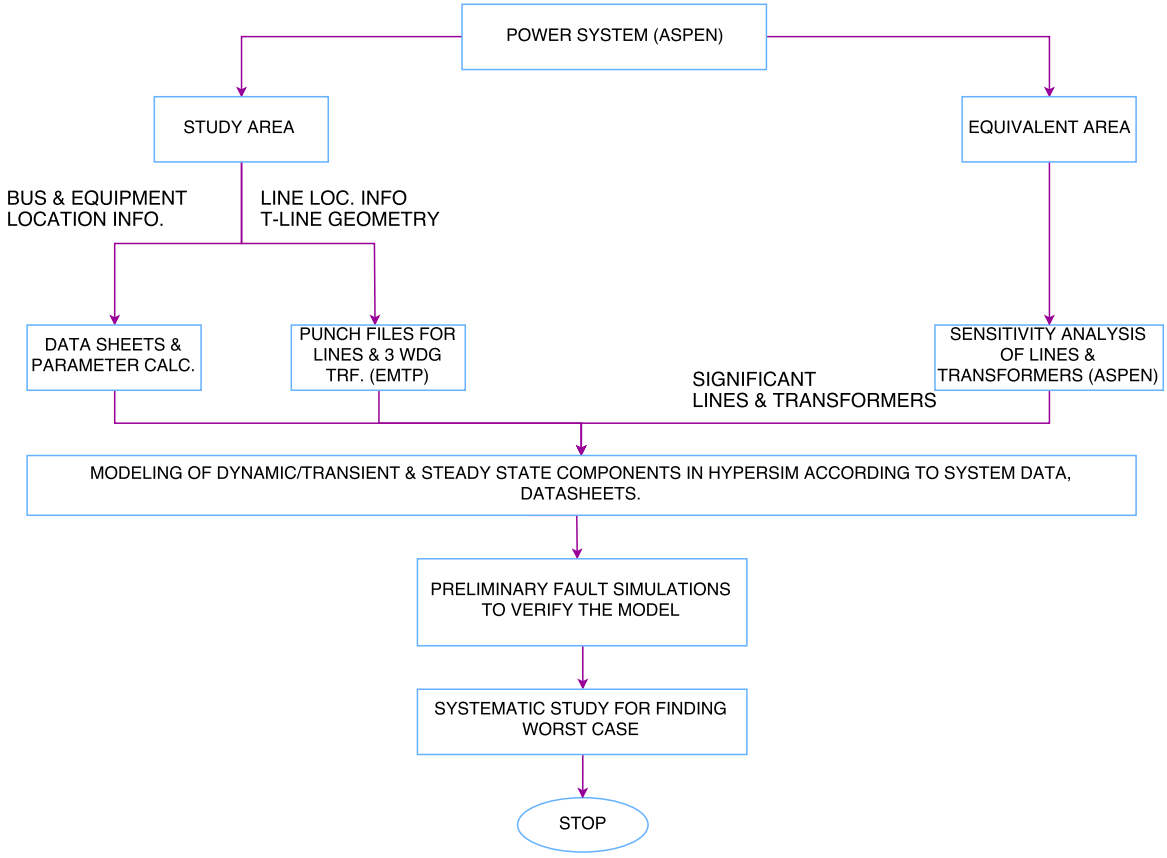

Figure 3.2: Work Flow

An original ASPEN equivalent power system model of an electric utility is used in this thesis. This ASPEN model consists of study area and equivalence area with all components shown in Figure 3.1. Study area is two bus deep from series capacitor line with actual power system components and equivalence area is rest of the power system with equivalent lines and equivalent transformers connected between boundary buses of study area. Equivalent sources are connected to boundary buses in study area. Study area is modeled with bus information, equipment

information and traveling wave line information. Equipment information is available in the form of data sheets and from the data sheets parameters required for modeling the power system elements in HYPERSIM are calculated. Sensitivity analysis is performed in ASPEN to remove equivalent lines and equivalent transformers whose presence does not impact fault current passing through series capacitor line.

The transmission lines data is available in T-Line geometry (Figure 3.3). These lines are modeled in HYPERSIM as Frequency distributed parameter line model, Constant distributed parameter line model and π line model. Lines whose length is less than 15KM are modeled as π lines. For modeling a traveling wave line in HYPERSIM, minimum length must be 15KM for a time step of $50\mu s$. In addition to lines, study area also consists of generators with step-up transformers, induction motor, series capacitor with surge arrester and bypass breaker in parallel and shunt capacitors. Generators are modeled as voltage sources and step-up transformers are modeled as two-winding transformers using the data from ASPEN/PSSE. Induction motor parameters are calculated using the data from the manufacturer's datasheet and entered into induction motor element control panel in HYPERSIM. Equivalent lines and equivalent transformers are modeled in HYPERSIM using the data from ASPEN/PSSE power system model. After developing the model with the above mentioned elements, faults at different locations and different incidence angle are applied for capturing the worst fault scenarios to test relays.

HYPERSIM provides a fairly large library of models for power elements and control blocks. The subsection 3.2.1 to subsection 3.2.3 explains the details of modeling lines, induction motor and three winding transformer.

3.2.1 Modeling of Transmission Lines

Two types of traveling wave line models are considered in this thesis; Constant distributed parameter line and Frequency distributed parameter line. JMARTI frequency distributed parameter line line model is suitable for switching transient studies [8]. Electrical parameters into HYPERSIM "transmission line" and "JMARTI" model can be entered in two different ways; Hyperline Line data module in Hyperview and load file function with EMTP files. All transmission lines in this thesis are modeled using the load file function in HYPERSIM line control panel. The punch file generated in EMTP is loaded into HYPERSIM line element control panel.

T-Line geometry shown in Figure 3.3 includes configuration, conductor type, sag, bundled conductor spacing and separation angle, number of shields, and their type. This data is available in an excel file. A python code parses the excel file and outputs data required for generating punch files, to a text file. An example of the python output is shown in Figure 3.4.

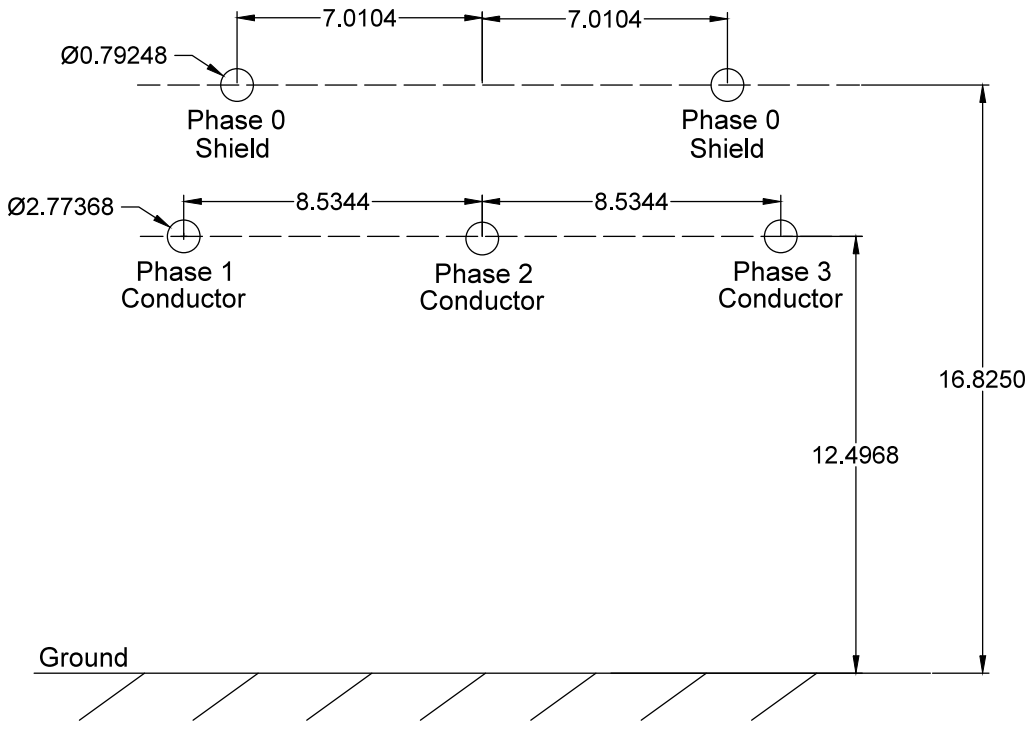

Figure 3.3: T-Line Geometry

```
STR-207A - STR-301    :    Length of Line [km]  =  24.6711822
Structure Type  =  HORIZONTAL
Conductor Type  =  795 ACSR "Condor"
Shield Type-1  =  5/16 EHS Steel
Shield Type-2  =  5/16 EHS Steel
 Phase     DC Resistance   Outside          Horizontal     Vertical Ht.      Vertical Ht.
 Number    Ohm/Km          Diameter[cm]     distance[m]    at tower[m]       at Midspan[m]
 1         0.08003         2.77368          -8.5344        12.4968           7.9248
 2         0.08003         2.77368          0              12.4968           7.9248
 3         0.08003         2.77368          8.5344         12.4968           7.9248
 0         4.1197          0.79248          -7.0104        16.82496          15.30096
 0         4.1197          0.79248          7.0104         16.82496          15.30096
No. of Conductors in Bundles  =  2.0
Bundle Conductor Spacing[cm]  =  30.48
Separation Angle[deg]  =  180.0
```

Figure 3.4: Python Output of Transmission Line of Figure 3.3

Data from the text file when entered into EMTPs line data block, creates punch files. Punch file for each section of transmission line in the study area is created. For a multi-section line, punch file of the longest section is used to represent the entire line. The length of the line is the sum of lengths of individual sections. In this way, punch files for Constant parameter (CP) type and Frequency Distributed (FD) type are created in EMTP for all transmission lines in study area. Series capacitor line on which faults will be applied is modeled as Frequency distributed parameter line, Lines whose length is less than 15KM are modeled as π lines and all other lines are modeled as Constant distributed parameter line. Transmission line element in HYPERSIM is used to model Constant distributed parameter lines and J-Marti line element is used to model Frequency distributed parameter lines in HYPERSIM. Punch files created in EMTP for CP and FD type lines can be loaded directly into control panels of "transmission line" and "J-Marti"line elements in HYPERSIM respectively. Control Panels for an unTransposed Line and J-Marti FD line are shown in Figure 3.5 and Figure 3.6.

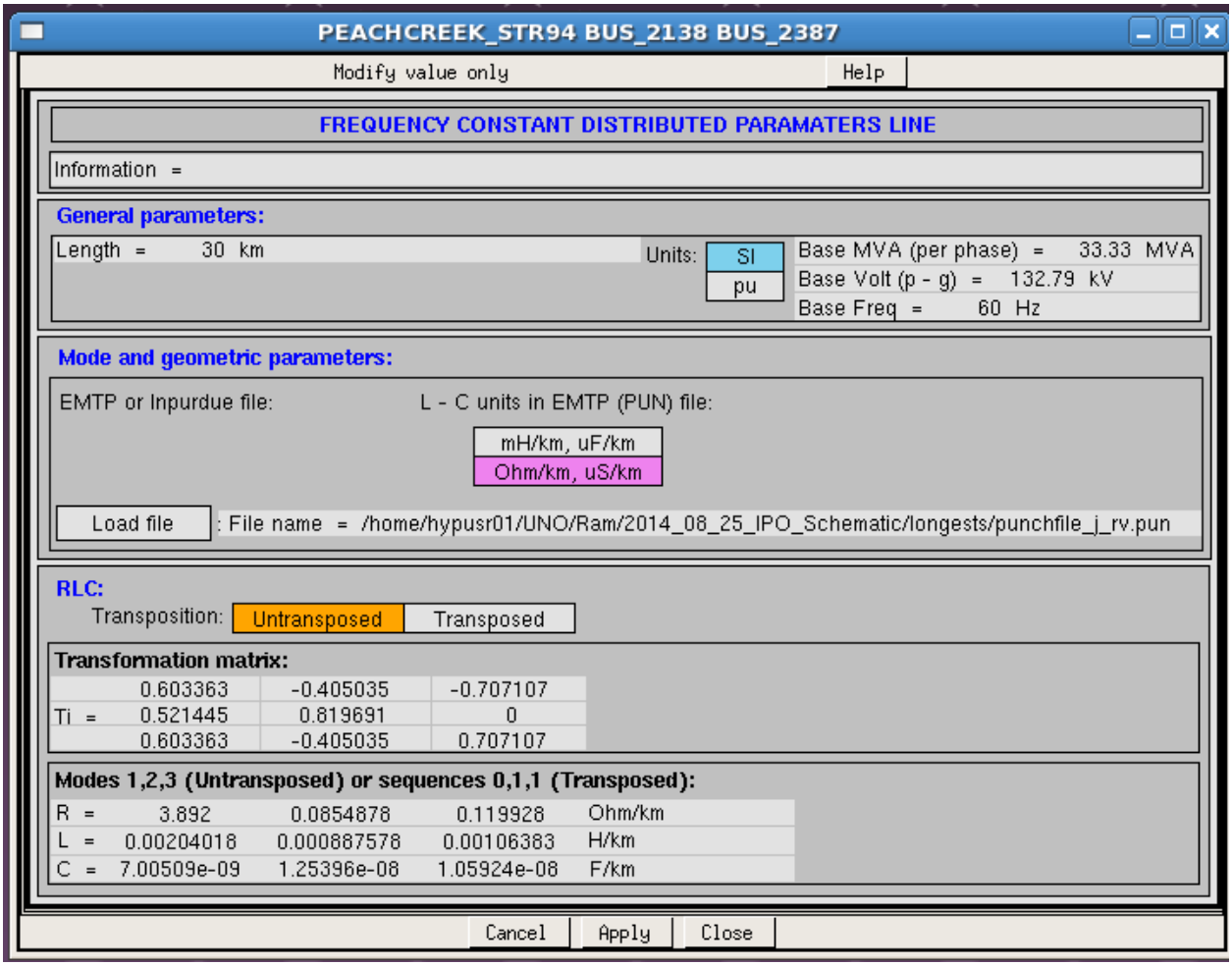

Figure 3.5: Control Panel of an Untransposed Line

3.2.2 Modeling of Induction Motor

In this section, modeling of Induction motor element in HYPERSIM will be discussed. An induction motor is connected at the end of series capacitor line via power transformer. Induction motor and its power transformer being part of study area, accurate modeling of these components is required.

The general parameters of induction motor are provided in a data sheet. This datasheet includes no-load and locked rotor test results and also specifications of the Induction Motor. From the data, the stator resistance and inductance values and rotor resistance and inductance values are calculated. These calculations are performed with reference to mathematical equations of no-load and locked rotor tests in [4].

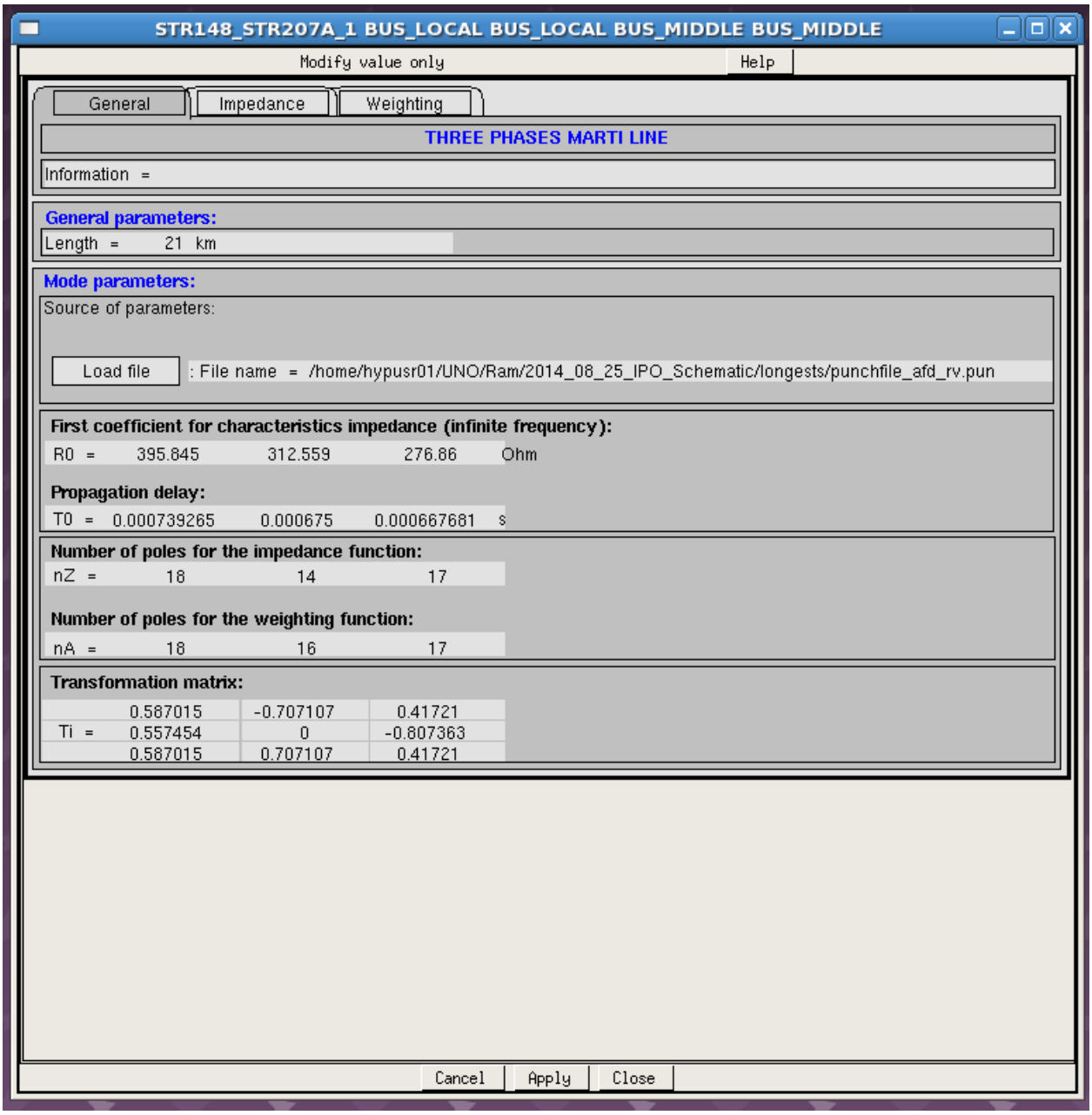

Figure 3.6: Control Panel of a J-Marti Line

Calculation of Induction Motor Parameters

The constant values of induction motor are:

Applied Voltage = 6600V (line-line)

Applied Phase Voltage v_{ph} = 3810.62V (line-neutral)

No Load Current I_0 = 96.2A

No Load PF = 0.0048

Locked Rotor Current I_{sc} = 3156A

Locked Rotor PF = 0.118

No load parameters r_0 and x_0 are determined using Equation 3.1 to Equation 3.6.

$$\cos\phi_0 = 0.048 \tag{3.1}$$

$$\phi_0 = 87.24^0 \tag{3.2}$$

$$I_m = I_0 \sin\phi_0 = 96.08A. \tag{3.3}$$

$$I_c = I_0 \cos\phi_0 = 4.63A. \tag{3.4}$$

$$x_0 = V_{ph}/I_m = 39.65\Omega \tag{3.5}$$

$$r_0 = V_{ph}/I_c = 823.004\Omega \tag{3.6}$$

Locked rotor parameters r_l and x_l are determined using Equation 3.7 to Equation 3.11:

$$\cos\phi_{sc} = 0.118 \tag{3.7}$$

$$\phi_{sc} = 83.22^0 \tag{3.8}$$

$$z_{sc} = v_{ph}/I_{sc} = 1.207\Omega \tag{3.9}$$

$$r_l = z_{sc}\cos\phi_{sc} = 0.142\Omega \tag{3.10}$$

$$x_l = z_{sc}\sin\phi_{sc} = 1.198\Omega \tag{3.11}$$

Stator parameters r_s, x_s and rotor parameters r_r, x_r are determined by Equation 3.12 to Equation 3.14

$$x_s = x_r = 0.5x_l = 0.599\Omega \tag{3.12}$$

$$x_m = x_0 - x_s = 39.051\Omega \tag{3.13}$$

$$r_s = r_r = (r_l - r_s)\left[\frac{x_r + x_m}{x_m}\right]^2 == 0.072\Omega \tag{3.14}$$

The stator and rotor resistance's and reactances along with general parameters are entered into induction motor control panel in HYPERSIM shown in Figure 3.7.

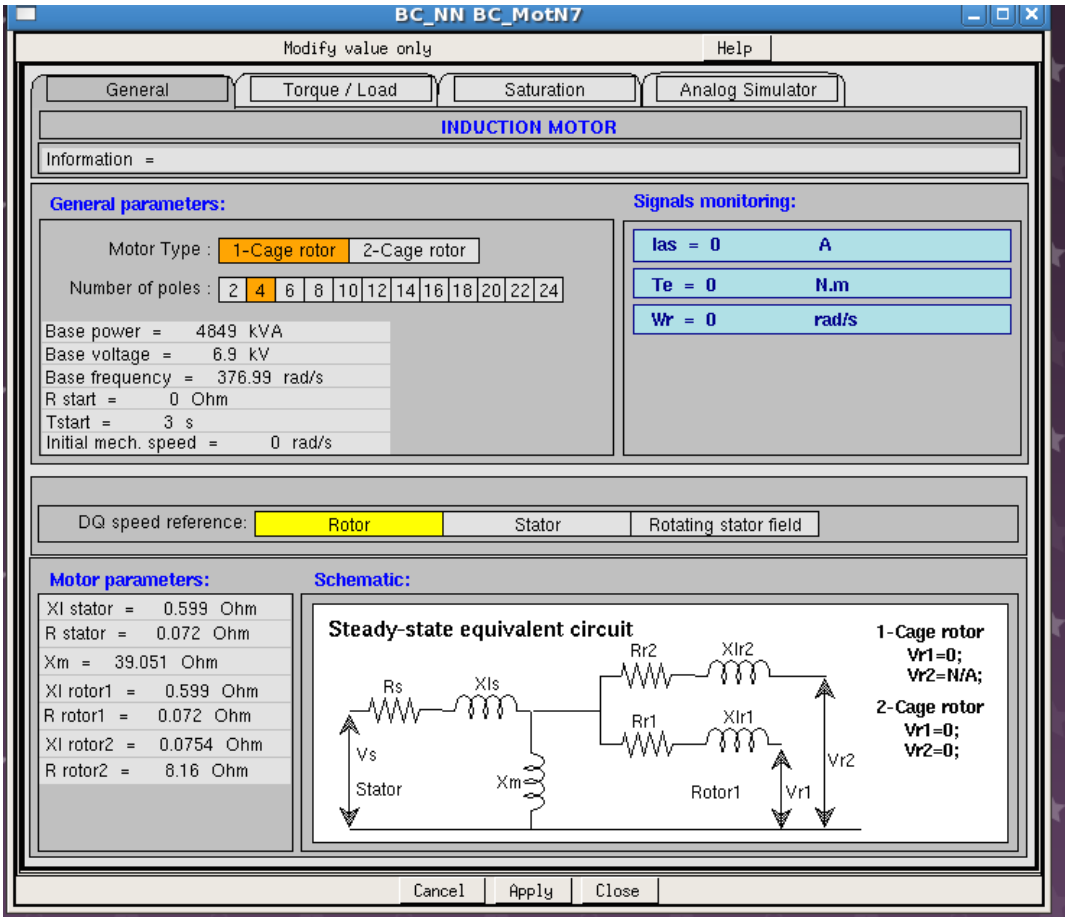

Figure 3.7: Control Panel of an Induction Motor

The p.u resistance and reactance values of two-winding transformer connected to the induction motor are available in the ASPEN equivalent. These values along with primary and secondary voltages and type of transformer are entered into control panel of two-winding transformer element in HYPERSIM. Control panel is shown in Figure 3.8.

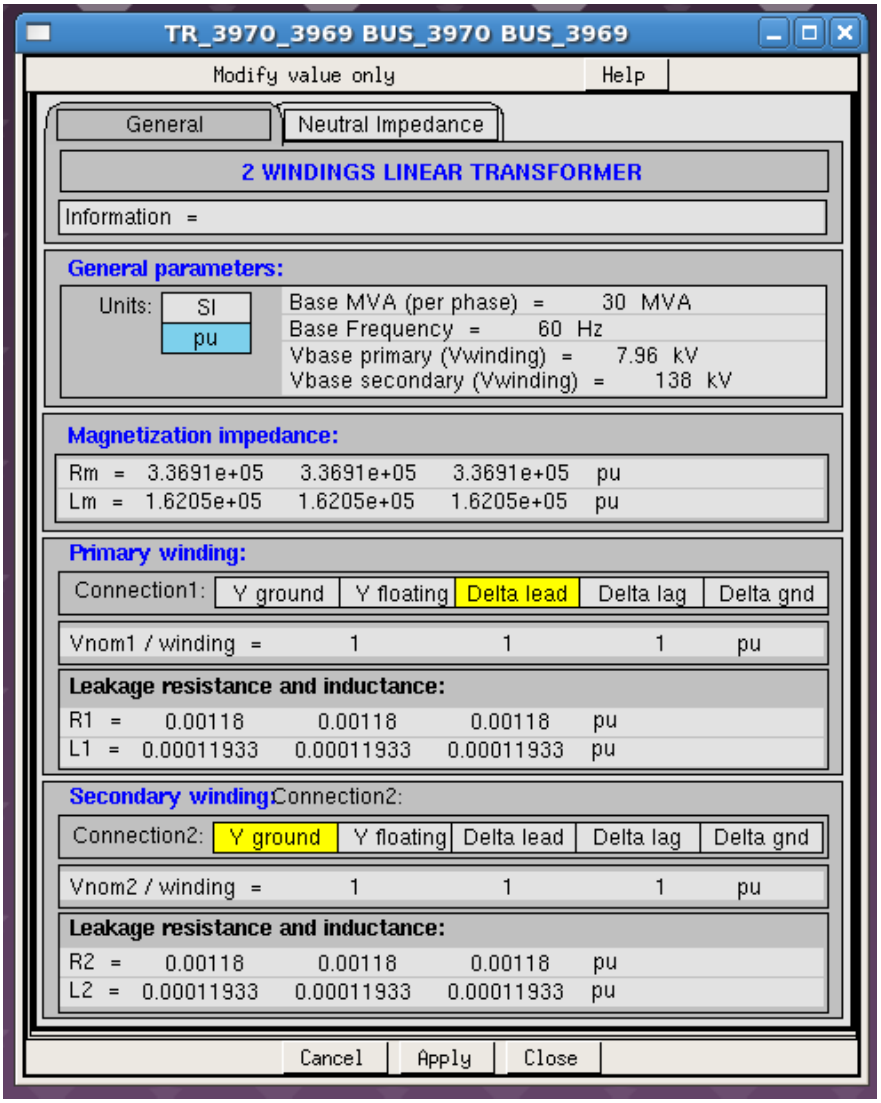

Figure 3.8: Control Panel of a Two-Winding Transformer

3.2.3 Modeling of Three-Winding Transformer

In this section, another major power system element; three-winding transformer modeling in HYPERSIM will be discussed. These transformers are to be accurately modeled for capturing the exact transient phenomenon. The original equipment manufacturers data for these transformers is available in datasheets and are modeled in EMTP using "BC-Tran block". The data sheet contains all the data needed for modeling the transformers except the zero-sequence test data. According to the EMTP theory book [46], a good approximation is to take zero sequence test results as equal to the positive sequence test results. The transformers modeled have a delta tertiary winding which causes the excitation test to be equivalent to a short circuit test.

When all the required data entered into respective fields, EMTP generates output files. The .pun and .out files are of interest to us. The .out file contains all the data that was entered during the process and also the output parameters that are calculated. The .pun file contains the calculated parameters, i.e., the resistances and the reactances of the windings. The .pun file has the resistance R in ohms and reactance ωL in ohms. The three-winding transformer element model in HYPERSIM accepts the winding resistance in ohms, Ω and inductance in Henry, H. The resistance values can be obtained directly from the .pun file and the inductance of the windings is calculated using Equation 3.15 with ω being the angular frequency and f = 60Hz the system frequency.

$$L = \frac{X}{\omega} \tag{3.15}$$

$$\omega = 2\pi f \tag{3.16}$$

Figure 3.9 shows the parameters window for entering the data from the .pun file into HYPERSIM. The data in the .pun file is in R (Ω) and X = ωL (Ω) format. The data for the transformer element in HYPERSIM is in R and L matrices format.

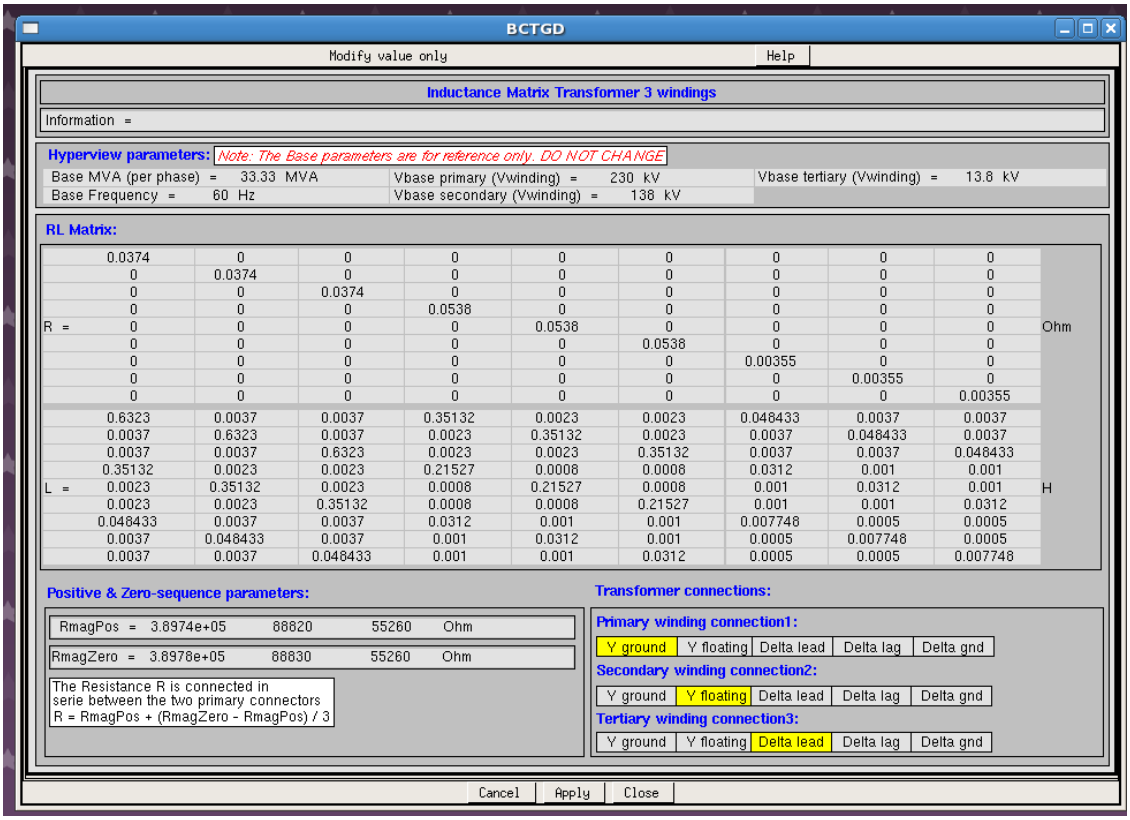

Figure 3.9: Control Panel of a Three Winding Transformer

3.2.4 Miscellaneous

All other power system components (Generators, shunt capacitor, series capacitor and MOV) in study area are modeled using the data from the ASPEN/PSSE equivalent file. Generators are modeled as voltage sources. The data of each component is entered into control panels of respective power system elements in HYPERSIM. In addition to these, breaker/bus configurations at each end of series capacitor line are also modeled in HYPERSIM.

3.2.5 Equivalent Area

Equivalent two winding transformers and equivalent π lines are connected between the boundary buses in study area. The total number of equivalent π lines and equivalent transformers are initially 17 and 20 respectively. Sensitivity analysis is performed in ASPEN to remove some equivalent lines

and equivalent transformers whose presence does not impact fault current value. The criteria followed for performing sensitivity analysis is illustrated in Figure 3.10. A single line-to-ground and three-phase-to-ground faults were applied at each terminal bus of series capacitor line. Fault current through the line, voltages at the terminal buses of series capacitor line are captured. The scenario is repeated by removing one equivalent line at a time and compared with values when there is no line removed. The criteria followed for removal of an equivalent line is as follows:

1. Change in voltage is less than 1 Volt
2. Change in current is less than 10 A
3. Change in angle is less than 1 degree

This process eliminated 17 equivalent components (lines & transformers). π line and two winding transformer elements in HYPERSIM are used to model remaining equivalent π lines and equivalent two winding transformers using the data from ASPEN/PSSE. Because of presence of some lines & transformer elements in HYPERSIM, four transmission lines sending and receiving end buses are terminated on same station. To overcome this, decoupling inductor element is connected at one end of each of these four lines. Presence of decoupling inductors made the power system unable to produce signals at buses in the model. Different values of inductance were tried for this decoupling inductor until signals are available at buses.

3.3 Modeling of Fault Arc

In section 3.2, modeling of power system elements in HYPERSIM was discussed. This section discusses modeling of fault arc phenomenon in HYPERSIM. In this thesis realistic arc models are developed and incorporated in HYPERSIM based on mathematical models developed by A.T. Johns, R.K. Aggarwal and Y.H. Song [40]. Literature shows that fault arc was represented as a

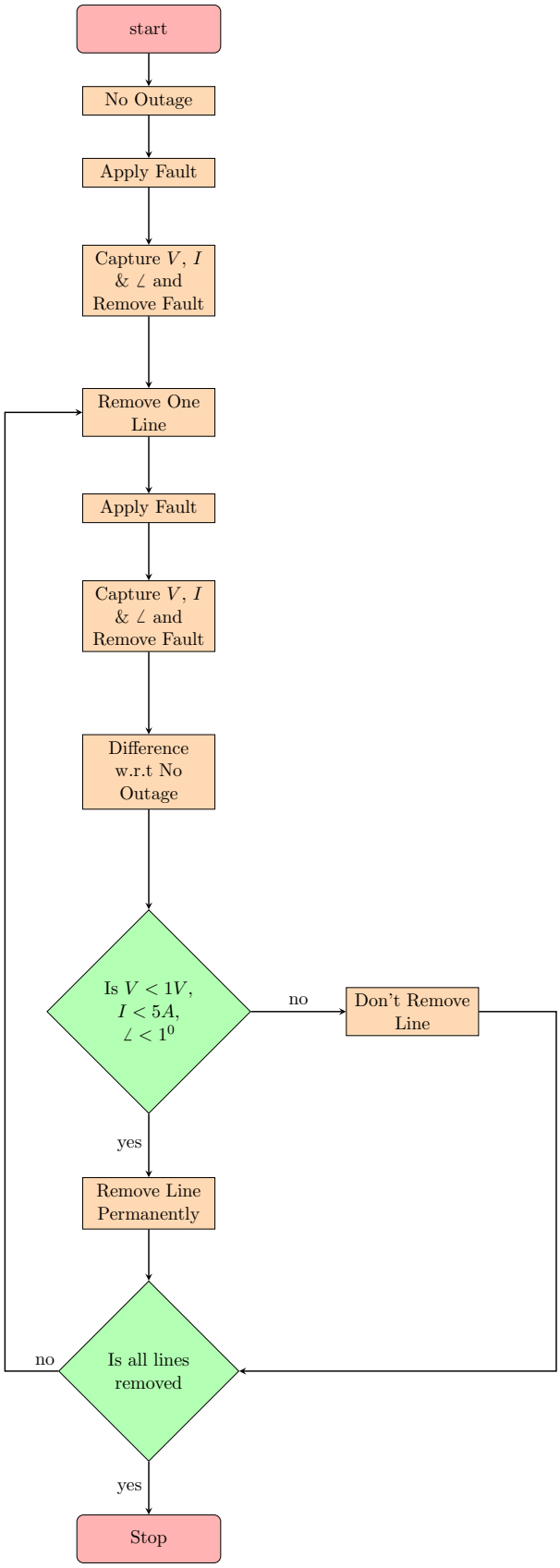

Figure 3.10: Sensitivity Analysis FLowchart

time varying resistor. This element is readily available in EMTP whereas in HYPERSIM, it is required to build this time varying resistor element. To build a time varying resistor element in HYPERSIM, User Code Model (UCM) component is used to develop this element.

UCM component is composed of a power part and a control part. The power part has external nodes to which other power system elements are connected and control part node accepts signals from external control blocks to perform user defined functions. A script should be developed to build this UCM component for using it to perform user defined functions.

Fault arc phenomenon in this thesis is modeled using UCM time varying resistor and an ideal switch. UCM time varying resistor element simulates fault arc and ideal switch is used to simulate arc extinction and re-strike. The control node of UCM resistor element is connected to external control blocks. These control blocks update the value of resistance in UCM time varying resistor element for every time step.

The block diagram shown in Figure 3.11 computes primary arc resistance value. In Figure 3.11 $|i|$ is fault current, g is primary arc conductance and r_p is primary arc resistance. The descriptions of blocks *k1* and *k2* are given in Equation 3.17 and Equation 3.18 respectively. Using the values given in Equation 3.19 and Equation 3.20, *k1* and *k2* are computed and used for modeling primary arc phenomenon in HYPERSIM.

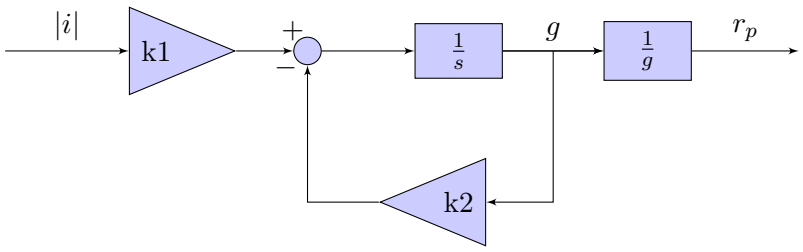

Figure 3.11: Primary Arc Block Diagram

$$k_1 = \frac{1}{\alpha V_p I_p} \tag{3.17}$$

$$k_2 = \frac{L_p}{\alpha I_p} \tag{3.18}$$

$$\alpha = 2.81 \times 10^{-5}, V_p = 15V/cm \tag{3.19}$$

$$L_p = 100cm \tag{3.20}$$

The block diagram shown in Figure 3.12 computes secondary arc resistance value. In Figure 3.12 $|i|$ is fault current, g is secondary arc conductance and r_s is secondary arc resistance. The descriptions of blocks *k3* and *k4* are given in Equation 3.21 and Equation 3.22 respectively. Using the values given in Equation 3.23, *k3* and *k4* are computed and used for modeling secondary arc phenomenon in HYPERSIM.

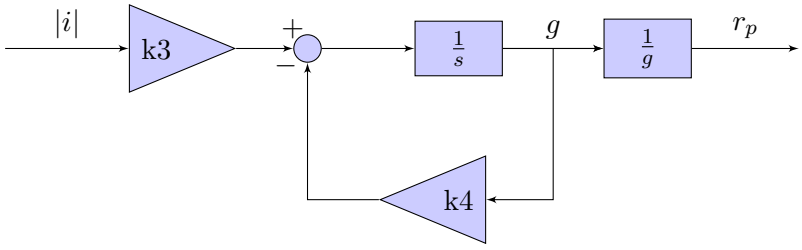

Figure 3.12: Secondary Arc Block Diagram

$$k_3 = \frac{1}{75\beta I_s} \tag{3.21}$$

$$k_4 = \frac{1}{\beta I_s^{1.4}} \tag{3.22}$$

$$\beta = 2.51 \times 10^{-3} \tag{3.23}$$

UCM time varying resistor element in HYPERSIM is updated with either primary arc resistance value or secondary arc resistance value depending on the status of series breaker. Flowchart shown in Figure 3.13 illustrates the condition to output primary arc resistance value or secondary arc resistance value to UCM time varying resistor element. The decision block in Figure 3.13 outputs primary arc resistance value until the series breaker opens and outputs secondary arc resistance value after series breaker opens.

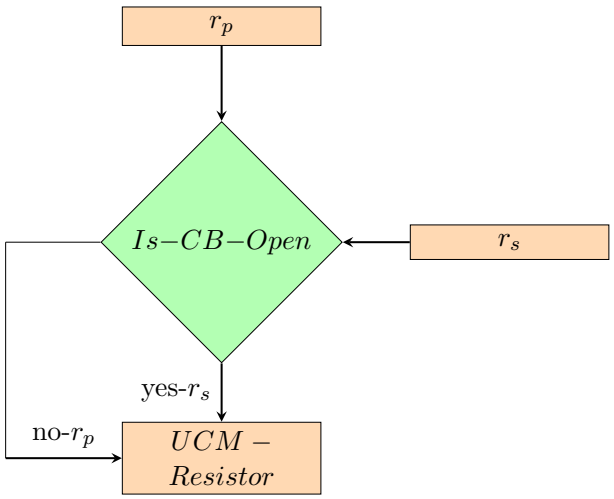

Figure 3.13: User Code Module Simulation Flowchart

The status (open/close) of control switch simulates arc extinction and re-strike phenomenon. Flowchart shown in Figure 3.14 illustrates the condition for opening or closing of the control switch to simulate arc extinction and arc re-strike respectively. Voltage impressed across the arc path is compared against re-ignition voltage. When the former is less than the later, control switch opens simulating arc extinction phenomenon and when the former is greater than the later, control switch closes simulating arc re-strike phenomenon. When the re-ignition voltage is permanently greater than recovery voltage, control switch remains open simulating permanent extinction of fault arc.

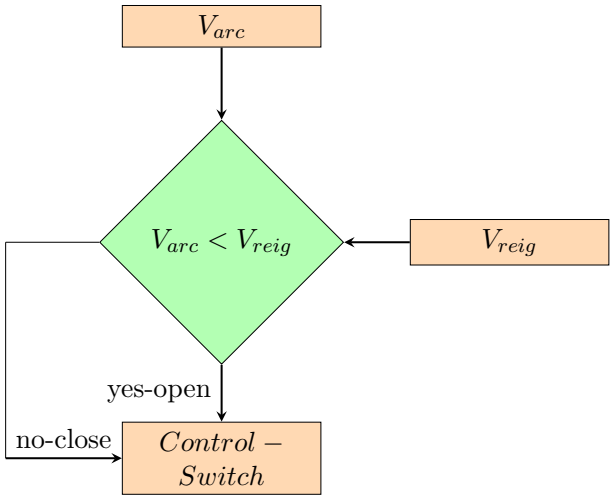

Figure 3.14: Switch Simulation Flowchart

3.4 Systematic Study Using Testview

In this section, automatic simulations of power system models using Testview software in HYPERSIM will be discussed. TestView is a simple powerful graphical interface designed for users to perform automatic test sequences, automatic data analysis and graph generation [47]. It can find automatically worst case. Testing relay for faults at different locations and different point of incidences is a tedious process to do manually. This process can be automated in HYPERSIM using Testview software. In Testview, scripts can be developed for applying different types of faults at different locations and different point of incidences. Also the software outputs result in excel format which can be used later.

Using the TestView software of HYPERSIM, a script is developed to apply faults automatically. User can define different times for switching breakers. The type of switching used is "Uniform Type" in which user defines minimum and maximum time in seconds with reference to t=0 of the POW for opening or closing at some random timings between specified minimum and maximum times.

3.5 Design of Protection Philosophy

The first part of this research work (section 3.2 to section 3.4) describes building of a power system model suitable for testing relays used in SPS applications. Now the second part of this research work deals with design of a protection scheme for series capacitor line to test the performance of SPS relays. In the following sections, Protection scheme description for series capacitor line, Relay test set-up description, and relay signals required for testing SPS relays will be discussed.

3.5.1 Protection Scheme

The topology of protection scheme for series capacitor line is shown in Figure 3.15. This topology includes two sets of two-line differential relays and two overcurrent relays. Each set is connected in closed loop to local bus and remote bus of series capacitor line model in HYPERSIM Real-Time Simulator. Line differential relays are tested for analyzing their performance for both temporary and permanent single-line to ground faults at local end, middle and remote end of series capacitor line. The topology also includes breaker configuration connected at each end of series capacitor line. This breaker configuration includes independent pole operated (IPO) breakers. For all temporary single-line to ground faults, single pole of these IPO breakers are opened by line differential relays and close signal is sent to these IPO breakers by overcurrent relays. The IPO breakers connected to local bus receive/send digital signals from/to relays connected at the local end of series capacitor line and IPO breakers connected to remote bus of series capacitor line receive/send digital signals from/to relays connected at the remote end of series capacitor line.

3.5.2 Relay Test Set-up

Figure 3.16 illustrates the overview of relay test set-up for testing relays using HYPERSIM Real-Time Simulator.

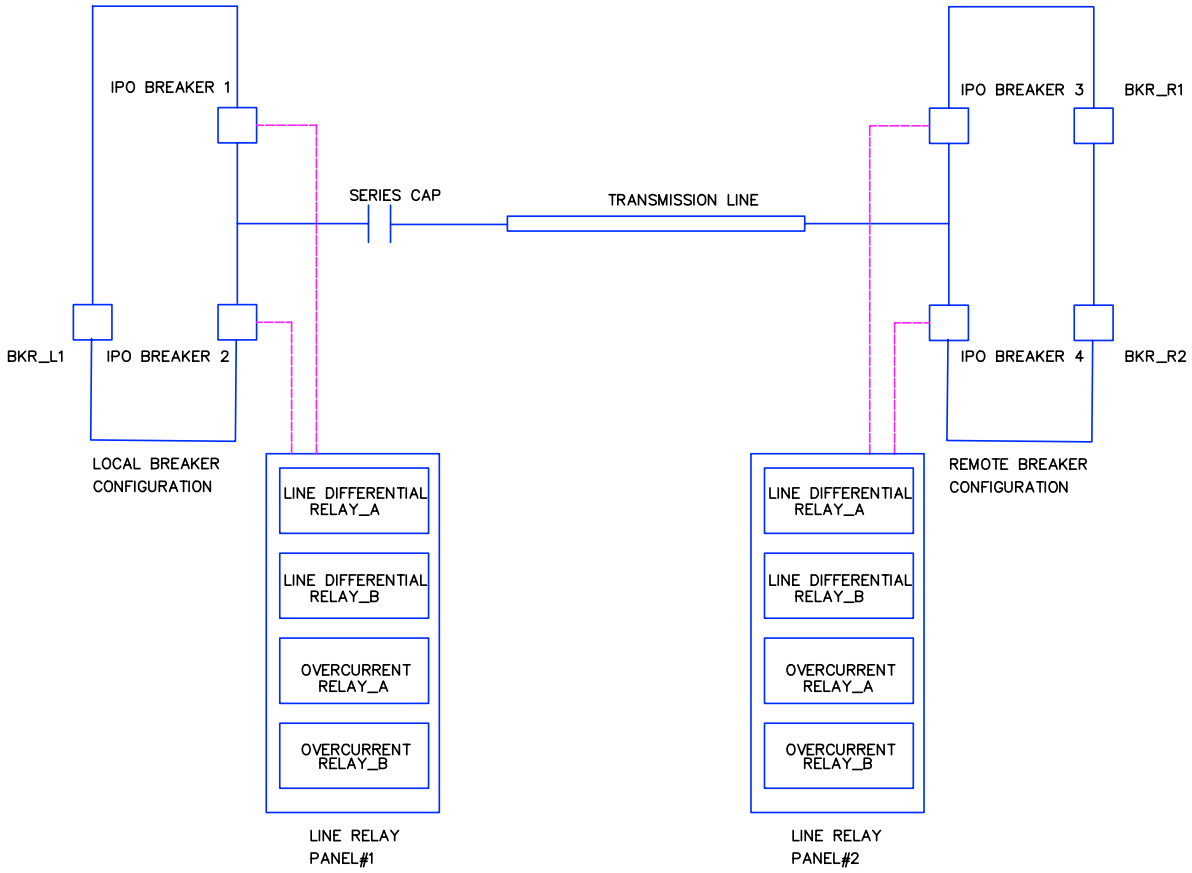

Figure 3.15: Relay Topology

The Relay test set up includes the following items:

- Workstation with HYPERSIM Software.
- Real-Time Simulator.
- Input/Output (I/O) Module.
- Amplifiers.
- Line Relay Panel 1 & 2.

The Real-Time Simulator with HYPERSIM software acts as a power system for performing digital simulations and testing relays. During simulations, the real-time simulator together with

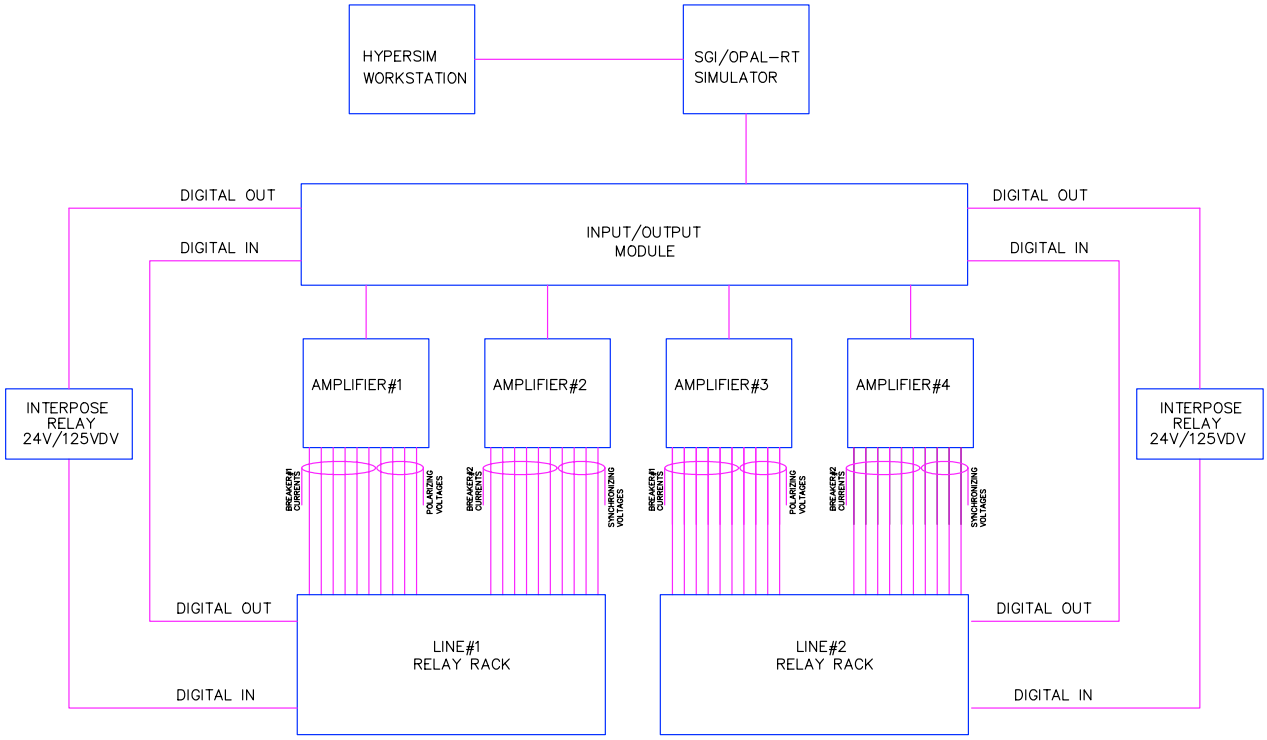

Figure 3.16: Relay Test Setup

I/O module outputs low level analogue signals to voltage and current amplifiers. These amplifiers are used to bring the simulators low level analogue signals up to values normally seen by the relays under testing. The simulator also has output contacts so that breaker status can be provided to the line differential and overcurrent relays at the auxiliary voltage level. To close the test loop, the trip signals from line differential relay output contacts and close signals from overcurrent relay output contacts are connected to the simulator.

3.5.3 Relay Design

All relays in line relay panels are interconnected with each other and with HYPERSIM I/O module. Each relay performs specific functions according to the design. Determination of these functions performed by each relay is illustrated in the following sections. Each line relay panel includes input

signals to the line relay panel from HYPERSIM, output signals from line relay panel to HYPERSIM and interface signals required for the protecting series capacitor line. These signals are determined for one-line relay panel and they are identical for other line relay panel.

Relay Inputs

Relay inputs include Breaker fail DTT send, Close status of independent pole operated (IPO) breaker model & series capacitor bypass breaker model in HYPERSIM and Series capacitor DTT receive.

- DTT Send Breaker 1 or Breaker 2 fail: This input contact initiates direct transfer trip (DTT) from line differential relays in the event of breaker failure.
- IPO Breaker Status: The status (open/close) of individual pole of IPO Breaker-1 & IPO Breaker-2 models in HYPERSIM is provided to both line differential relays and also to each IPO breakers respective overcurrent relays.
- Series Capacitor DTT Received: This input contact initiates series capacitor by-pass breaker close signal from line differential relays.
- Bypass Breaker Status: The status (open/close) of series capacitor by-pass breaker model in HYPERSIM is provided to each overcurrent relay in the line relay panel.
- DFR: All the relay inputs are provided to DFR for event recording.

Relay Outputs

Relay outputs include single pole and three pole trip signals, Breaker fail protection trip signal, pole disagreement trip signal, and close signal to IPO breaker models in HYPERSIM.

- Trips: Line differential relays send single pole trip and three pole trip signals to IPO Breaker-1 & IPO Breaker-2 models in HYPERSIM.

- Protection trips close by-pass breaker send DTC: In the event of fault, the series capacitor is to be by-passed. When fault occurs, close by-pass breaker signal is sent by each line differential relay to series capacitor by-pass breaker model in HYPERSIM.

- Breaker Fail Protection: In the event of fault, when a particular line differential relay fails to trip IPO breakers or fails to clear the fault, then a direct transfer trip signal is sent to all IPO breakers connected to series capacitor line.

- Pole Disagreement: Circuit Breaker can get different states even when there is no fault. This conditions is defined as Pole Disagreement. If there is a Pole Disagreement condition, overcurrent relays send trip signals to IPO breaker models in HYPERSIM.

- Breaker Close: Three phase close signal is sent by each overcurrent relay to its respective IPO Breaker model in HYPERSIM.

- DFR: All the relay output signals are provided to DFR for event recording.

Interface Signals

Relay interface signals include close input, re-close initiate, re-close drive to lockout and breaker failure.

- Close Input: A close signal is send by overcurrent relay to its respective IPO Breaker model in HYPERSIM only when its close input is initiated.

- Re-close initiate: In the event of fault, when the line differential relay trips IPO breaker model in HYPERSIM, overcurrent relay re-close initiate input is initiated.

- Re-close Drive to Lockout: If fault still persists when IPO Breaker models in HYPERSIM receive close input from overcurrent relays, then re-close drive to lockout is initiated and re-closing relay goes into lockout state.

- Breaker failure: Breaker failure condition is a situation in which breaker fails to trip or fails to clear the fault. Each overcurrent relay receives individual pole breaker failure input and three pole breaker failure input from each line differential relay and breaker fail input signal from adjacent overcurrent relay. Each individual pole and three pole breaker failure input initiates when IPO breaker fails to trip or fails to clear the fault.

Chapter 4

Test System

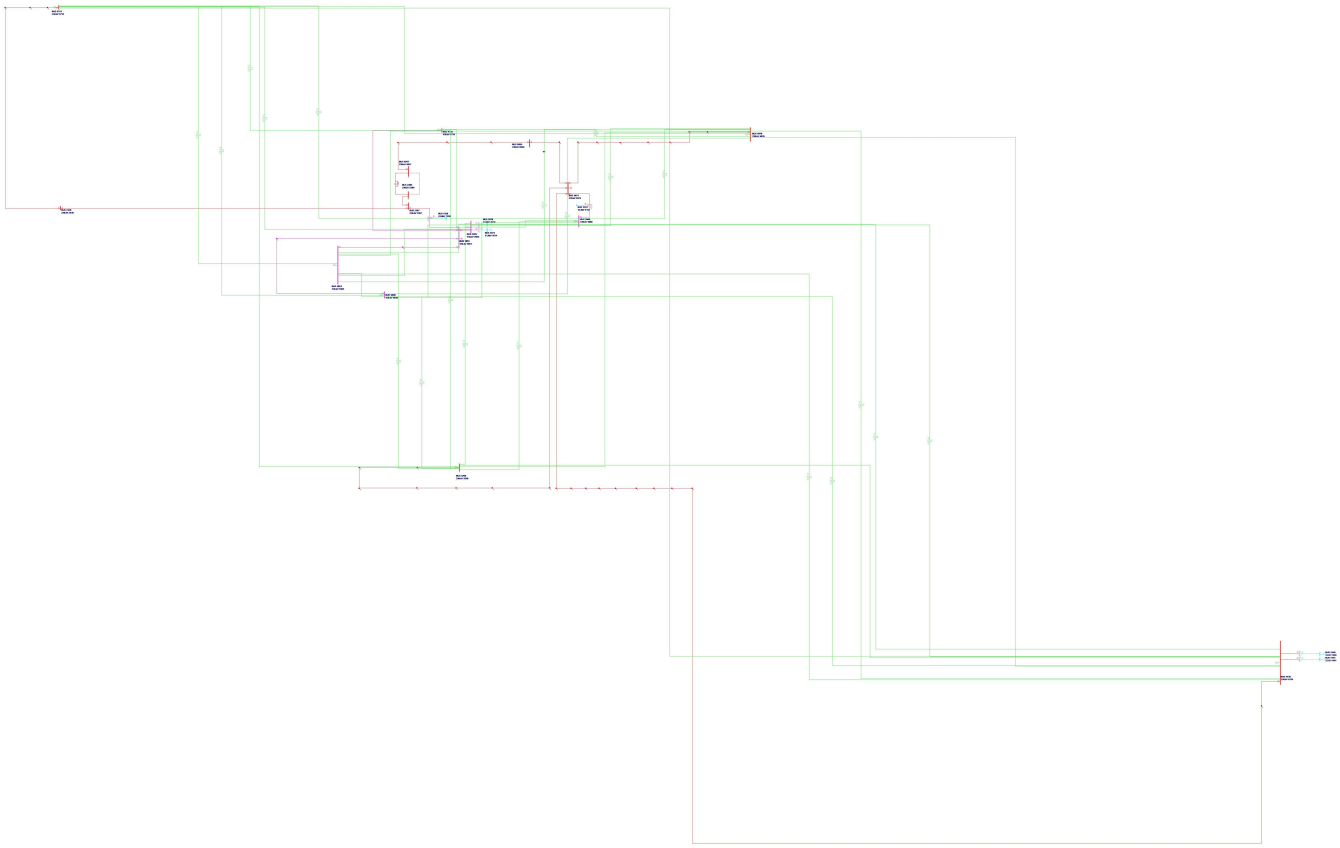

Figure 4.1: Test System

Figure 4.1 shows a Test System that is a portion extracted from an actual power system of an electric utility. Zoomed-in portion of an area within the test system is shown in Figure 4.2 to show the series-capacitor line where SPS relays will be connected to. Magenta and Red colored lines represent study area and Green colored lines represent equivalent system. Magenta colored lines represent 230kV system and Red colored lines represent 138kV System.

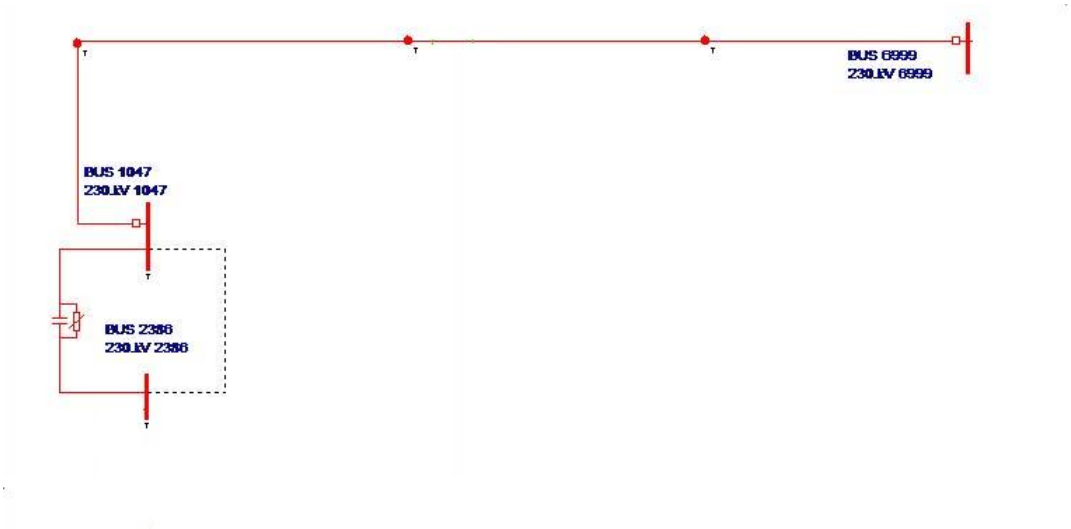

Figure 4.2: Main Study Area

The study area has a total of 11 transmission lines out of which 2 lines are modeled as frequency distributed parameter line, 6 lines are modeled as constant distributed parameter line and 3 lines are modeled as π line since the length of these lines is less than 15KM. Test system also consists of 4 generators with step-up transformers, 1 motor with step down power transformer, 2 three winding transformers, 1 series capacitor with MOV and by-pass capacitor, and 3 shunt capacitors. The equivalent area has 11 equivalent transformers and 9 equivalent π lines connected between boundary buses of study area. Equivalent area also consists of 9 equivalent voltage sources behind source impedance connected to boundary buses in study area. This chapter will give the information about the test system in the form that HYPERSIM can accept the data.

4.1 Transmission Lines

HYPERSIM accepts transmission line data file in .pun format (EMTP Generated Punch file). This file can be loaded directly into HYPERSIM control panel. This .pun file contains the T-line geometry data, Resistance, Reactance, Time constant, and length of line (KM) for each conductor. This .pun file when loaded into HYPERSIM control panel, distributed line parameters R, L, and C are calculated internally and the line is modeled. There are 8 lines that are modeled as either frequency-dependent or constant parameters lines. The data for these 8 lines are available in form of EMTP punch files as shown in Figure 4.3 to Figure 4.14 .

The data for the lines modeled as π lines in HYPERSIM is shown in Table 4.1. The resistance and reactance values are shown in per unit.

Table 4.1: π Line Data

From Bus	Voltage (KV)	To Bus	Voltage (KV)	R (p.u)	X (p.u)	L (p.u)
1054	138	5	138	0.003010	0.012610	3.3E-05
5	138	1051	138	0.000380	0.001650	4E-06
1054	138	1733	138	0.007990	0.036700	5.43E-05
3969	138	1054	138	0.004450	0.020470	0.0009739

```
C LINE DATA, FD,  3
C                                    49        51
C LINE-MODEL         FD-LINE   QREAL     LOG               .1        10
C METRIC
C   1    0  .08003 4       1 2.77368 -8.5344 12.4968  7.9248   30.48   180
C   2    0  .08003 4       1 2.77368       0 12.4968  7.9248   30.48   180
C   3    0  .08003 4       1 2.77368  8.5344 12.4968  7.9248   30.48   180
C   0    0  4.1197 4       1  .79248 -7.010416.8249615.30096
C   0    0  4.1197 4       1  .79248  7.010416.8249615.30096
C LINE LENGTH =  2.0000E+02  KM
C TRANSFORMATION MATRIX AT F =  3.1866E+03  HZ
C
-1                            1.                    -2 3
      18      3.9584471103501761035 7E+02
  3.4583553986654879 96D+02  2.9007359790860969 04D+03  5.2609103067000553 72D+01
 -2.9995219432196145 14D+03  1.9915274552963273 89D+03  3.1328812877601290 41D+01
  1.3086800456773919 45D+03  3.4617659900332392 91D+02  2.6902973699895123 90D+03
  1.2963073839995709 93D+04  6.8164694352564678 41D+04  8.2382033721634594 26D+04
  1.0909342477587201 57D+05  5.6657244297227892 09D+05  9.8583020500884344 80D+05
  1.0106837021021211 52D+07  2.3432165275012280 79D+07  1.1842020589335653 19D+08
  3.0673926145507383 72D-03  1.3420323561157943 00D+00  1.7145185771711981 55D+00
  2.0133682868176592 25D+00  2.0494339049062193 50D+00  2.9831466716784431 63D+00
  1.0590017191799100 62D+01  1.2737502871417705 21D+01  6.7226834592461869 99D+01
  3.0482428161007874 22D+02  8.3720390969683876 39D+02  1.4959592330654434 14D+03
  4.1159363616987584 46D+03  3.9096589492507126 12D+04  7.3869866493982131 94D+04
  3.8627702578793704 74D+05  1.8872479501276118 68D+06  9.8552330263042058 80D+06
      18      7.3926539095484566 3142E-04
  3.8890521288353820 80D-05  1.3166560040947430 24D-03  3.4827119812827415 75D-03
  1.9847934061315588 26D-03  1.7428280913511010 75D-02  4.2242203111550344 35D-02
  6.5726635158576085 52D-01  2.7050198094866630 96D+00  1.8045125337643774 80D+01
  1.3963876521302182 71D+02  6.4170959326613015 61D+01  1.7363693602993766 52D+01
  1.6192739571449550 34D+02  1.8694253597421707 13D+03  9.3347782196836662 48D+04
  5.3897634924437606 24D+05 -5.7575043499283507 47D+07  5.6940445367764063 18D+07
  1.9849702021162988 35D-02  1.8393955529181464 93D+00  2.4422641716462329 95D+00
  2.8221746667680354 11D+00  1.2238854349761417 95D+01  2.9405855901423606 72D+01
  1.1035940138050598 59D+02  2.2073188079643259 13D+02  5.8916373321652201 87D+02
  9.4807972261295606 13D+02  1.1381481834544265 44D+03  1.2095190155089824 20D+03
  2.4184604858127713 67D+03  8.7911829945820063 59D+03  3.0013122531359389 54D+04
  3.8671271051092087 87D+04  4.1618779651436194 84D+04  4.1660027313957674 78D+04
-2                            1.                    -2 3
```

Figure 4.3: Punchfile of Transmission Line Section BUS-1047 - BUS-6999 Part 1

```
     14      3.125591716372591690 74E+02
  3.333268641041751721D+02  1.906645527373382265D+03  3.016845969075052949D+02
 -5.180704109734518426D+01  4.137574529068651827D+02 -6.286152256030989065D+02
  1.213204761018982208D+04 -1.023671675672115271D+04  8.443062041960916986D+02
  2.974077256855056248D+02  4.835278663015885172D+02  1.829832389370962176D+02
  2.084513522321321943D+04  1.727545574228869751D+07
  2.942525142816906827D-03  1.257705787906041373D+00  1.613871816946121029D+00
  1.988884326429332106D+00  2.516695328747037497D+00  2.548893295378801493D+00
  1.151914720345485144D+01  1.210235577588838751D+01  1.294197240443434715D+01
  2.443958781077420639D+01  5.211027543598430611D+01  7.709933568919377933D+01
  6.989626616676497179D+03  2.921763664152513258D+06
     16      6.750004558494695355 85E-04
  4.491808274796823961D-05  2.437289408512994734D-03  4.619985321217452007D-03
  1.199488742216882169D-02  1.648330264705118176D-01  2.038664183409007435D+01
  8.815525123253783022D+02  9.488164567319732669D+03  4.723629148457432893D+04
  2.323636865519160929D+05  5.304886848028606037D+05  3.762550220672306061D+10
 -7.561995653735737610D+10  3.799363602470868683D+10 -2.778028830475386349D+05
  2.756298577780050109D+05
  1.984667866497095978D-02  1.744248973287775950D+00  3.297252772612280225D+00
  4.342266616665459544D+00  2.983887837688948963D+01  1.828602703412561823D+03
  3.067984713020085110D+04  9.048250320207020559D+04  1.460268434736945492D+05
  2.233830863429179008D+05  3.151882399168554111D+05  5.192165627044717548D+05
  5.197308996243741713D+05  5.202457460474126274D+05  5.419562064100171439D+06
  5.424930692644581199D+06
-3                           1.                    -2 3
     17      2.768601966018080702 27E+02
  3.238359461394135224D+02  1.817411586543497606D+03  1.695149658220408639D+02
  1.900036587824800449D+01  3.003770736125484291D+02 -4.211348835707377134D+02
  2.907377583235328075D+03  1.016535369255186670D+05 -1.019860148905655806D+05
  2.150715130054545341D+02  5.143831972637475758D+01  2.776211140420326160D+02
  3.344031038477415336D+02  2.827239820433609339D+02  2.274909635235861174D+02
  1.807257837010769776D+02  2.855510872395917090D+02
  2.860077327771865137D-03  1.261034621251599264D+00  1.606711594721633940D+00
  2.014397912265156521D+00  2.615206478943999713D+00  2.728345930170970490D+00
  1.099732896595146947D+01  1.271471023082610152D+01  1.271938339441311605D+01
  1.546677265719338656D+01  1.759370209145505370D+01  2.620979809302523122D+01
  4.304718166197337581D+01  6.725828798215215443D+01  9.975291827109188603D+01
  1.499981184242850532D+02  2.336387977223178609D+02
```

Figure 4.4: Punchfile of Transmission Line Section BUS-1047 - BUS-6999 Part 2

```
      17      6.676806249991263774 58E-04
  4.772614644183157854D-05  2.238499758248318431D-03  3.368241183350828560D-03
  1.880664913351099560D-02  1.949181641008368784D-02  3.402003346841440262D-02
  4.183371826030564080D+03  1.855558449239449692D+04  7.934611636286627618D+04
  3.556787889066339121D+05  1.457967602872346761D+06  4.398762096438303590D+06
  4.019370080230001221D+11 -8.066000591310991211D+11  4.046567527261318359D+11
 -1.946246936479042983D+06  1.930135249951983104D+06
  1.984526968129588301D-02  1.736648719046103739D+00  2.625765820713696019D+00
  7.144030927432226896D+00  7.820100331024580242D+00  1.348176868452481614D+01
  2.888258197078077937D+05  4.995107922241432825D+05  7.829726442378211068D+05
  1.188108292353657074D+06  1.742750070720160613D+06  2.517604822448275052D+06
  4.192185340092204511D+06  4.196338126906732097D+06  4.200495027479812503D+06
  4.503234250940705091D+07  4.507695163401123136D+07
C   Q MATRIX BY ROWS (IMAGINARY PART = 0)
  0.58701475 -0.70710678  0.41721038
  0.00000000  0.00000000  0.00000000
  0.55745449  0.00000000 -0.80736305
  0.00000000  0.00000000  0.00000000
  0.58701475  0.70710678  0.41721038
  0.00000000  0.00000000  0.00000000
```

Figure 4.5: Punchfile of Transmission Line Section BUS-1047 - BUS-6999 Part 3

```
C LINE-MODEL         CP-LINE   QREAL
C METRIC
C   1    0  .09165 4       1 2.35458 -4.419613.59408 9.02208       0     0       1
C   2    0  .09165 4       0 2.35458       013.59408 9.02208       0     0       1
C   3    0  .09165 4       1 2.35458  4.419613.59408 9.02208       0     0       1
C   0    0  4.1197 4       1  .79248 -2.895621.1226419.59864
C   0    0  4.1197 4       1  .79248  2.895621.1226419.59864
C UNTRANSPOSED MODELLING. PARAMETERS AT F =  5.0106E+03  HZ
$VINTAGE,1
C R' IN OHMS/KM, ZC IN OHMS, TAU IN SEC, LENGTH IN KM
-1                        6.20488E+00 6.56154E+02 5.52173E-05-1.44841E+01 2 03
-2                        9.22229E-02 3.41453E+02 4.83200E-05-1.44841E+01 2 03
-3                        1.19061E-01 3.94159E+02 4.85982E-05-1.44841E+01 2 03
$VINTAGE,0
  0.59585492 -0.40902575 -0.70710678
  0.00000000  0.00000000  0.00000000
  0.53842766  0.81571596  0.00000000
  0.00000000  0.00000000  0.00000000
  0.59585492 -0.40902575  0.70710678
  0.00000000  0.00000000  0.00000000
```

Figure 4.6: Punchfile of Transmission Line Section BUS-1054 - BUS-1733

```
C LINE-MODEL         CP-LINE   QREAL
C METRIC
C   1    0   .0671 4       1 3.03784   3.048 24.0792 19.5072   30.48   180       2
C   2    0   .0671 4       1 3.03784   3.048  19.812   15.24   30.48   180       2
C   3    0   .0671 4       1 3.03784   3.048 15.5448 10.9728   30.48   180       2
C   0    0 1.15979 4       1 1.09982       0   30.48  28.956
C UNTRANSPOSED MODELLING. PARAMETERS AT F =  3.2773E+03  HZ
$VINTAGE,1
C R' IN OHMS/KM, ZC IN OHMS, TAU IN SEC, LENGTH IN KM
-1                          4.58966E+00 6.19052E+02 1.07725E-04-2.77772E+01 2 03
-2                          3.37724E-02 2.34495E+02 9.26544E-05-2.77772E+01 2 03
-3                          5.19390E-02 2.89501E+02 9.27929E-05-2.77772E+01 2 03
$VINTAGE,0
  0.44217667 -0.49371729  0.69708154
  0.00000000  0.00000000  0.00000000
  0.48861951  0.80485271  0.16658734
  0.00000000  0.00000000  0.00000000
  0.75165644 -0.32873387 -0.69682227
  0.00000000  0.00000000  0.00000000
```

Figure 4.7: Punchfile of Transmission Line Section BUS-1071 - BUS-1070

```
C LINE-MODEL         CP-LINE   QREAL
C METRIC
C   1    0  .09165 4       1 2.35458  -3.04814.38656 9.81456   30.48   180       2
C   2    0  .09165 4       1 2.35458   3.04814.38656 9.81456   30.48   180       2
C   3    0  .09165 4       1 2.35458   3.04815.9715211.39952   30.48   180       2
C   0    0  4.1197 4       1  .79248       019.5986418.07464
C UNTRANSPOSED MODELLING. PARAMETERS AT F =  3.1881E+03  HZ
$VINTAGE,1
C R' IN OHMS/KM, ZC IN OHMS, TAU IN SEC, LENGTH IN KM
-1                          5.06929E+00 6.09714E+02 1.31713E-04-3.35547E+01 2 03
-2                          5.34925E-02 3.03959E+02 1.12405E-04-3.35547E+01 2 03
-3                          4.93599E-02 1.97157E+02 1.11944E-04-3.35547E+01 2 03
$VINTAGE,0
  0.68938361 -0.80847136 -0.01405863
  0.00000000  0.00000000  0.00000000
  0.55958418  0.45965992 -0.67754298
  0.00000000  0.00000000  0.00000000
  0.45970695  0.36751723  0.73532083
  0.00000000  0.00000000  0.00000000
```

Figure 4.8: Punchfile of Transmission Line Section BUS-1071 - BUS-1139

```
C LINE-MODEL         CP-LINE   QREAL
C METRIC
C   1    0   .0671 4       1 3.03784 -5.4864 14.3256  9.7536   30.48   180       2
C   2    0   .0671 4       1 3.03784       0 14.3256  9.7536   30.48   180       2
C   3    0   .0671 4       1 3.03784  5.4864 14.3256  9.7536   30.48   180       2
C   0    0  4.1197 4       1  .79248 -3.9624 18.8976 17.3736
C   0    0  4.1197 4       1  .79248  3.9624 18.8976 17.3736
C UNTRANSPOSED MODELLING. PARAMETERS AT F =  3.1906E+03  HZ
$VINTAGE,1
C R' IN OHMS/KM, ZC IN OHMS, TAU IN SEC, LENGTH IN KM
-1                        3.92563E+00 5.12845E+02 3.98296E-04-1.02451E+02 2 03
-2                        3.46899E-02 2.49160E+02 3.41854E-04-1.02451E+02 2 03
-3                        6.88316E-02 2.99430E+02 3.45113E-04-1.02451E+02 2 03
$VINTAGE,0
  0.60244209 -0.40679666 -0.70710678
  0.00000000  0.00000000  0.00000000
  0.52357038  0.81794413  0.00000000
  0.00000000  0.00000000  0.00000000
  0.60244209 -0.40679666  0.70710678
  0.00000000  0.00000000  0.00000000
```

Figure 4.9: Punchfile of Transmission Line Section BUS-1071 - BUS-3299

```
C LINE-MODEL         CP-LINE   QREAL
C METRIC
C   1    0  .16857 4       1 1.73736 -5.486416.8249612.25296   30.48   180       2
C   2    0  .16857 4       1 1.73736       016.8249612.25296   30.48   180       2
C   3    0  .16857 4       1 1.73736  5.486416.8249612.25296   30.48   180       2
C   0    0 1.15979 4       1 1.09982 -3.962421.1226419.59864
C   0    0 1.15979 4       1 1.09982  3.962421.1226419.59864
C UNTRANSPOSED MODELLING. PARAMETERS AT F =  3.2480E+03  HZ
$VINTAGE,1
C R' IN OHMS/KM, ZC IN OHMS, TAU IN SEC, LENGTH IN KM
-1                        3.00437E+00 5.36721E+02 7.41617E-05-1.96339E+01 2 03
-2                        8.48603E-02 2.66080E+02 6.55015E-05-1.96339E+01 2 03
-3                        1.04966E-01 3.16792E+02 6.59034E-05-1.96339E+01 2 03
$VINTAGE,0
  0.60399415 -0.40435066 -0.70710678
  0.00000000  0.00000000  0.00000000
  0.51997151  0.82036417  0.00000000
  0.00000000  0.00000000  0.00000000
  0.60399415 -0.40435066  0.70710678
  0.00000000  0.00000000  0.00000000
```

Figure 4.10: Punchfile of Transmission Line Section BUS-2138 - BUS-5711

```
C LINE-MODEL         CP-LINE   QREAL
C METRIC
C   1    0  .16857 4       1 1.73736 -5.486416.8249612.25296   30.48   180       2
C   2    0  .16857 4       1 1.73736       016.8249612.25296   30.48   180       2
C   3    0  .16857 4       1 1.73736  5.486416.8249612.25296   30.48   180       2
C   0    0  4.1197 4       1  .79248 -3.962421.1226419.59864
C   0    0  4.1197 4       1  .79248  3.962421.1226419.59864
C UNTRANSPOSED MODELLING. PARAMETERS AT F =  3.2480E+03  HZ
$VINTAGE,1
C R' IN OHMS/KM, ZC IN OHMS, TAU IN SEC, LENGTH IN KM
-1                        3.89200E+00 5.39669E+02 1.00325E-04-2.65380E+01 2 03
-2                        8.54878E-02 2.66049E+02 8.85346E-05-2.65380E+01 2 03
-3                        1.19928E-01 3.16913E+02 8.90844E-05-2.65380E+01 2 03
$VINTAGE,0
  0.60336323 -0.40503536 -0.70710678
  0.00000000  0.00000000  0.00000000
  0.52144546  0.81969057  0.00000000
  0.00000000  0.00000000  0.00000000
  0.60336323 -0.40503536  0.70710678
  0.00000000  0.00000000  0.00000000
```

Figure 4.11: Punchfile of Transmission Line Section BUS-2387 - BUS-2138

```
C LINE DATA, FD,  3
C                                    45        51
C LINE-MODEL         FD-LINE   QREAL     LOG               .1        10
C METRIC
C   1    0  .08003 4       1 2.77368 -5.4864  16.764  12.192   30.48   180
C   2    0  .08003 4       1 2.77368       0  16.764  12.192   30.48   180
C   3    0  .08003 4       1 2.77368  5.4864  16.764  12.192   30.48   180
C   0    0 1.15979 4       1 1.09982 -3.962421.1226419.59864
C   0    0 1.15979 4       1 1.09982  3.962421.1226419.59864
C LINE LENGTH =  2.0000E+02  KM
C TRANSFORMATION MATRIX AT F =  3.2467E+03  HZ
C
-1                            1.                    -2 3
      17      4.6276983701689283634 6E+02
  3.588297213000404895D+02  1.234268858351346898D+04 -1.211216082381471278D+04
  1.886311315848947288D+03  1.358151951681313676D+02  1.843515523735833995D+03
  5.821378042732459335D+02  1.978593619164194388D+04  5.812103389859105846D+03
  2.710430101697738064D+04  1.827513582435597709D+04  2.435516685830047572D+04
  2.390051905816885119D+05  8.163501315614135237D+05  2.920249036595042795D+06
  8.982209837354730815D+06  7.569164098876936734D+07
  3.197558801033473577D-03  1.539327253106812066D+00  1.682626308643832891D+00
  1.862776873885295892D+00  3.119862418203416699D+00  1.845380646696493443D+01
  2.012533217377021444D+01  1.859045234439035426D+02  2.023236718642551466D+02
  4.161488484154673415D+02  7.121399342739274516D+02  1.718542670909992694D+03
  1.558782094455411061D+04  5.495505513096057257D+04  2.021039316760178481D+05
  6.484158822511786129D+05  5.585686665456472896D+06
```

Figure 4.12: Punchfile of Transmission Line Section BUS-6999 - BUS-1071 Part 1

```
     19      7.0524528883839435 1894E-04
  3.587611164093538118D-05  1.040987124982439707D-03  1.423845888243098186D-03
  3.583591424950899242D-03  1.383527012305535778D-02  2.687026893578304057D-02
  5.646330605590685892D-01  2.891917487651767704D+00  1.724294361146593246D+01
 -1.331031685598574654D+00  3.289647051161980329D+01  2.920934086954123927D+02
  9.849090551402617848D+02  2.947180155689940875D+03  3.844167133990861203D+03
  3.127837328324187183D+04  2.584528139885620028D+07 -2.593007952822408453D+07
  4.539909460838253290D+04
  1.985121348874332309D-02  1.650567257145291844D+00  2.259064089384510865D+00
  2.862041160943454621D+00  1.009938480221625326D+01  2.126959175195089813D+01
  1.068405450200238107D+02  2.269245983475600497D+02  2.801741572027170832D+02
  2.894223516651977093D+02  8.722289318089367498D+02  5.184956435064764264D+03
  8.327264094861953708D+03  1.465689844682732291D+04  1.833880794611891906D+04
  3.489513857719091175D+04  5.117245541660551680D+04  5.122314694879723538D+04
  8.189087287786658271D+04
-2                            1.                     -2 3
     14      2.5201257453445793 9990E+02
  3.162696286650091224D+02  1.678029206770588871D+03  3.249521277219903368D+02
  1.423629931359721468D+02 -2.952543669771623627D+02 -5.736067353880980590D+01
  2.782567400782729237D+03  9.475210561544979555D+02 -9.308489234707145670D+02
  5.411938355825004976D+01  8.637906058758029815D+01  2.590985598422423095D+02
  3.383592291241468502D+02  5.624185680719493803D+02
  2.798319771264327210D-03  1.263648777219529062D+00  1.650582907438595370D+00
  2.114341296944423743D+00  2.476592360827428063D+00  2.763023510143975070D+00
  1.170354435136610860D+01  1.348238376217778622D+01  1.421723810509717367D+01
  1.620766965878715382D+01  1.882174212677081115D+01  2.753093084416484260D+01
  4.593204328468901565D+01  7.241589872464759026D+01
     16      6.6712575422519 1599373E-04
  5.004221062710410942D-05  1.917693358421415422D-03  1.951275832153553458D-03
  1.078669345010387429D-02  1.584379081231391748D-02  2.827148643624591284D-02
  1.430613928205734520D-01  1.863348360775870560D+03  3.441486666654784494D+04
  1.057927376562585123D+05  5.612569609172971686D+05  1.195378341601126827D+06
  3.048824282012185082D+06  1.664178756761551369D+06  1.296091164578723431D+09
 -1.282225472762602568D+09
  1.984410747132010419D-02  1.673943206721950405D+00  1.771750467705296872D+00
  4.797273675217018862D+00  7.121088760518894389D+00  1.270154537495968405D+01
  3.232549133524074847D+01  4.045853074899736675D+05  1.628019171891246689D+06
  2.552269387413735967D+06  5.447464598451180384D+06  8.058700426781466231D+06
  1.593491820129632205D+07  2.085701749008598551D+07  4.853858632417216152D+07
  4.873912919267771393D+07
-3                            1.                     -2 3
```

Figure 4.13: Punchfile of Transmission Line Section BUS-6999 - BUS-1071 Part 2

```
     14      3.0101734229495434 6471E+02
  3.306044669278208517D+02  1.84863323584184 6727D+03  3.67036342384437 4324D+02
  2.031173698461694599D+01 -2.62744467868512 6291D+02 -6.55349727070807 5462D+01
  2.239039060900378536D+04 -2.04057324795872 7370D+04  8.51382808971592 4534D+02
  2.910389952480943521D+02  3.38243979048711 0258D+02  3.07646546154392 6949D+02
  2.700143618954374460D+02  6.30813832294948 3991D+05
  2.917444780175141878D-03  1.25873708890584 9566D+00  1.63048322420607 0947D+00
  2.035337744759834422D+00  2.39270815011668 3807D+00  2.63296858409366 0525D+00
  1.209649918274399560D+01  1.24230007211748 4611D+01  1.33937261921806 0478D+01
  2.498728693169366011D+01  4.16154997535262 7229D+01  6.61706718565623 7882D+01
  1.084001302953773802D+02  2.17584802786388 5509D+05
     16      6.6810182540187872 8072E-04
  4.574259588608474848D-05  2.39888624493042 843D-03  2.44566035234133 3301D-03
  1.729582783810684060D-02  2.84932546594086 6914D-02  5.18318219300039 2818D-02
  1.946385585751149847D+02  3.65973258021519 3138D+03  1.83524397381074 5229D+04
  3.729060147170955315D+04  1.31140866265756 8930D+05  1.76618009696927 6667D+06
  9.119066785938014984D+08 -9.23522117392466 1875D+08  6.88705079939705 2526D+08
 -6.790464596191515923D+08
  1.984626501589444383D-02  1.81185809235832 6067D+00  1.92670796595238 2695D+00
  6.670538650977436035D+00  1.10776971686560 4259D+01  2.02735302810688 0473D+01
  1.793341691201518188D+04  1.15759742729879 0717D+05  1.98945188780080 6435D+05
  2.532170202276949422D+05  3.99901085094478 7962D+05  8.35027210698457 9004D+05
  1.303806430751867592D+06  1.30509798389541 1016D+06  1.59665404072442 4412D+06
  1.598235689270412549D+06
C   Q MATRIX BY ROWS (IMAGINARY PART = 0)
  0.60511992 -0.40449644 -0.70710678
  0.00000000  0.00000000  0.00000000
  0.51734928  0.82022096  0.00000000
  0.00000000  0.00000000  0.00000000
  0.60511992 -0.40449644  0.70710678
  0.00000000  0.00000000  0.00000000
```

Figure 4.14: Punchfile of Transmission Line Section BUS-6999 - BUS-1071 Part 3

4.2 Generators

All the generators available in study area are modeled as voltage sources behind impedance's in HYPERSIM. The information about these generators is obtained from ASPEN/PSSE model and the data for HYPERSIM voltage source elements, in the form that HYPERSIM accepts is shown in Table 4.2. The voltage, resistance, reactance and inductance values in Table 4.2 are in per unit.

Table 4.2: Voltage Sources Data

Bus	Bus Name	Base KV	V (p.u)	Angle(deg)	Base MVA	R (p.u)	X (p.u)	L (p.u)
1140	BUS 1140	24	1	0	680	0.0038	0.16	0.000424628
1141	BUS 1141	22	1	0	583.2	0.0039	0.17	0.000451168
3970	BUS 3970	13.8	1	0	101.8	0.00303	0.117	0.00031051
3971	BUS 3971	13.8	1	0	101.8	0.00303	0.117	0.00031051

4.3 Two-Winding Transformers

Study area contains step-up transformers connected to generators. The information about these step-up transformers is obtained from ASPEN/PSSE model. Table 4.3 shows the information available in PSSE about these transformers. Resistance and Reactance values in the table are in per unit. All transformers are star connected high voltage winding and delta connected low voltage winding type.

Table 4.3: Two-Winding Transformer Data

From Bus	Primary-KV	To Bus	Secondary-KV	R (p.u)	X (p.u)	Wdg-1 Ratio	Wdg-2 Ratio
1140	24	1139	230	0.0004	0.0167	1	0.975
1141	22	1139	230	0.00052	0.02037	1	0.95
3970	13.8	3969	138	0.00237	0.08997	1	1
3971	13.8	3969	138	0.00237	0.08997	1	1

In HYPERSIM, it is required to enter data for each winding individually. According to [48], the winding reactance of an individual winding is given by Equation 4.1.

$$X_1 = X_2/K^2 = X_{01}/2. \tag{4.1}$$

Where K is turns ratio, X_{01} total equivalent reactance and X_1, X_2 are primary, secondary windings individual reactances. Above statement is based on a assumption that the transformers are well designed. Table 4.4 shows the data for these transformers in the form that HYPERSIM accepts. Subscript p represents primary side and subscript s represents secondary side values.

Table 4.4: Two-Winding Transformer Data (HYPERSIM)

From Bus	To Bus	R_p (p.u)	L_p (p.u)	R_s (p.u)	L_s(p.u)
1140	1139	0.0002	2.215E-05	0.0002	2.215E-05
1141	1139	0.00026	2.70E-05	0.0026	2.70E-05
3970	3969	0.00118	1.193265E-04	0.00118	1.193265E-04
3971	3969	0.00118	1.193265E-04	0.00118	1.193265E-04

4.4 Three-Winding Transformers

Study area also contains 2 three-winding transformers. The information about these transformers is available in datasheets. From the datasheets, only the data required for BC-TRAN element in EMTP is extracted. The extracted data is shown in Table 4.5 to Table 4.10. Figure 4.15 and Figure 4.16 are .pun files of three-winding transformers. These .pun files are generated by EMTP BC-TRAN element. The resistance and reactance values from these .pun format files are entered into HYPERSIM's three-winding transformer element control panel.

Table 4.5: Bus 1071 & Bus 2387 Three-Winding Transformer Excitation Data

Bus	Windings per core leg	Rated Frequency (Hz)
1071	3	60
2387	3	60

Table 4.6: Bus 1071 & Bus 2387 Three-Winding Transformer Positive & Zero Sequence Data

Bus	Exciting Current (%)	Three-Phase Power Rating (MVA)	Excitation Loss (kW)
1071	0.56	300	137.879
2387	100	250	31.7

Table 4.7: Bus 1071 Three-Winding Transformer Winding Data

Winding	Voltage (kV)	R(Ω)
1	128.752887	0.26951
2	79.676644	0.661556
3	13.8	0.05304

Table 4.8: Bus 2387 Three-Winding Transformer Winding Data

Winding	Voltage (kV)	R(Ω)
1	132.794457	0.37434
2	79.6766744	0.05388
3	13.8	0.0035562

Table 4.9: Bus 1071 Three-Winding Transformer Short Circuit Data

Winding Pair	P(KW)	Z Pos(%)	S Pos rating (MVA)	Z Zero(%)	S Zero rating (MVA)
1,2	145.422	3.82	180	3.82	180
1,3	38.548	3.14	29.6	3.14	29.6
2,3	43.695	2.4	29.6	2.4	29.6

Table 4.10: Bus 2387 Three-Winding Transformer Short Circuit Data

Winding Pair	P(KW)	Z Pos(%)	S Pos rating (MVA)	Z Zero(%)	S Zero rating (MVA)
1,2	346.21	10.96	250	10.96	250
1,3	118.28	17.3	50	17.3	50
2,3	117.42	12.96	50	12.96	50

```
C BCTRAN BRANCH DATA - RESISTANCE MATRIX (OHMS) AND REACTANCE MATRIX (OHMS) AT
C F= 60.00
$VINTAGE, 1
 1HAK   HAM              0.2695100000E+000.2970115712E+05
 2XAK   XAM              0.0000000000E+000.1837896068E+05
                         0.6615600000E+000.1137686971E+05
 3YAK   YAM              0.0000000000E+000.3183502666E+04
                         0.0000000000E+000.1970702317E+04
                         0.5304000000E-010.3418275742E+03
 4HBK   HBM              0.0000000000E+000.0000000000E+00
                         0.0000000000E+000.0000000000E+00
                         0.0000000000E+000.0000000000E+00
                         0.2695100000E+000.2970115712E+05
 5XBK   XBM              0.0000000000E+000.0000000000E+00
                         0.0000000000E+000.0000000000E+00
                         0.0000000000E+000.0000000000E+00
                         0.0000000000E+000.1837896068E+05
                         0.6615600000E+000.1137686971E+05
 6YBK   YBM              0.0000000000E+000.0000000000E+00
                         0.0000000000E+000.0000000000E+00
                         0.0000000000E+000.0000000000E+00
                         0.0000000000E+000.3183502666E+04
                         0.0000000000E+000.1970702317E+04
                         0.5304000000E-010.3418275742E+03
 7HCK   HCM              0.0000000000E+000.0000000000E+00
                         0.0000000000E+000.0000000000E+00
                         0.0000000000E+000.0000000000E+00
                         0.0000000000E+000.0000000000E+00
                         0.0000000000E+000.0000000000E+00
                         0.0000000000E+000.0000000000E+00
                         0.2695100000E+000.2970115712E+05
 8XCK   XCM              0.0000000000E+000.0000000000E+00
                         0.0000000000E+000.0000000000E+00
                         0.0000000000E+000.0000000000E+00
                         0.0000000000E+000.0000000000E+00
                         0.0000000000E+000.0000000000E+00
                         0.0000000000E+000.0000000000E+00
                         0.0000000000E+000.1837896068E+05
                         0.6615600000E+000.1137686971E+05
 9YCK   YCM              0.0000000000E+000.0000000000E+00
                         0.0000000000E+000.0000000000E+00
                         0.0000000000E+000.0000000000E+00
                         0.0000000000E+000.0000000000E+00
                         0.0000000000E+000.0000000000E+00
                         0.0000000000E+000.0000000000E+00
                         0.0000000000E+000.3183502666E+04
                         0.0000000000E+000.1970702317E+04
                         0.5304000000E-010.3418275742E+03
$VINTAGE, 0
```

Figure 4.15: EMTP Punch file for BC-Tran Three Winding Transformer At Bus-1071

```
C BCTRAN BRANCH DATA - RESISTANCE MATRIX (OHMS) AND REACTANCE MATRIX (OHMS) AT
C F= 60.00
$VINTAGE, 1
 1HAK   HAM               0.3743400000E-010.2383800479E+03
 2XAK   XAM               0.0000000000E+000.1324506961E+03
                          0.5388000000E-010.8115746532E+02
 3YAK   YAM               0.0000000000E+000.1825937157E+02
                          0.0000000000E+000.1176262280E+02
                          0.3556200000E-020.2921039889E+01
 4HBK   HBM               0.0000000000E+000.0000000000E+00
                          0.0000000000E+000.0000000000E+00
                          0.0000000000E+000.0000000000E+00
                          0.3743400000E-010.2383800479E+03
 5XBK   XBM               0.0000000000E+000.0000000000E+00
                          0.0000000000E+000.0000000000E+00
                          0.0000000000E+000.0000000000E+00
                          0.0000000000E+000.1324506961E+03
                          0.5388000000E-010.8115746532E+02
 6YBK   YBM               0.0000000000E+000.0000000000E+00
                          0.0000000000E+000.0000000000E+00
                          0.0000000000E+000.0000000000E+00
                          0.0000000000E+000.1825937157E+02
                          0.0000000000E+000.1176262280E+02
                          0.3556200000E-020.2921039889E+01
 7HCK   HCM               0.0000000000E+000.0000000000E+00
                          0.0000000000E+000.0000000000E+00
                          0.0000000000E+000.0000000000E+00
                          0.0000000000E+000.0000000000E+00
                          0.0000000000E+000.0000000000E+00
                          0.0000000000E+000.0000000000E+00
                          0.3743400000E-010.2383800479E+03
 8XCK   XCM               0.0000000000E+000.0000000000E+00
                          0.0000000000E+000.0000000000E+00
                          0.0000000000E+000.0000000000E+00
                          0.0000000000E+000.0000000000E+00
                          0.0000000000E+000.0000000000E+00
                          0.0000000000E+000.0000000000E+00
                          0.0000000000E+000.1324506961E+03
                          0.5388000000E-010.8115746532E+02
 9YCK   YCM               0.0000000000E+000.0000000000E+00
                          0.0000000000E+000.0000000000E+00
                          0.0000000000E+000.0000000000E+00
                          0.0000000000E+000.0000000000E+00
                          0.0000000000E+000.0000000000E+00
                          0.0000000000E+000.0000000000E+00
                          0.0000000000E+000.1825937157E+02
                          0.0000000000E+000.1176262280E+02
                          0.3556200000E-020.2921039889E+01
$VINTAGE, 0
```

Figure 4.16: EMTP Punch file for BC-Tran Three Winding Transformer At Bus-2387

4.5 Load: Induction Motor with Power Transformer

Study area also contains induction motor with step-down transformer as load element. The information about induction motor is available in a data sheet. The information required for induction motor element in HYPERSIM is extracted and shown in Table 4.11 and Table 4.12. The induction motor general data from Table 4.11 can be entered directly into HYPERSIM induction motor element. The Induction motor performance data from Table 4.12 was used to calculate the induction motor parameters i.e., resistance and reactances.

Table 4.11: Induction Motor General Data

Power (MW)	Synchronous Speed(RPM)	Poles	Rotor Type	Voltae (V)	Phases	Frequency (Hz)
4.9236	1800	4	1-Cage Rotor	6600	3	60

Table 4.12: Induction Motor Performance Data

Description	Percent Power Factor	Currents (A)
No Load	4.8	96.2
Locked Rotor	11.8	3156

Table 4.13 shows the data in the form that HYPERSIM accepts for induction motor element. Subscript s represents stator side values and subscript r represents rotor side values.

Table 4.13: Induction Motor Data (HYPERSIM)

$r_s(\Omega)$	$x_s(\Omega)$	$r_r(\Omega)$	$x_r(\Omega)$	$x_m(\Omega)$
0.072	0.599	0.072	0.599	39.051

The information about power transformer is obtained from ASPEN model and is shown in Table 4.14. The data for this power transformer in the form that HYPERSIM accepts is shown Table 4.15. Subscript p represents primary side subscript s represents secondary side values and subscript 0 represents magnetizing branch values.

Table 4.14: Power Transformer Data

From Bus	Primary-KV	To Bus	Secondary-KV	R (p.u)	X (p.u)	R_0 (p.u)	X_0 (p.u)
BUS_LOAD	230	BUS_MOTOR	6.9	0.02155	0.44945	0.02047	0.42698

Table 4.15: Power Transformer Data (HYPERSIM)

From Bus	To Bus	R_p (p.u)	L_p (p.u)	R_s (p.u)	L_s (p.u)	R_0 (p.u)	L_m (p.u)
BUS_LOAD	BUS_MOTOR	0.010775	0.001192	0.010775	0.001192	0.02047	0.00113

4.6 Series Capacitor

Table 4.16 shows the information about Series Capacitor component which was obtained from ASPEN. The data from Table 4.16 can be entered into HYPERSIM Series Capacitor element control panel shown in Figure 4.17.

Table 4.16: Series Capacitor Data (HYPERSIM)

Bus	Base KV	C (F)
2387	230	0.0001087

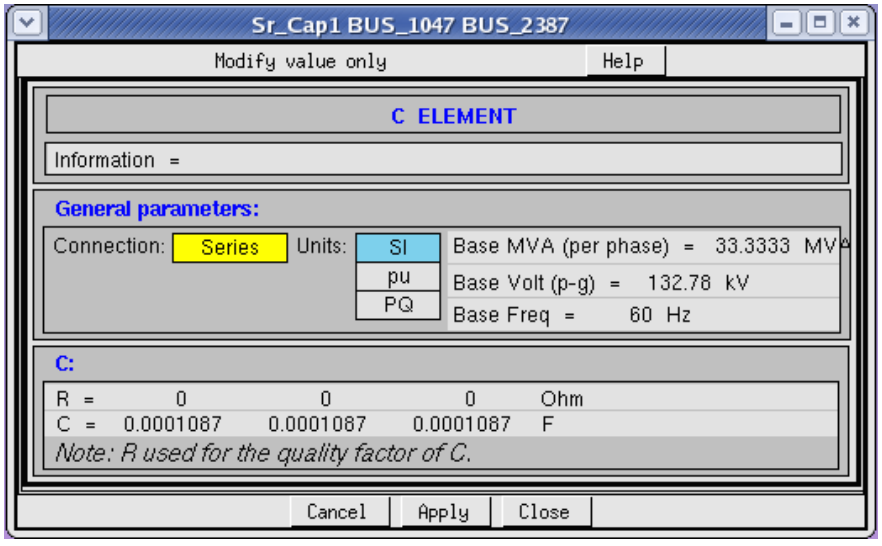

Figure 4.17: Control Panel of Series Capacitor

4.7 Surge Arrester

Table 4.17 shows the information about surge arrester component which was also obtained from ASPEN. The data from Table 4.17 can be entered into HYPERSIM Non-Linear resistor element control panel shown in Figure 4.18.

Table 4.17: Surge Arrester Data (HYPERSIM)

Vmin	P	Q
0.928077	0.3622	17.244
1.06066	0.036088	56.4055
1.10485	0.006829	73.101
1.1402	0.129967	50.648
1.1932	0.319977	45.5486
1.2552	74.4342	21.566

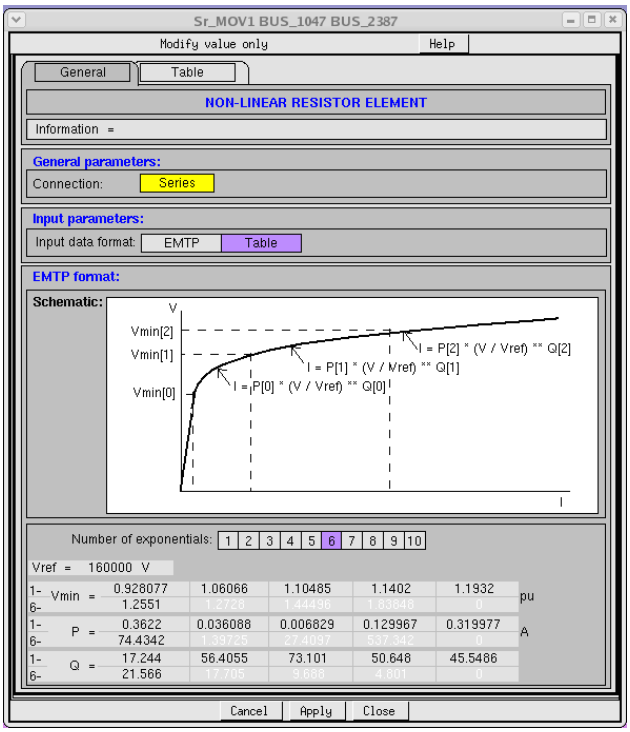

Figure 4.18: Control Panel of Surge Arrester

4.8 Shunt Capacitor

Table 4.18 shows the information about Shunt Capacitor components which were obtained from ASPEN/PSSE. The data from Table 4.18 can be entered into HYPERSIM Shunt Capacitor element control panel shown in Figure 4.19.

Table 4.18: Shunt Capacitor Data (HYPERSIM)

Bus	Base KV	Gshunt(MW)	Bshunt(Mvar)
1054	138.00	0	30.61
1071	230.00	0	81.41
1071	230.00	0	81.41

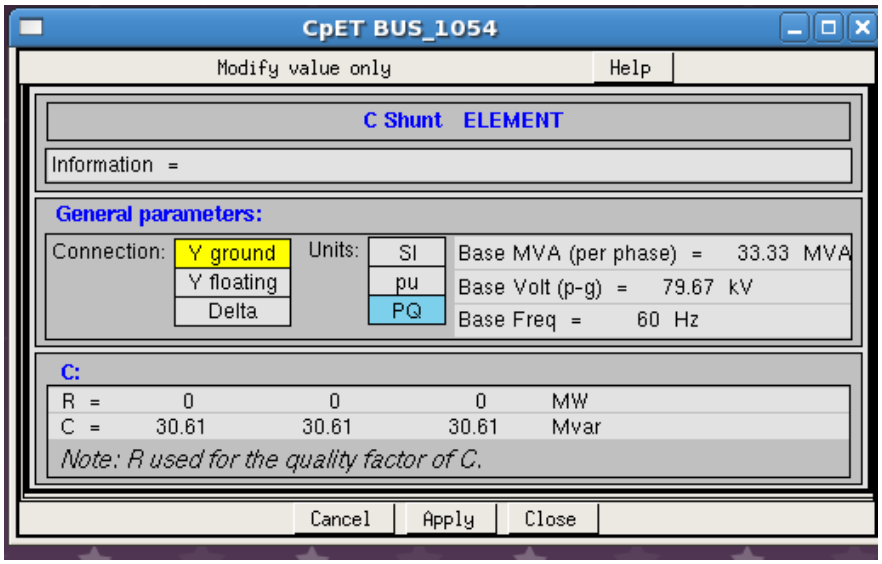

Figure 4.19: Control Panel of Shunt Capacitor

4.9 Equivalent Voltage Sources

The ASPEN power system model has 9 equivalent sources connected to boundary buses in study area. The information about these equivalent sources is obtained from ASPEN/PSSE and the data for HYPERSIM voltage source element, in the form that HYPERSIM accepts is shown in Table 4.19. The voltage, resistance, reactance and inductance values in Table 4.19 are in per unit.

Table 4.19: Equivalent Voltage Sources Data

Bus	Bus Name	Base KV	V (p.u)	Angle	Base MVA	R (p.u)	X (p.u)	L (p.u)
1051	BUS 1051	138	1	0	100	0.103337	0.364468	0.000967272
1070	BUS 1070	230	1	0	100	0.002522	0.0299	7.93524E-05
1080	BUS 1080	138	1	0	100	0.056244	0.870916	0.002311348
1139	BUS 1139	230	1	0	100	0.001116	0.015391	4.08466E-05
1733	BUS 1733	138	1	0	100	0.061917	0.364744	0.000968004
1890	BUS 1890	138	1	0	100	1E-05	1.62105	0.00430215
3298	BUS 3298	230	1	0	100	0.030877	0.121605	0.000322731
3969	BUS 3969	138	1	0	100	0.055609	0.313783	0.000832757
5711	BUS 5711	230	1	0	100	1E-05	0.094234	0.00025009

4.10 Equivalent Transformers

The ASPEN power system model has 11 equivalent transformers connected between boundary buses. The information about these equivalent transformers is obtained from ASPEN/PSSE and is shown in Table 4.20. The data for HYPERSIM two-winding transformer element, in the form that HYPERSIM accepts is shown in Table 4.21. The resistance and reactance values of equivalent transformers are in per unit. All equivalent transformers primary and secondary windings are star-grounded type.

4.11 Equivalent π Lines

The ASPEN power system model has 9 equivalent π lines connected between boundary buses. The information about these equivalent π lines is obtained from ASPEN/PSSE and the data for HYPERSIM π line element, in the form that HYPERSIM accepts is shown in Table 4.22. The resistance and inductance values of π lines are in per unit. These values can be entered into HYPERSIM π line element control panel shown in Figure 4.20.

Table 4.20: Two-Winding Equivalent Transformer Data

From Bus	Primary-KV	To Bus	Secondary-KV	R (p.u)	X (p.u)	Wdg-1 Ratio	Wdg-2 Ratio
1051	138	1070	230	1.50777	2.56086	1	1
1051	138	1139	230	0.807052	1.58549	1	1
1051	138	3298	230	0.140268	0.238189	1	1
1051	138	5711	230	0.051922	0.341828	1	1
1070	230	1733	138	0.121842	0.524834	1	1
1070	230	3969	138	0.28782	1.11169	1	1
1080	138	1139	230	0.213633	1.2435	1	1
1139	230	1733	138	1 .3192 8	4.64704	1	1
1890	138	3298	230	0.020951	0.066493	1	1
3298	2 30	3969	138	0.403799	0.899047	1	1
3969	138	5711	230	0.086979	0.550353	1	1

Table 4.21: Two-Winding Equivalent Transformer Data (HYPERSIM)

From Bus	To Bus	R_P (p.u)	L_P (p.u)	R_S (p.u)	L_S (p.u)
1051	1070	0.753885	0.003396446	0.753885	0.003396446
1051	1139	0.403526	0.002102821	0.403526	0.002102821
1051	3298	0.070134	0.000315908	0.070134	0.000315908
1051	5711	0.025961	0.000453363	0.025961	0.000453363
1070	1733	0.060921	0.000696083	0.060921	0.000696083
1070	3969	0.14391	0.001474425	0.14391	0.001474425
1080	1139	0.1068165	0.001649243	0.1068165	0.001649243
1139	1733	0.65964	0.006163328	0.65964	0.006163328
1890	3298	0.0104755	8.82E-05	0.0104755	8.82E-05
3298	3969	0.2018995	0.001192398	0.2018995	0.001192398
3969	5711	0.0434895	0.000729928	0.0434895	0.000729928

Table 4.22: Equivalent π Lines Data

From Bus	Voltage (KV)	To Bus	Voltage (KV)	R (p.u)	X (p.u)	L (p.u)
1047	230	2386	230	0.0001	0.0001	2.65258E-07
1047	230	2386	230	0	-0.0397	-0.000105308
1051	138	1080	138	0.284179	0.710957	0.001885872
1051	138	3969	138	1.2793	3.27475	0.008686544
1070	230	1139	230	0.009303	0.054905	0.00014564
1070	230	5711	230	0.728477	3.26854	0.008670072
1139	230	3298	230	0.375677	1.32461	0.003513637
2386	230	2387	230	0.0001	0.0001	2.65258E-07
3298	230	5711	230	0.020907	0.104125	0.0002762

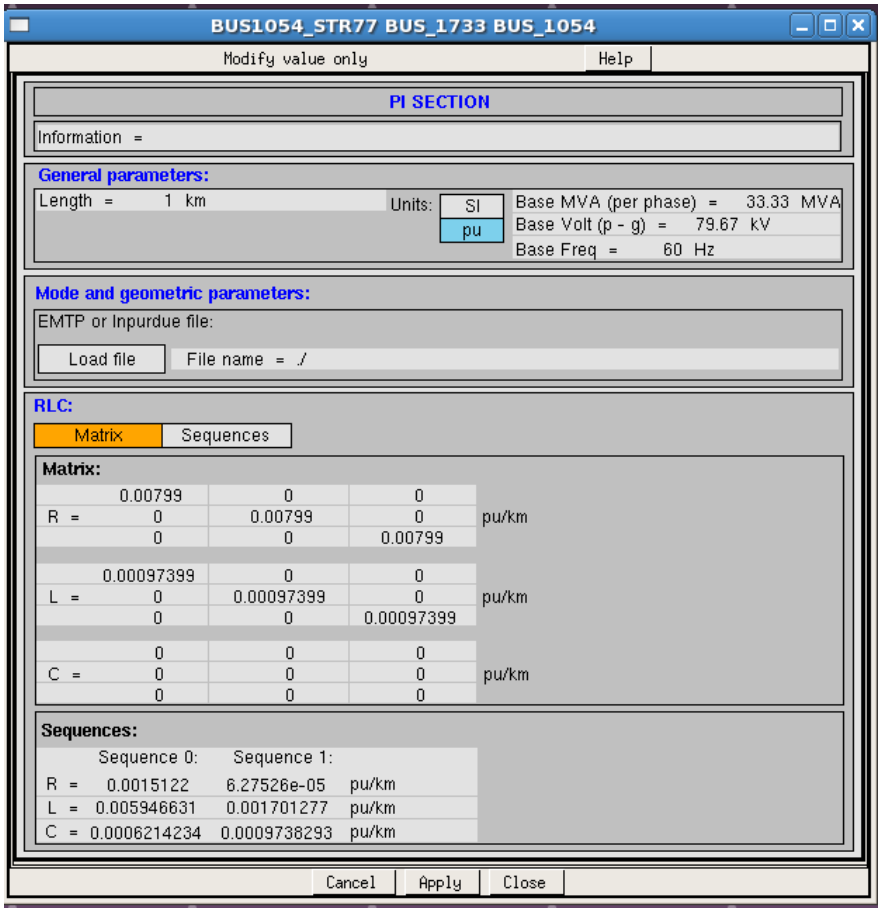

Figure 4.20: Control Panel of π Line

Chapter 5

Simulation Results & Discussion

5.1 Model of IPO System

The Power system model built for fault simulation, analysis and relay testing is shown in Figure 5.1. Model includes all HYPERSIM elements namely Frequency dependent distributed parameter lines, Constant parameter distributed lines, π lines, Voltage Sources, Two-Winding and Three-Winding transformers, Induction motor, Series capacitor with MOV protection, and Shunt capacitors.

Voltage sources with step-up transformers, Frequency dependent and Constant parameter type lines were modeled first and connected to buses in study area. Induction motor load with step-down transformer was modeled and included in the model. Series capacitor, shunt capacitors were then included in the model. Breaker configurations with IPO breakers were modeled and connected to series capacitor line local bus and remote bus in the model. Equivalent voltage sources with source impedance were modeled and connected to the boundary buses in study area. Equivalent two-winding transformers and equivalent π lines were modeled and connected between the boundary buses in study area.

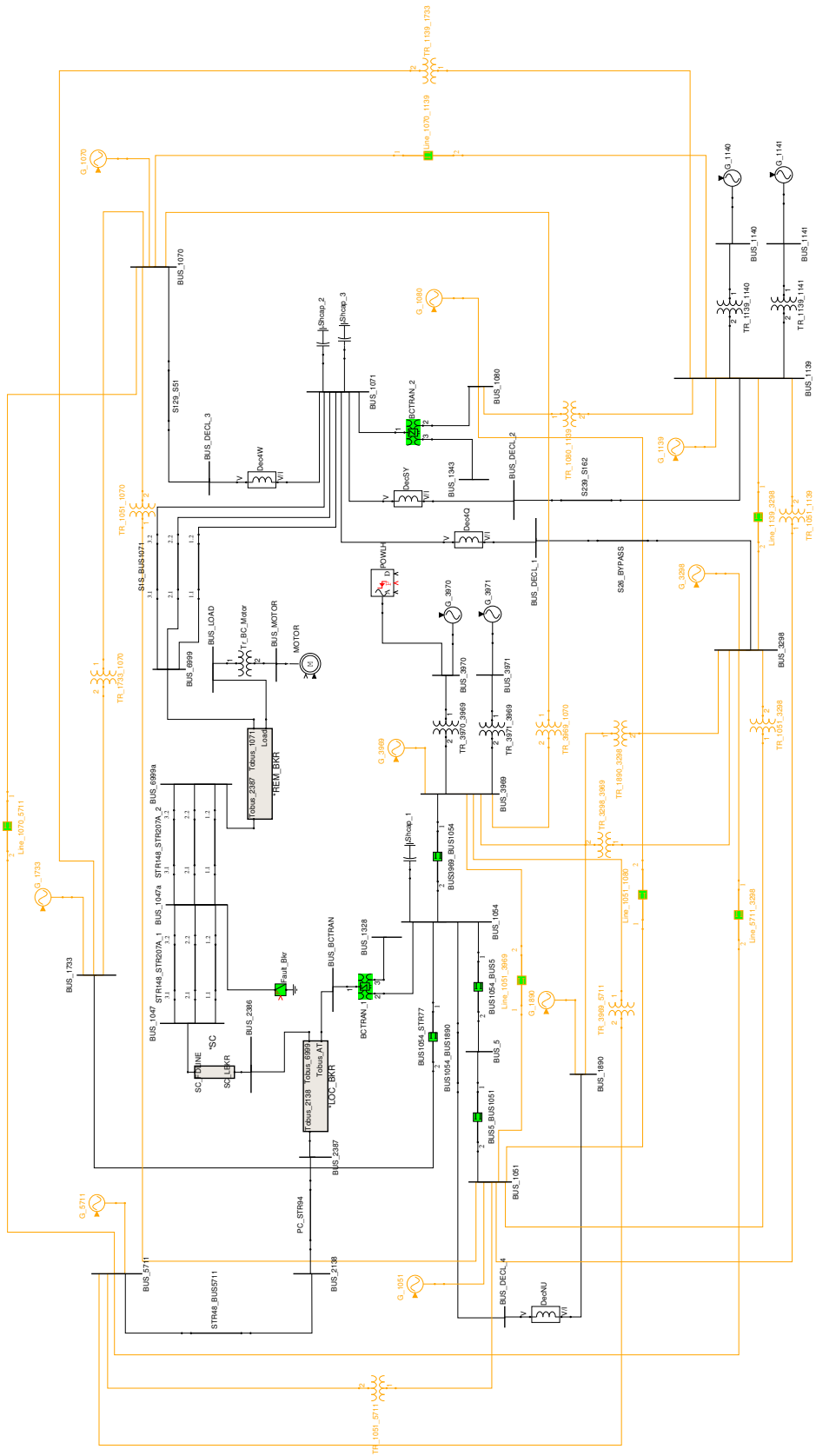

Figure 5.1: Model of IPO System

After inclusion of each HYPERSIM element, the model is tested for simulation time step and data acquisition at buses in scopeview software. Due to the presence of some power system elements of equivalent area (equivalent two-winding transformers and equivalent π lines), four distributed parameter transmission lines sending end and receiving terminals were terminated on same station. Decoupling inductors were used to split these lines. The inclusion of these decoupling inductors made the data acquisition at the buses unsuccessful as the model unable to find the point on wave to plot signals. The inductance value of these decoupling inductors are varied until data acquisition at buses is successful.

The series capacitor line to be protected is shown in Figure 5.2. IPO breakers are connected to the local bus and remote bus of line. Induction motor load is connected to load bus. Figure 5.3 and Figure 5.4 shows the breaker configuration at each end of the series capacitor line and Figure 5.5 shows series capacitor protection arrangement.

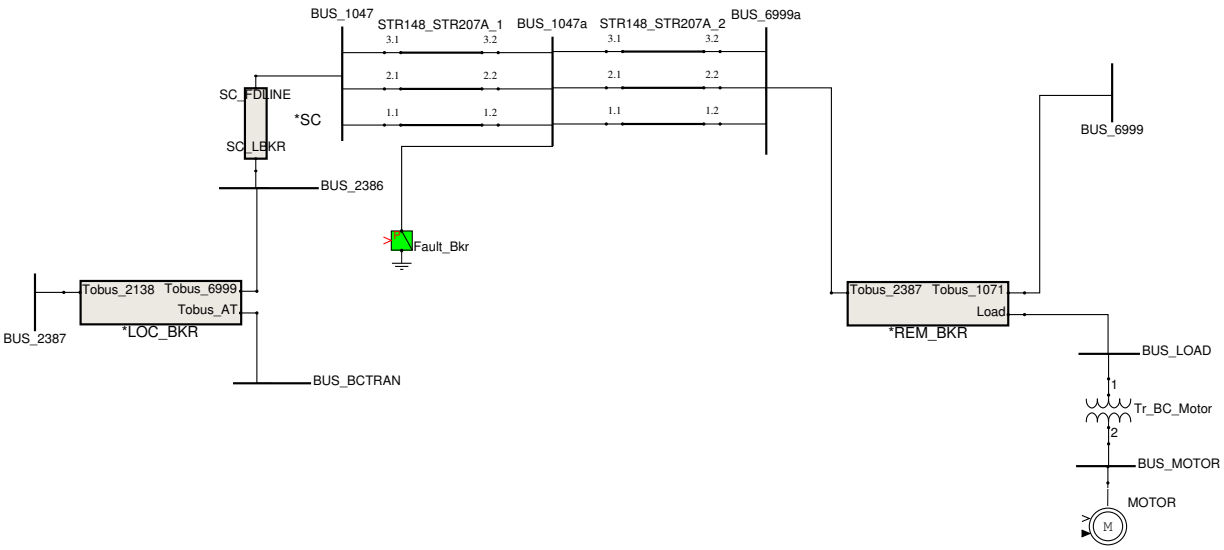

Figure 5.2: Series Capacitor Line

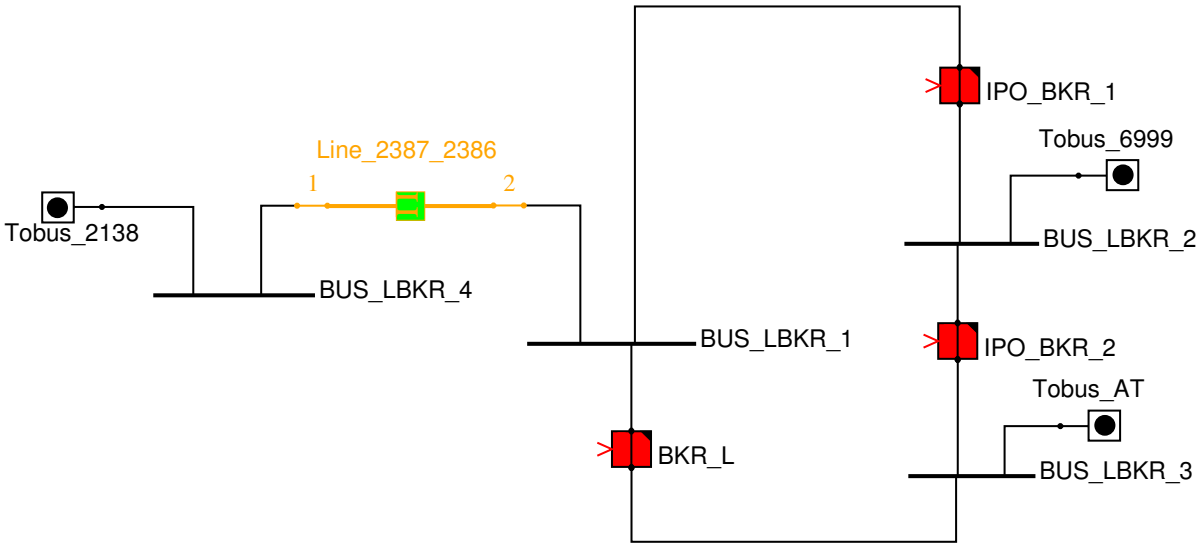

Figure 5.3: Local End Breaker Arrangement

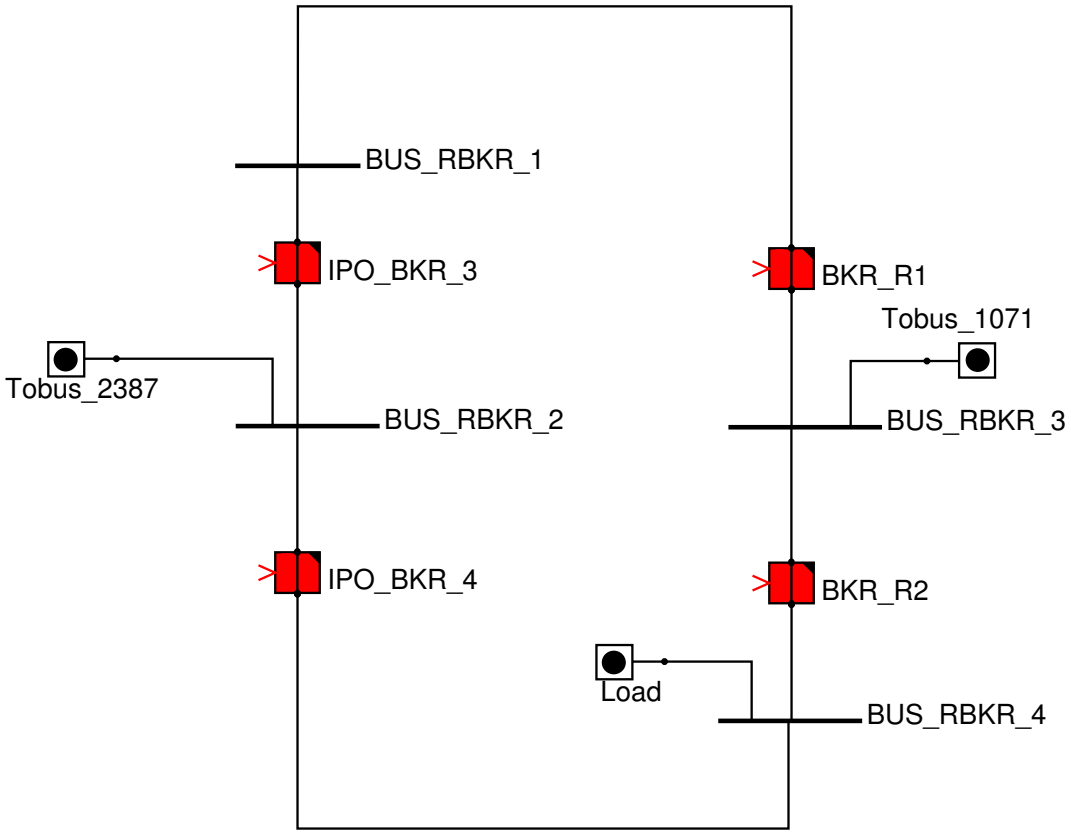

Figure 5.4: Remote End Breaker Arrangement

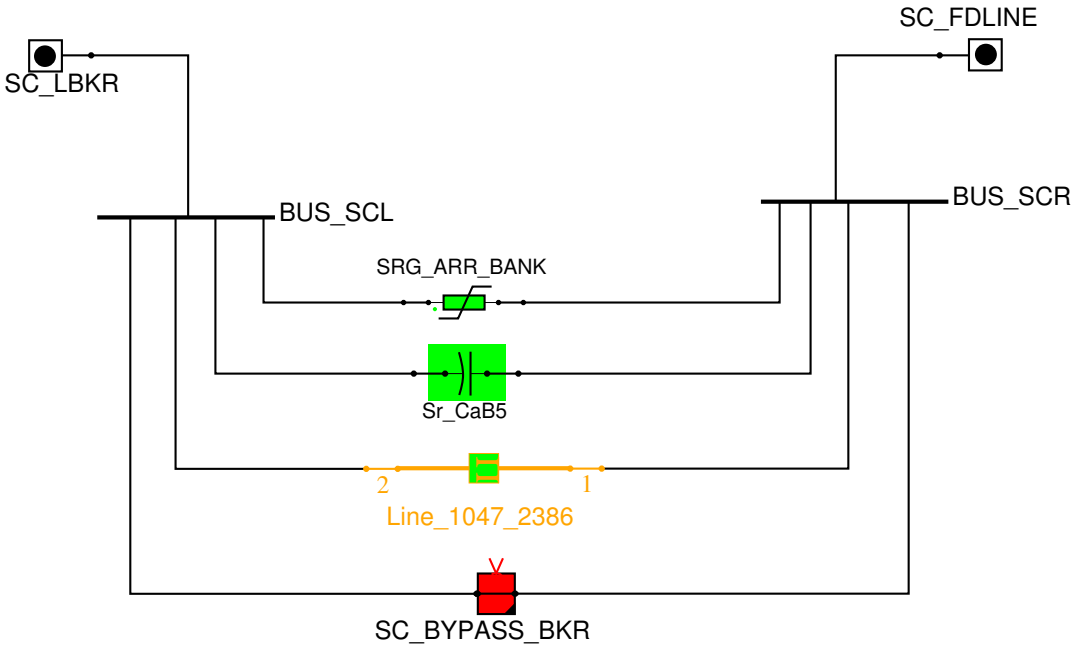

Figure 5.5: Series Capacitor Protection Arrangement

5.2 Open Loop Simulations

Using the Testview software in HYPERSIM, a script was developed for applying faults at different points on wave to determine worst scenarios. Fault breaker is closed 50 times at some random point on wave in a cycle (between 0.0166s and 0.0333s) and removed at 0.05s. For each fault scenario, time of fault application and maximum fault current were captured and presented as table out using the Testview software.

Table 5.1: Maximum Phase A to Ground Fault Currents (A) for Local End Fault ($1 \sim 25$)

T1(ms)	max_Ia	max_Ib	max_Ic
30.562	10799	145.14e-003	155.66e-003
32.148	8173.9	89.815e-003	90.712e-003
26.162	4107.8	96.35e-003	98.487e-003
25.948	3728.8	87.505e-003	89.529e-003
17.475	8628.3	86.113e-003	88.157e-003
29.448	5500.7	89.401e-003	100.23e-003
16.948	8770.5	88.36e-003	90.411e-003
20.848	6299.1	89.756e-003	90.447e-003
21.648	5680.8	88.081e-003	89.919e-003
131.348	7386.5	88.579e-003	91.161e-003
25.562	3845.4	89.61e-003	91.766e-003
32.048	8007.1	89.61e-003	90.463e-003
25.248	3798.5	87.272e-003	89.561e-003
30.148	6220.9	88.765e-003	98.535e-003
19.748	7606.5	87.982e-003	90.214e-003
31.475	7367.2	85.442e-003	88.598e-003
26.175	4205	98.566e-003	100.72e-003
17.948	8837.2	88.311e-003	90.443e-003
30.248	6303.7	88.611e-003	97.465e-003
33.048	8761.1	88.874e-003	90.16e-003
18.548	8614.4	88.109e-003	90.35e-003
31.548	7644.4	87.802e-003	90.668e-003
29.748	5826	88.847e-003	100.49e-003
18.348	8733.1	88.102e-003	90.409e-003
20.948	6235.4	89.637e-003	90.429e-003

Table 5.2: Maximum Phase A to Ground Fault Currents (A) for Local End Fault ($26 \sim 50$)

T1(ms)	max_Ia	max_Ib	max_Ic
16.948	8770.5	88.36e-003	90.411e-003
22.948	4798.2	88.432e-003	89.587e-003
27.948	4361.9	88.331e-003	90.005e-003
28.048	4389.9	88.435e-003	90.073e-003
29.262	5440.1	91.395e-003	102.24e-003
16.748	8699.7	88.237e-003	90.394e-003
27.048	3931.7	87.668e-003	89.671e-003
18.775	8959.1	92.787e-003	94.835e-003
26.948	3889.9	87.787e-003	89.636e-003
29.548	5578.9	89.355e-003	100.16e-003
19.748	7653.2	88.07e-003	90.227e-003
24.948	3875.3	87.67e-003	89.736e-003
25.148	3814.6	87.345e-003	89.584e-003
21.948	5467.4	88.431e-003	90.095e-003
28.348	4636	88.104e-003	91.161e-003
22.748	4931.2	88.118e-003	89.603e-003
31.348	7386.5	88.579e-003	91.161e-003
22.848	4879.4	88.279e-003	89.557e-003
25.362	3862.4	89.504e-003	91.779e-003
23.748	4340.6	87.602e-003	89.92e-003
25.775	3919.7	91.907e-003	94.003e-003
27.748	4268.2	87.961e-003	89.743e-003
19.448	7965.7	88.512e-003	90.308e-003
30.575	6455.3	86.766e-003	92.213e-003
31.048	7150.6	89.245e-003	91.195e-003

5.2.1 Simulation Results for Faults at Local End of Series Capacitor Line

Table 5.1 and Table 5.2 shows time of fault application and maximum values of fault current for single-line to ground faults applied in A-Phase at local end of series capacitor line. From Table 5.1 and Table 5.2, it is observed that the worst fault current occurs for fault applied at 30.562ms. Figure 5.6 shows plots for fault current through fault breaker and line current through local and remote IPO breakers for single-line (Phase A) to ground fault applied at local end of series capacitor line. The fault was applied at 0.02s and removed at 0.05s. Figure 5.7 shows plots for voltages at terminal buses of series capacitor line for single-line (Phase A) to ground fault applied at local end of series capacitor line. The fault was applied at 0.02s and removed at 0.05s.

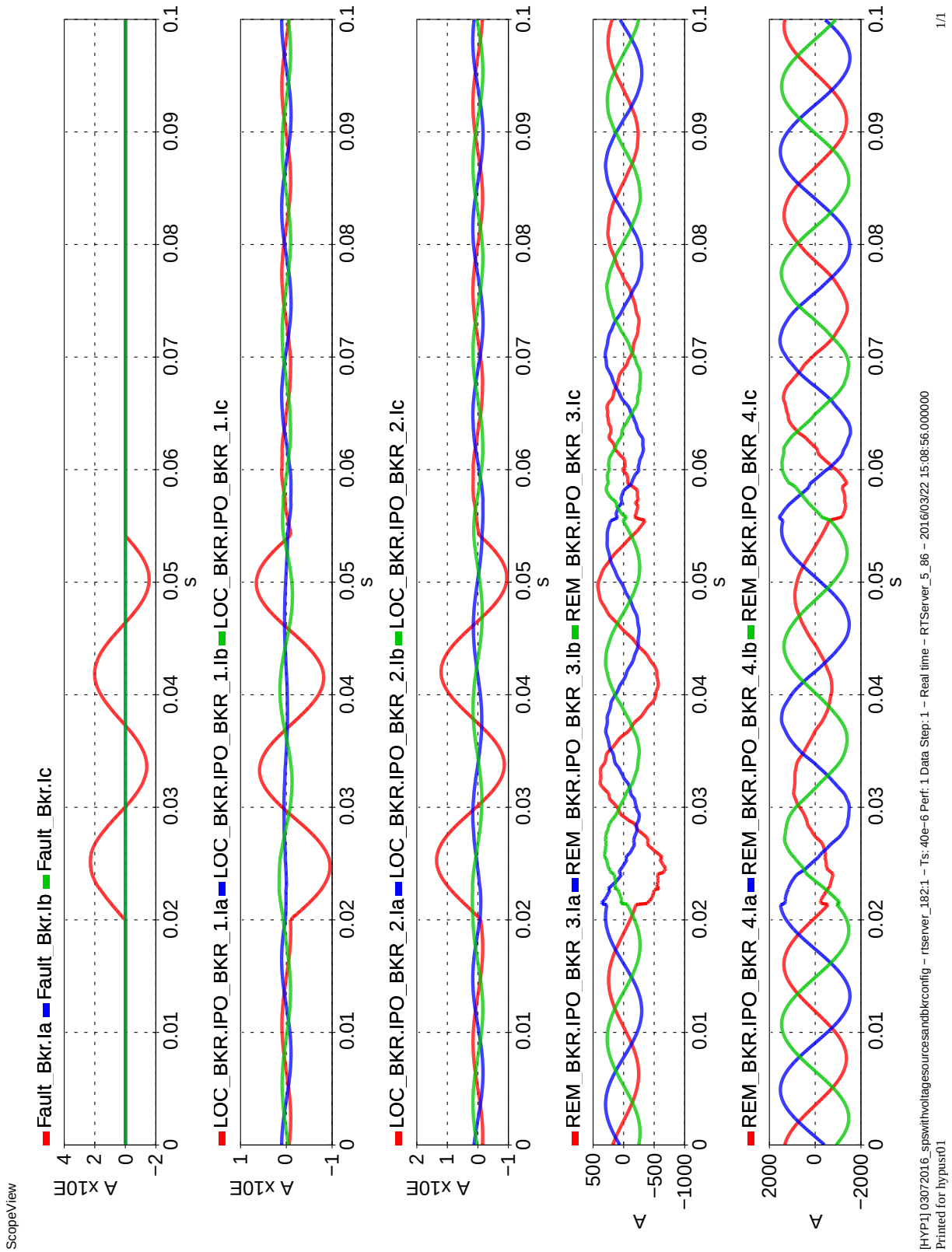

Figure 5.6: Fault & Line Currents for Phase A to Ground Faults at Local End

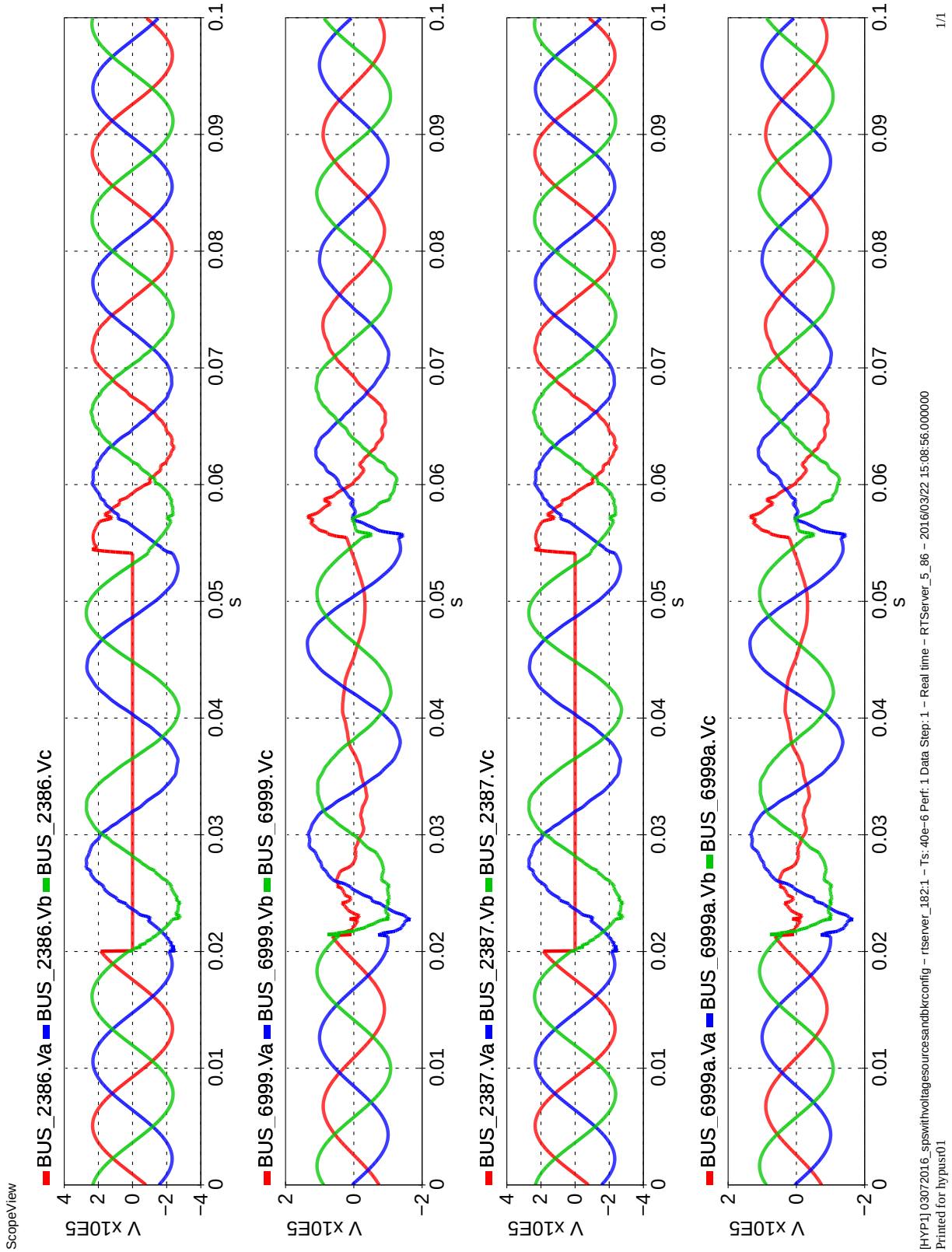

Figure 5.7: Voltages at Terminal Buses for Phase A to Ground Faults at Local End

Table 5.3: Maximum Phase A to Ground Fault Currents (A) for Mid-Line Fault ($1 \sim 25$)

T1(ms)	max_Ia	max_Ib	max_Ic
32.862	1636.5	139.76e-003	141.9e-003
17.175	1210.8	98.29e-003	98.861e-003
21.062	915.91	95.731e-003	96.821e-003
16.975	1194.1	98.308e-003	98.839e-003
18.062	1216.1	96.464e-003	97.034e-003
19.249	1141.6	95.492e-003	95.072e-003
18.562	1139.4	90.992e-003	91.495e-003
29.375	558.61	98.89e-003	115.35e-003
32.375	1001.3	90.866e-003	107.92e-003
18.862	1129.1	90.996e-003	91.454e-003
26.562	286.99	89.051e-003	90.111e-003
18.662	1135.2	90.995e-003	91.474e-003
26.649	299.59	92.614e-003	93.72e-003
17.775	1168.3	92.803e-003	93.375e-003
20.975	958.28	97.471e-003	98.659e-003
23.562	480.36	97.049e-003	95.323e-003
32.562	1129	100.24e-003	111.33e-003
22.549	630.47	94.139e-003	96.369e-003
16.962	1098.1	90.984e-003	91.492e-003
32.962	1062.1	90.682e-003	92.133e-003
29.375	574.52	98.923e-003	115.37e-003
31.075	799.91	91.596e-003	121.69e-003
23.375	504.17	98.427e-003	97.493e-003
31.162	795.19	89.686e-003	122.05e-003
17.275	1150.6	92.789e-003	93.367e-003

Table 5.4: Maximum Phase A to Ground Fault Currents (A) for Mid-Line Fault ($26 \sim 50$)

T1(ms)	max_Ia	max_Ib	max_Ic
20.162	1031.5	93.094e-003	91.193e-003
23.762	456.38	97.86e-003	94.371e-003
33.049	1125.5	94.885e-003	96.073e-003
26.175	327.91	101.61e-003	102.72e-003
26.275	292.03	90.848e-003	91.916e-003
24.462	383.26	97.282e-003	91.428e-003
24.462	387.26	97.334e-003	91.586e-003
29.375	542.51	93.395e-003	108.83e-003
21.762	714.3	90.494e-003	91.11e-003
23.675	478.29	99.481e-003	96.876e-003
18.262	1143.6	90.971e-003	91.524e-003
18.975	1142.8	92.841e-003	93.275e-003
28.262	389.45	92.749e-003	90.975e-003
19.662	1143.4	98.853e-003	96.821e-003
31.562	865.48	88.959e-003	115.17e-003
28.862	453.11	90.816e-003	99.431e-003
21.762	714.3	90.494e-003	91.11e-003
18.975	1137.2	92.91e-003	93.268e-003
30.462	689.38	91.168e-003	118.67e-003
24.062	422.83	98.114e-003	92.471e-003
26.562	286.68	89.056e-003	90.111e-003
32.949	1113.3	94.611e-003	95.91e-003
25.075	336.4	95.531e-003	91.924e-003
31.662	930.84	94.275e-003	121.79e-003
28.775	454.12	92.556e-003	100.35e-003

5.2.2 Simulation Results for Faults at Middle of Series Capacitor Line

Table 5.3 and Table 5.4 shows time of fault application and maximum values of fault current for single-line to ground faults applied in A-Phase at middle of series capacitor line. From Table 5.3 and Table 5.4, it is observed that the worst fault current occurs for fault applied at 32.862ms. Figure 5.8 shows plots for fault current through fault breaker and line current through local and remote IPO breakers for single-line (Phase A) to ground fault applied at middle of series capacitor line. The fault was applied at 0.02s and removed at 0.05s. Figure 5.9 shows plots for voltages at terminal buses of series capacitor line for single-line (Phase A) to ground fault applied at middle of series capacitor line. The fault was applied at 0.02s and removed at 0.05s.

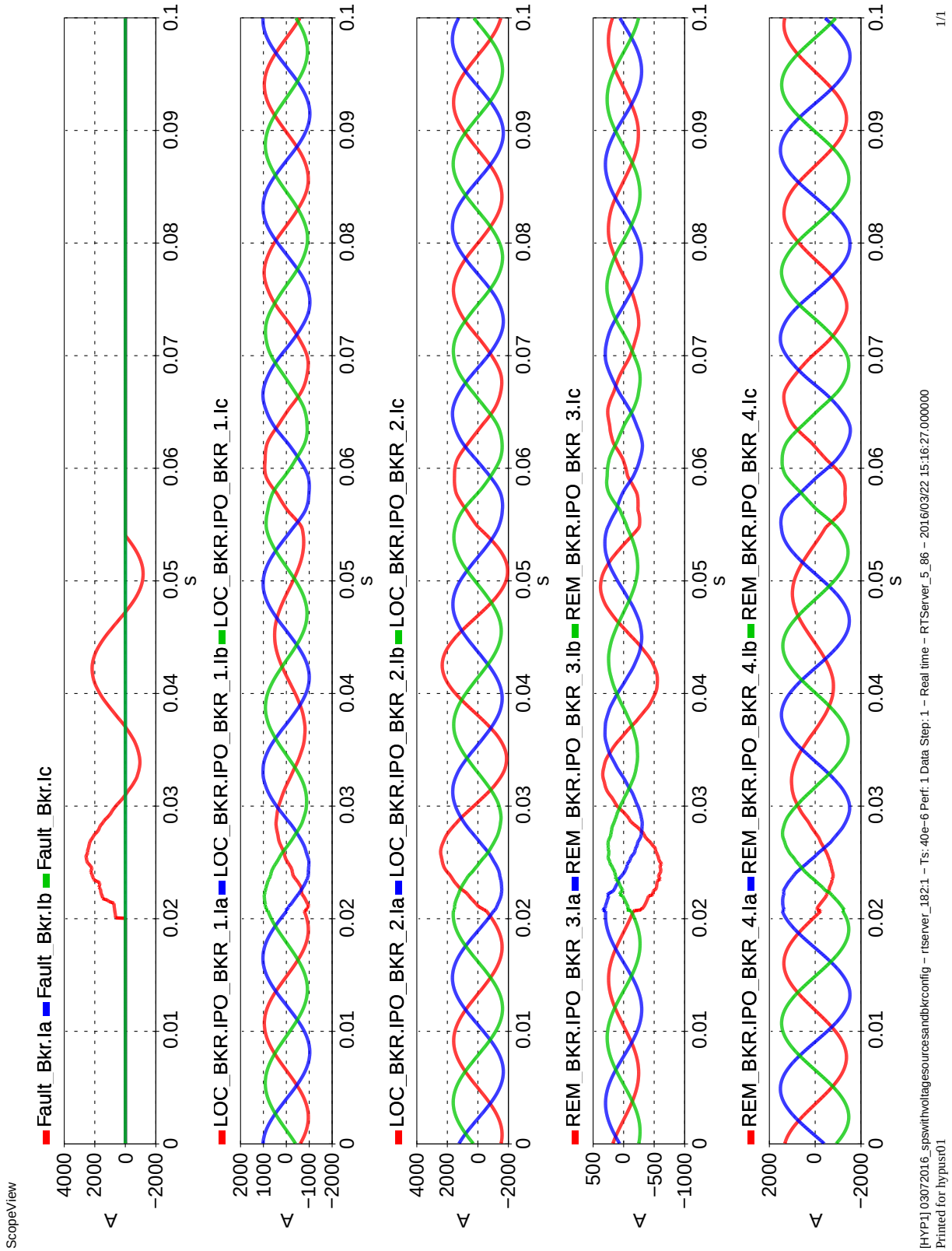

Figure 5.8: Fault & Line Currents for Phase A to Ground Faults at Mid-Line

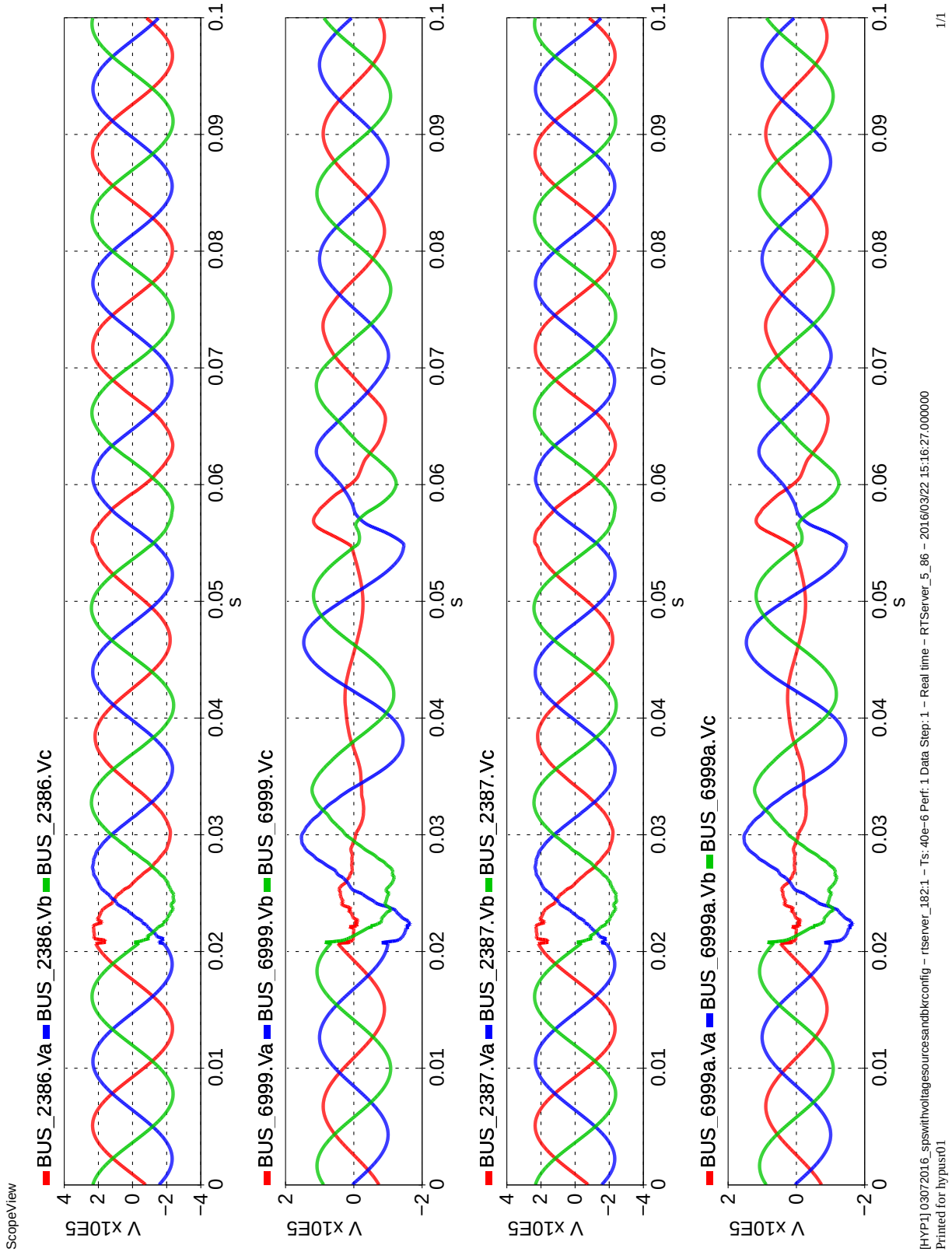

Figure 5.9: Voltages at Terminal Buses for Phase A to Ground Faults at Mid-Line

Table 5.5: Maximum Phase A to Ground Fault Currents (A) for Remote End Fault ($1 \sim 25$)

T1(ms)	max_Ia	max_Ib	max_Ic
25.362	539.73	99.398e-003	86.204e-003
24.975	417.82	69.511e-003	60.635e-003
31.362	526.46	68.611e-003	66.608e-003
29.562	372.57	69.482e-003	59.651e-003
17.662	750.72	68.691e-003	59.86e-003
18.662	798.39	68.752e-003	59.864e-003
25.749	345.87	66.831e-003	58.251e-003
22.349	644.02	71.199e-003	61.925e-003
24.275	454.79	69.728e-003	60.701e-003
26.575	332.58	69.443e-003	60.341e-003
26.449	324.45	66.809e-003	58.14e-003
17.749	742.25	67.409e-003	58.719e-003
30.349	437.51	71.286e-003	67.807e-003
23.349	510.07	67.034e-003	58.442e-003
26.449	324.45	66.809e-003	58.14e-003
19.875	815.91	70.053e-003	60.985e-003
31.562	512.32	65.085e-003	65.399e-003
19.675	771.07	66.147e-003	57.603e-003
20.149	776.26	67.427e-003	58.719e-003
18.575	812.19	70.056e-003	60.993e-003
19.362	804.06	68.76e-003	59.871e-003
33.262	682.35	69.08e-003	66.602e-003
28.062	311.16	68.04e-003	59.332e-003
30.162	415.3	68.595e-003	65.629e-003
27.349	301.07	66.79e-003	58.176e-003

Table 5.6: Maximum Phase A to Ground Fault Currents (A) for Remote End Fault ($26 \sim 50$)

T1(ms)	max_Ia	max_Ib	max_Ic
22.162	648.69	68.565e-003	59.718e-003
28.962	335.27	69.228e-003	59.277e-003
30.462	426.53	68.671e-003	65.965e-003
28.649	321.6	68.045e-003	58.149e-003
27.649	317.85	70.658e-003	61.534e-003
22.649	593.1	71.154e-003	61.867e-003
26.875	318.77	69.467e-003	60.364e-003
23.549	494.19	67.16e-003	58.373e-003
30.249	408.87	67.298e-003	63.405e-003
29.549	364.61	68.188e-003	58.526e-003
21.249	729.7	67.45e-003	58.709e-003
17.349	722.43	67.39e-003	58.749e-003
26.675	324.43	69.467e-003	60.339e-003
25.262	383.95	68.327e-003	59.324e-003
27.162	308.05	68.132e-003	59.29e-003
19.749	786.63	67.452e-003	58.737e-003
21.362	740.85	68.736e-003	59.829e-003
24.149	443.64	67.237e-003	58.43e-003
27.349	301.07	66.79e-003	58.176e-003
29.049	330.82	68.051e-003	58.206e-003
23.575	511.12	69.775e-003	60.607e-003
26.949	304.89	66.888e-003	58.138e-003
26.949	304.89	66.888e-003	58.138e-003
30.949	498.3	70.593e-003	69.582e-003
19.775	817.78	70.059e-003	60.992e-003

5.2.3 Simulation Results for Faults at Remote End of Series Capacitor Line

Table 5.5 and Table 5.6 shows time of fault application and maximum values of fault current for single-line to ground faults applied in A-Phase applied at middle of series capacitor line. From Table 5.5 and Table 5.6, it is observed that the worst fault current occurs for fault applied at 19.775ms. Figure 5.10 shows plots for fault current through fault breaker and line current through local and remote IPO breakers for single-line (Phase A) to ground fault applied at middle of series capacitor line. The fault was applied at 0.02s and removed at 0.05s. Figure 5.11 shows plots for voltages at terminal buses of series capacitor line for single-line (Phase A) to ground fault applied at middle of series capacitor line. The fault was applied at 0.02s and removed at 0.05s.

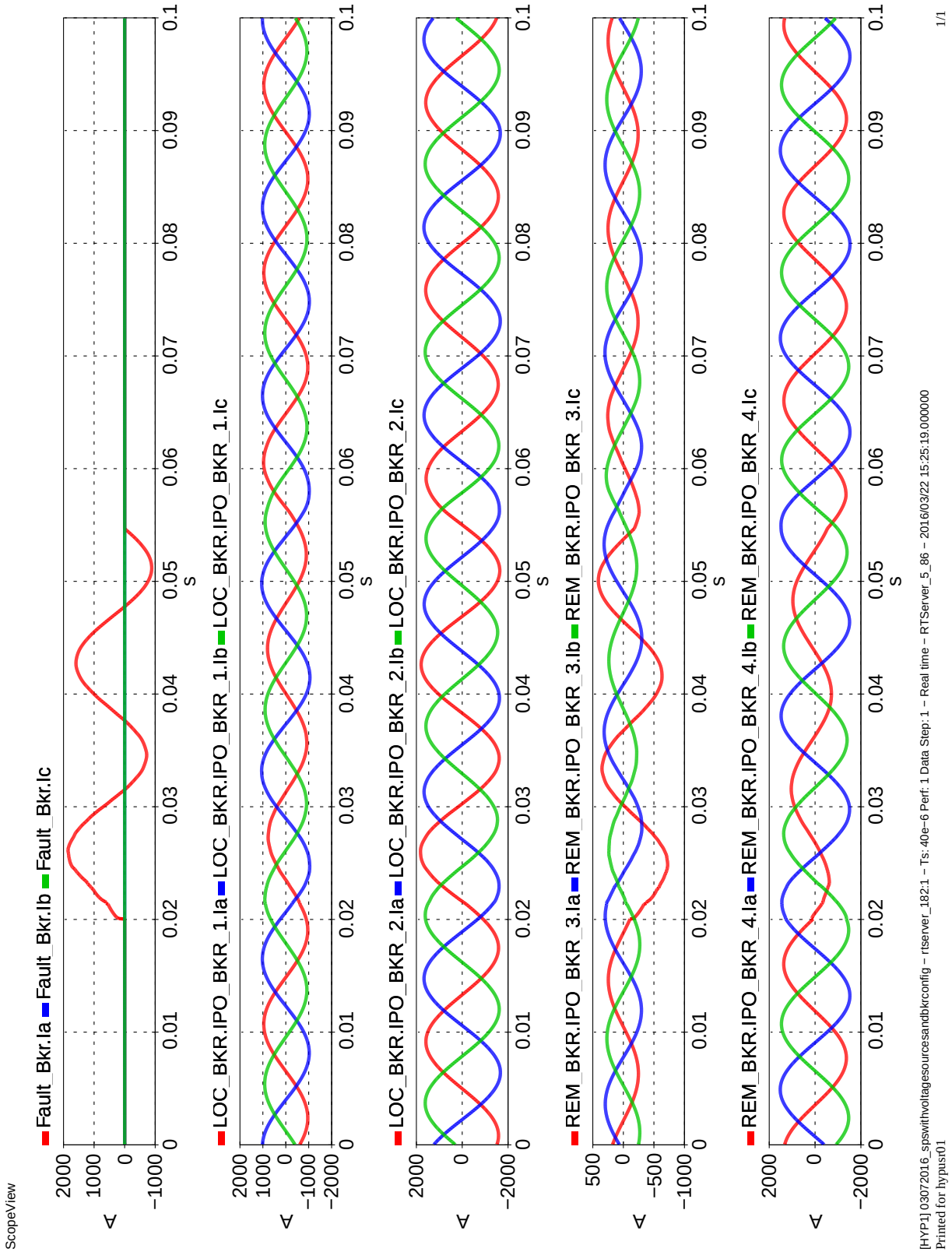

Figure 5.10: Fault & Line Currents for Phase A to Ground Faults at Remote End

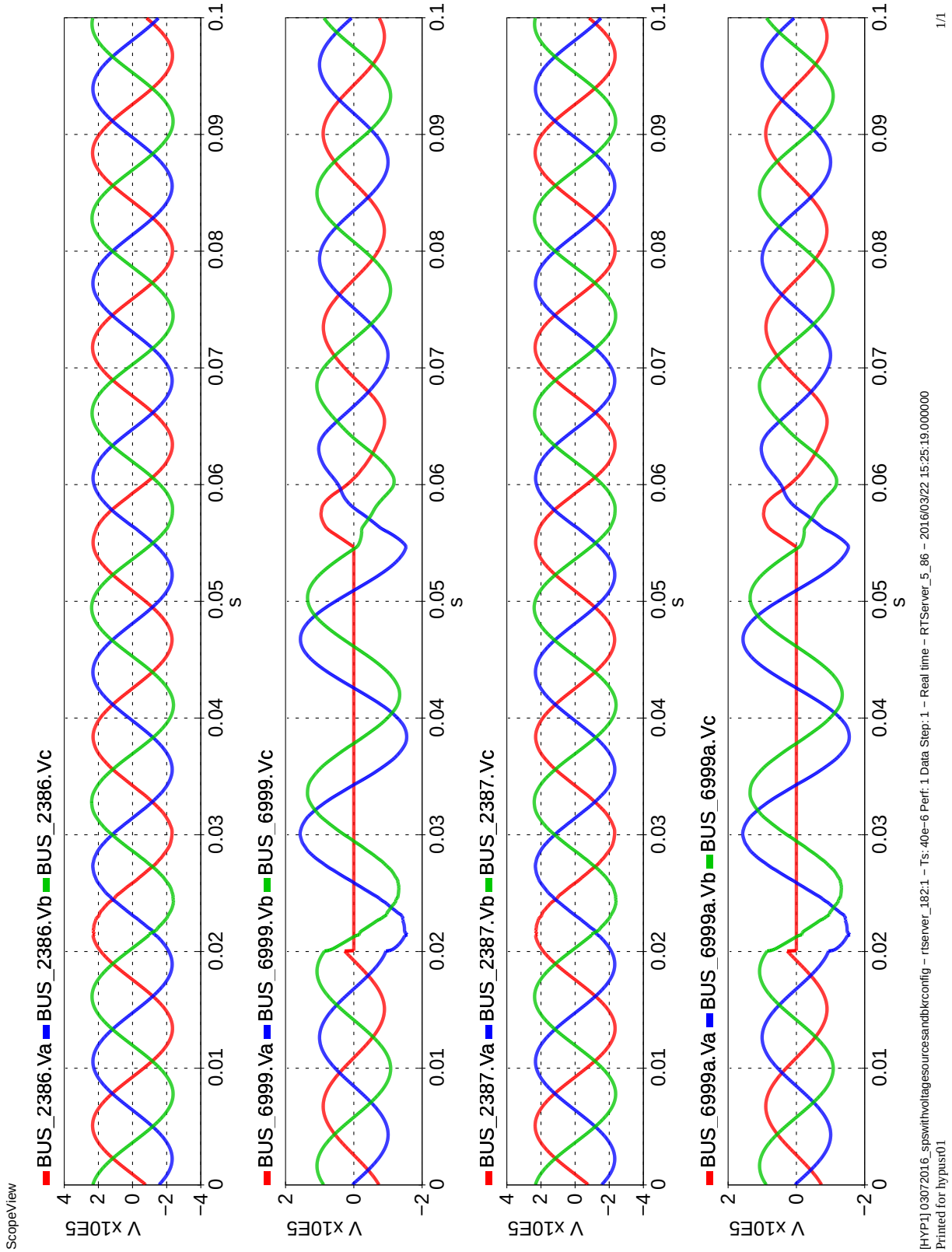

Figure 5.11: Voltages at Terminal Buses for Phase A to Ground Faults at Remote End

5.3 Fault Arc Model

Figure 5.12 shows the fault arc model. This model includes fault breaker, ideal switch and UCM controlled resistor element. Fault breaker is used to simulate fault conditions. Different types of faults can be simulated by this fault breaker. For observing primary and secondary arc phenomenon, single-line to ground faults are to be simulated. Ideal switch represents arc extinction and re-strike phenomenon and UCM control resistor element represents primary and secondary arc phenomenon. The block "Switch_Sim" lets the switch to remain in close position until primary arc extinguishes and during the secondary arc period the switch acts according to value computed by "SecArc" block. The block "Arc_Controller" updates the resistance of the "Arc_resistance" UCM element at every time step. The inputs to this block are primary arc resistance, secondary arc resistance and breaker trip command. This block outputs primary arc resistance to UCM element until trip command issued to line breakers and outputs secondary arc resistance to UCM Controlled Resistor" from the moment the line breakers were tripped.

Figure 5.13 shows the primary arc model. This model simulates primary arc phenomenon. The input to this model is fault current and the model computes primary arc resistance at every time step. The model updates the UCM "Arc_Resistance" element at every time step.

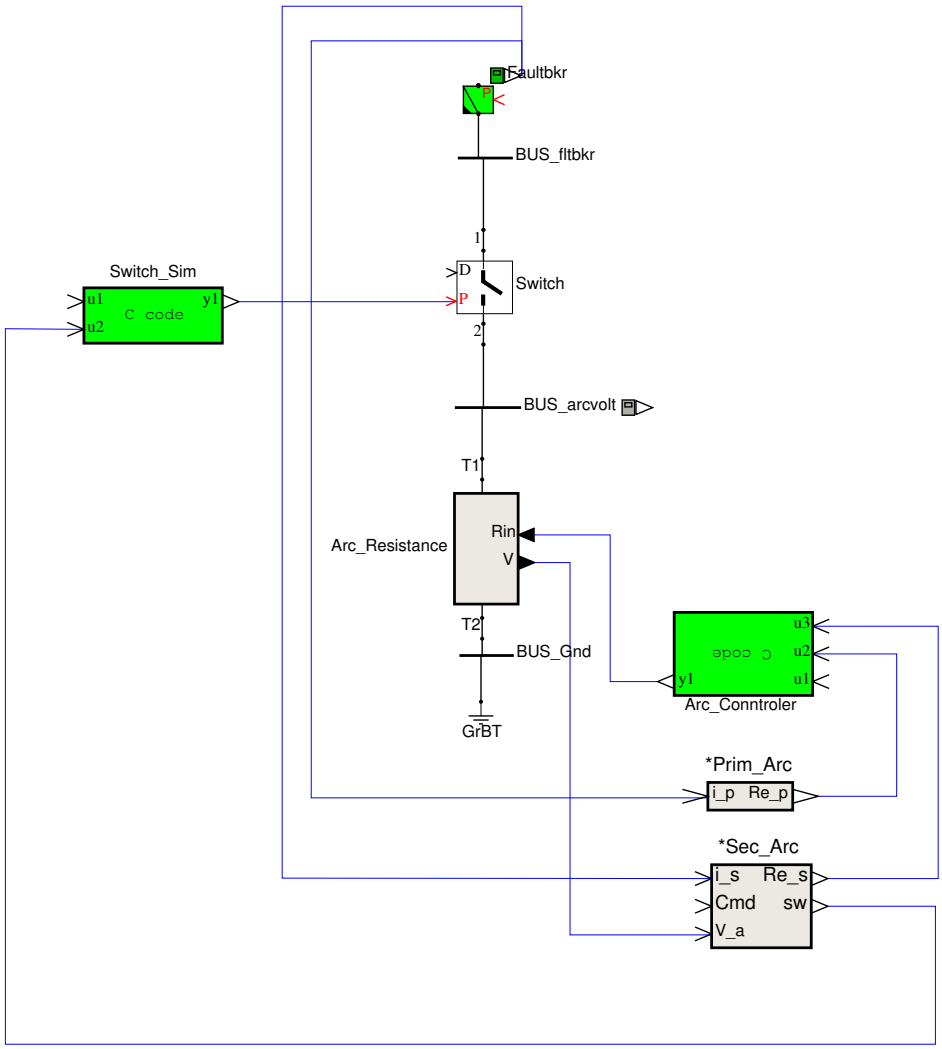

Figure 5.12: Fault Arc Model

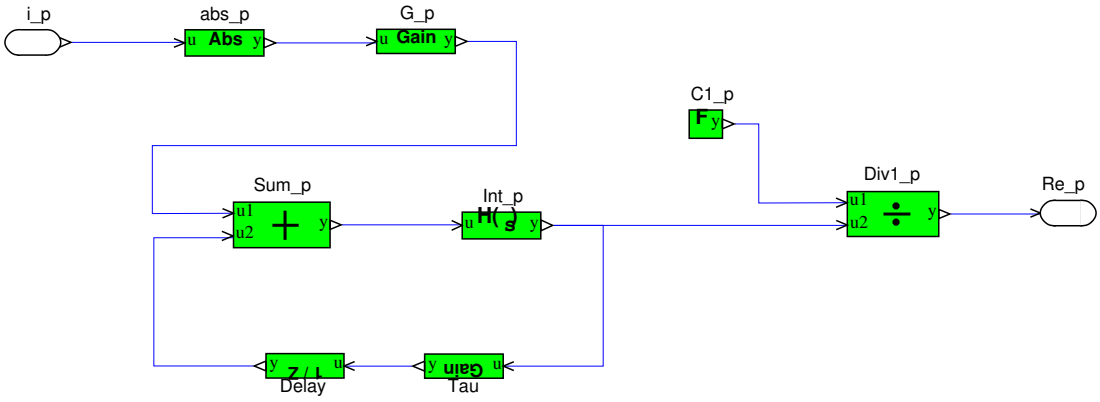

Figure 5.13: Primary Arc Block Diagram

Figure 5.14 shows the secondary arc model. The model simulates secondary arc phenomenon. This model takes the fault current as input and outputs secondary arc resistance value and switch command signal by performing computations. The block "Tau_s" computes time constant and arc length variations are computed by block "arclength_s". The reignition voltage is computed by block "V_r" and compared with the arc recovery voltage by the block "Switch_Controller". This block controls the ideal switch by opening it when arc recovery voltage is less than reignition voltage representing arc extinction and closing it when arc recovery voltage exceeds the reignition voltage representing re-strike. The model updates UCM "Arc_Resistance" element and controls ideal switch at every item step.

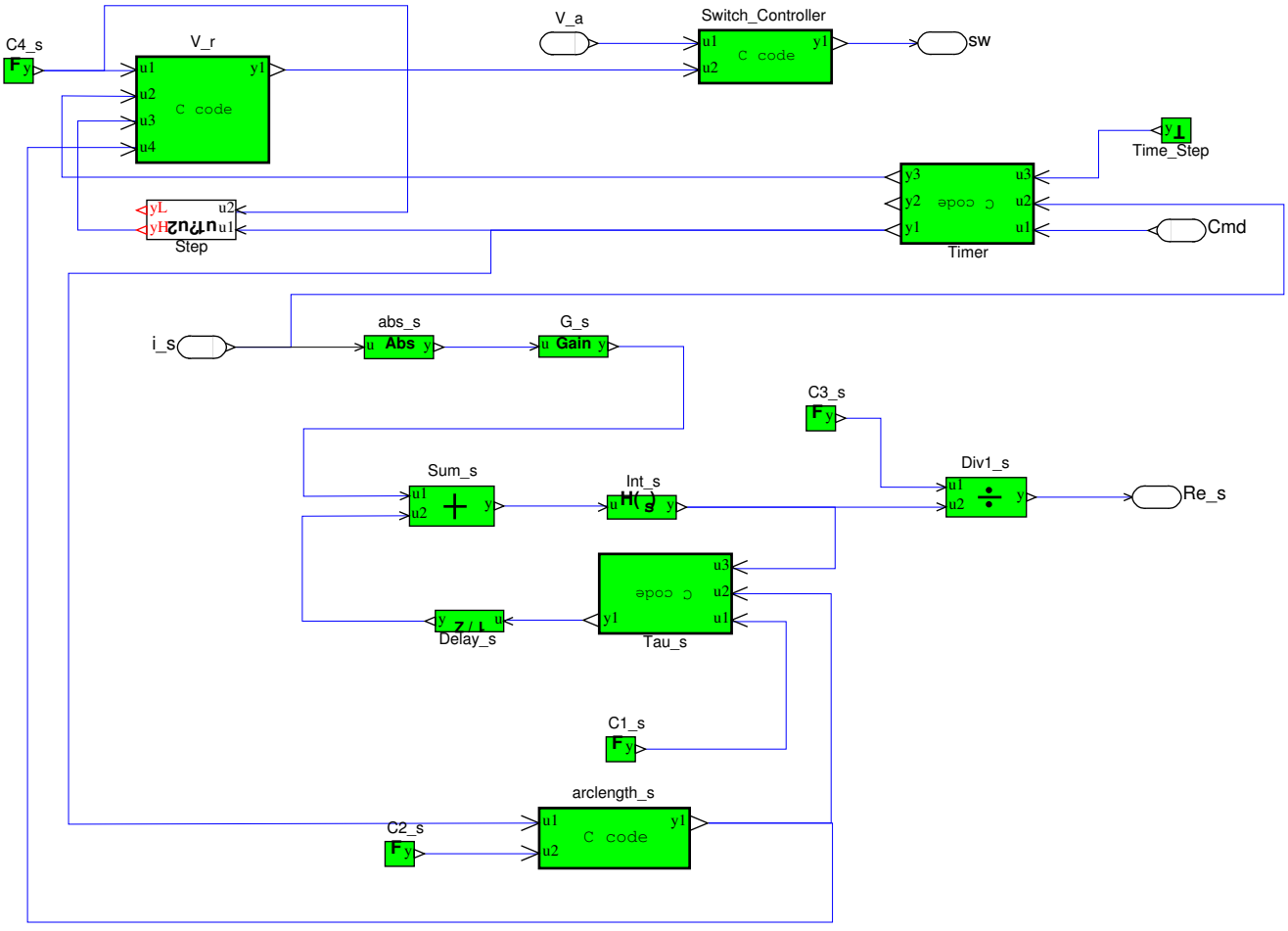

Figure 5.14: Secondary Arc Block Diagram

5.4 Fault Arc Model Test System and Plots

Figure 5.15 illustrates the test system used to verify the arc model. The system is an extract from main model. Fault arc model shown in Figure 5.12 is connected at mid-point of the transmission line. Fault was applied at 0.2s and removed at 0.7s.

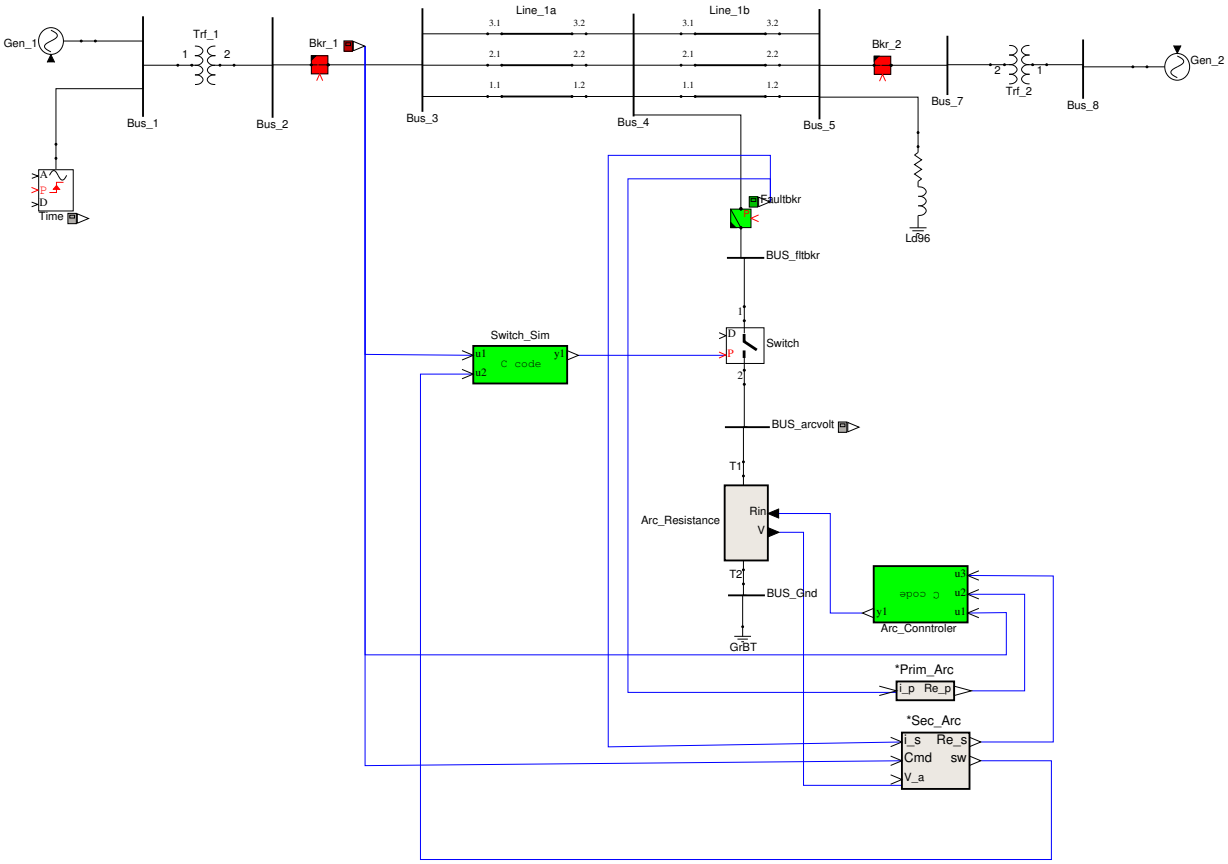

Figure 5.15: Fault Arc Model Test System

Figure 5.16 illustrates plots pertaining to primary arc simulation. Zoomed plots of primary arc resistance and primary arc voltage are shown in Figure 5.17 and Figure 5.18. Primary arc resistance value during the fault period is very less compared to pre-fault and post-fault periods.

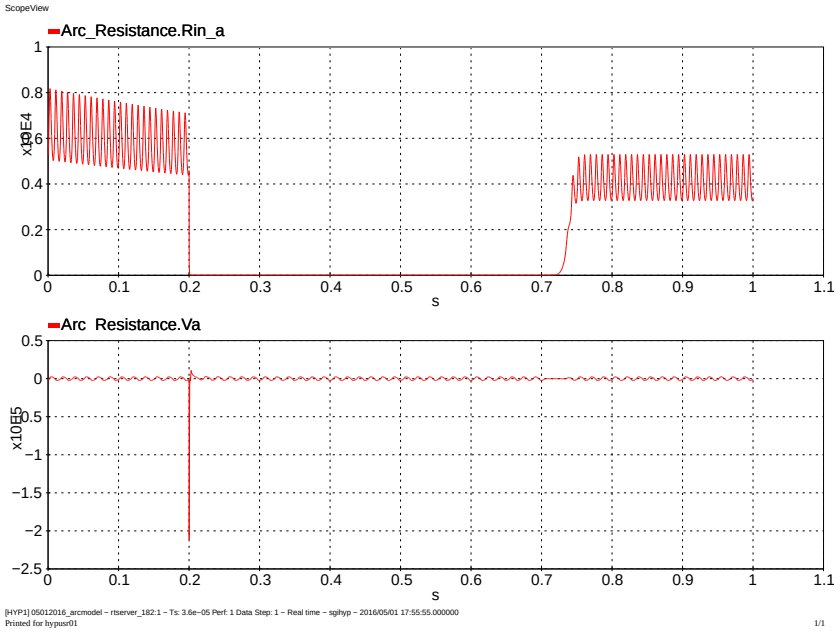

Figure 5.16: Primary Arc Plots

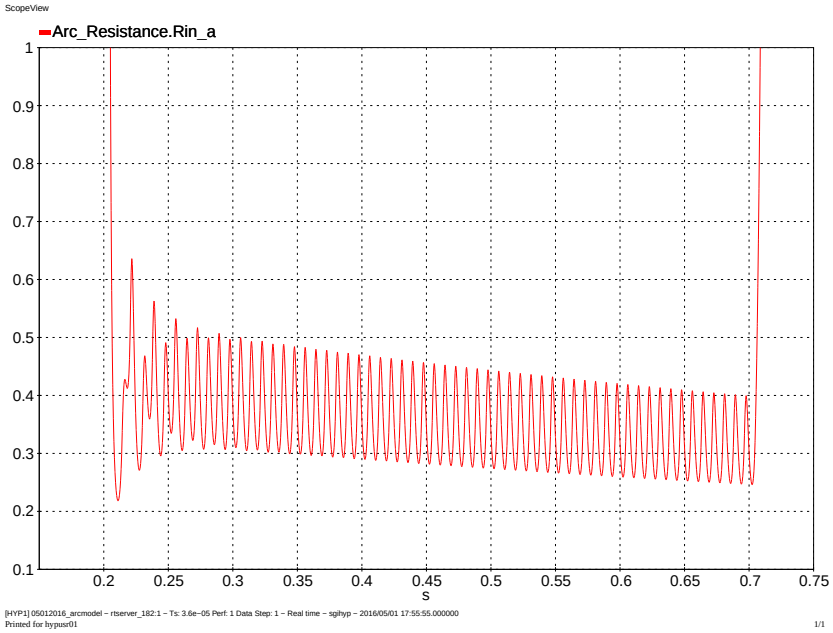

Figure 5.17: Primary Arc Resistance

Figure 5.19 illustrates plots pertaining to secondary arc simulations. Zoomed plots of secondary arc current, secondary arc voltage and switching action are shown in Figure 5.20,

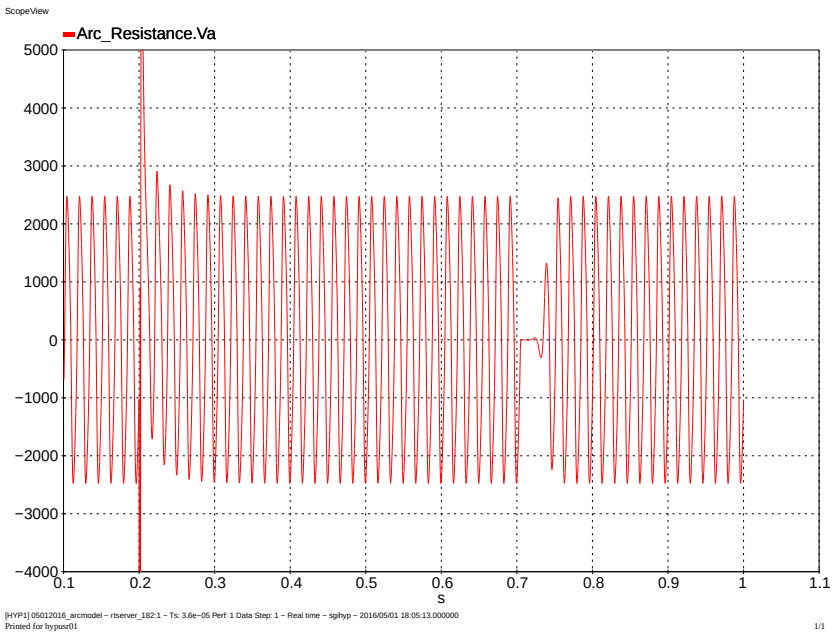

Figure 5.18: Primary Arc Voltage

Figure 5.21 and Figure 5.22. In Figure 5.19, the instant 0.2s corresponds to fault inception and instant 0.5s corresponds to breaker open. The current through the fault breaker from instant 0.2s to 0.5s is primary arc current. From the instant the breaker opens, the current through the fault breaker is secondary arc current as shown in Figure 5.20. The fault was removed at 0.7s and the secondary arc current continues to flow until arc extinguishes. Ideal switch simulates arc extinguish and re-strike. The simulation is shown in Figure 5.22. The switch remains in close position until the instant breaker opens and from the instant breaker opened, the switch opens when arc voltage is less than the reignition voltage simulating arc extinguishing phenomenon and closes when arc voltage exceeds reignition voltage simulating arc re-strike phenomenon. The arc re-strikes and extinguishes until reignition voltage is permanently greater than the recovery voltage and indicated by switch open condition in the plot at approximately 0.75s in Figure 5.22. From Figure 5.22, we can say that the secondary arc extinguished with in 250ms from the instant the breaker opened.

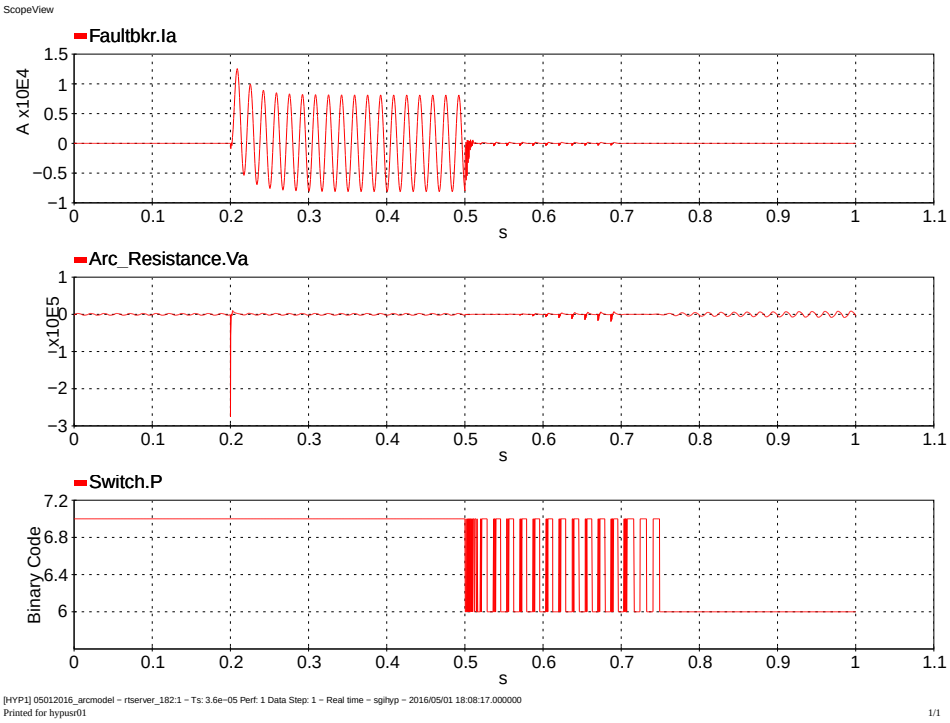

Figure 5.19: Secondary Arc Plots

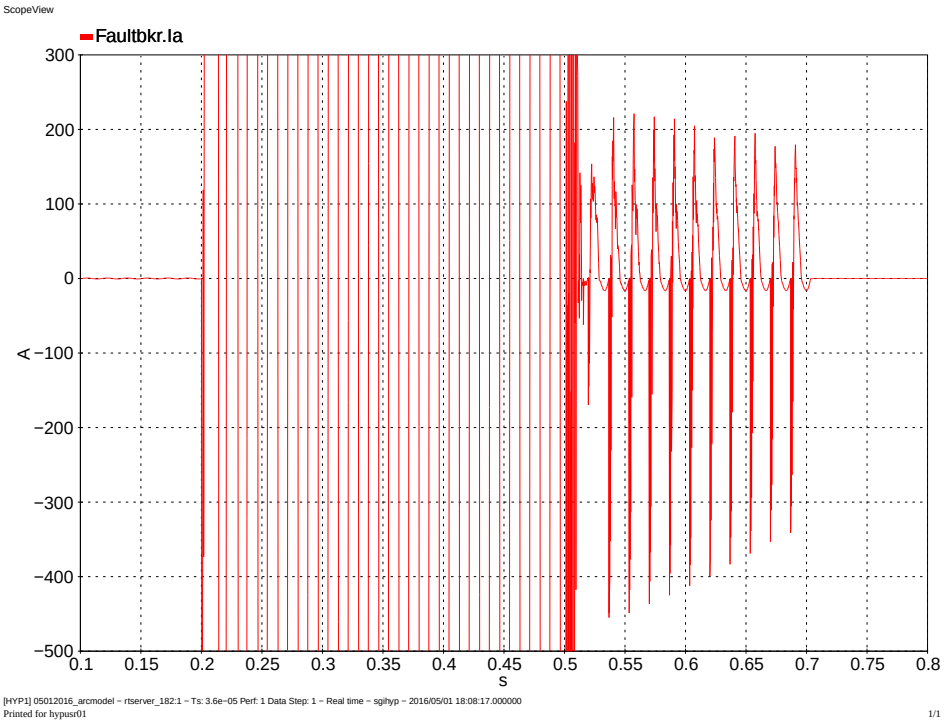

Figure 5.20: Secondary Arc Current

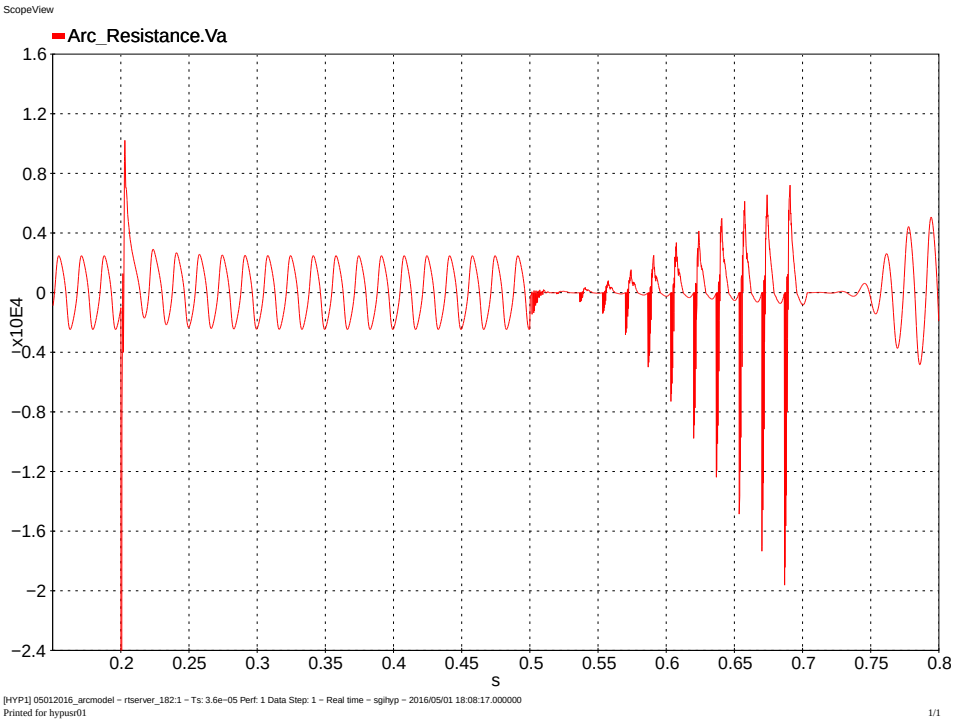

Figure 5.21: Secondary Arc Voltage

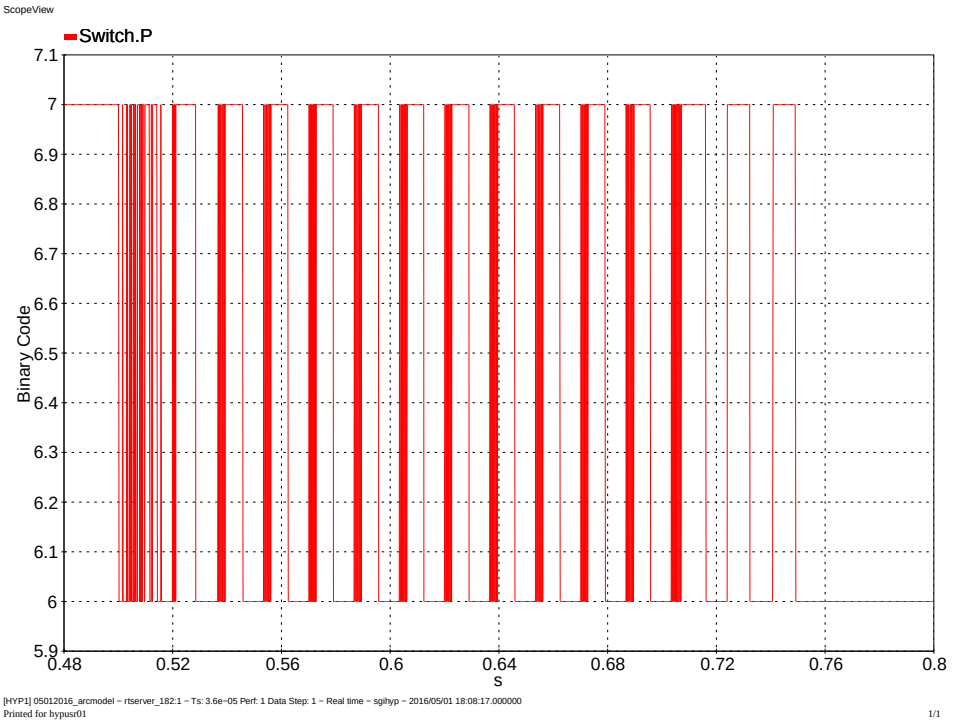

Figure 5.22: Switch Simulation

5.5 Relay Wiring Drawings

Figure 5.23 shows the logic circuit diagram for all the HYPERSIM outputs. This drawing includes logic for status of IPO breakers connected to local bus of series capacitor line and series capacitor by-pass breaker status. These breakers status was given as inputs to relays in line relay panel-1.

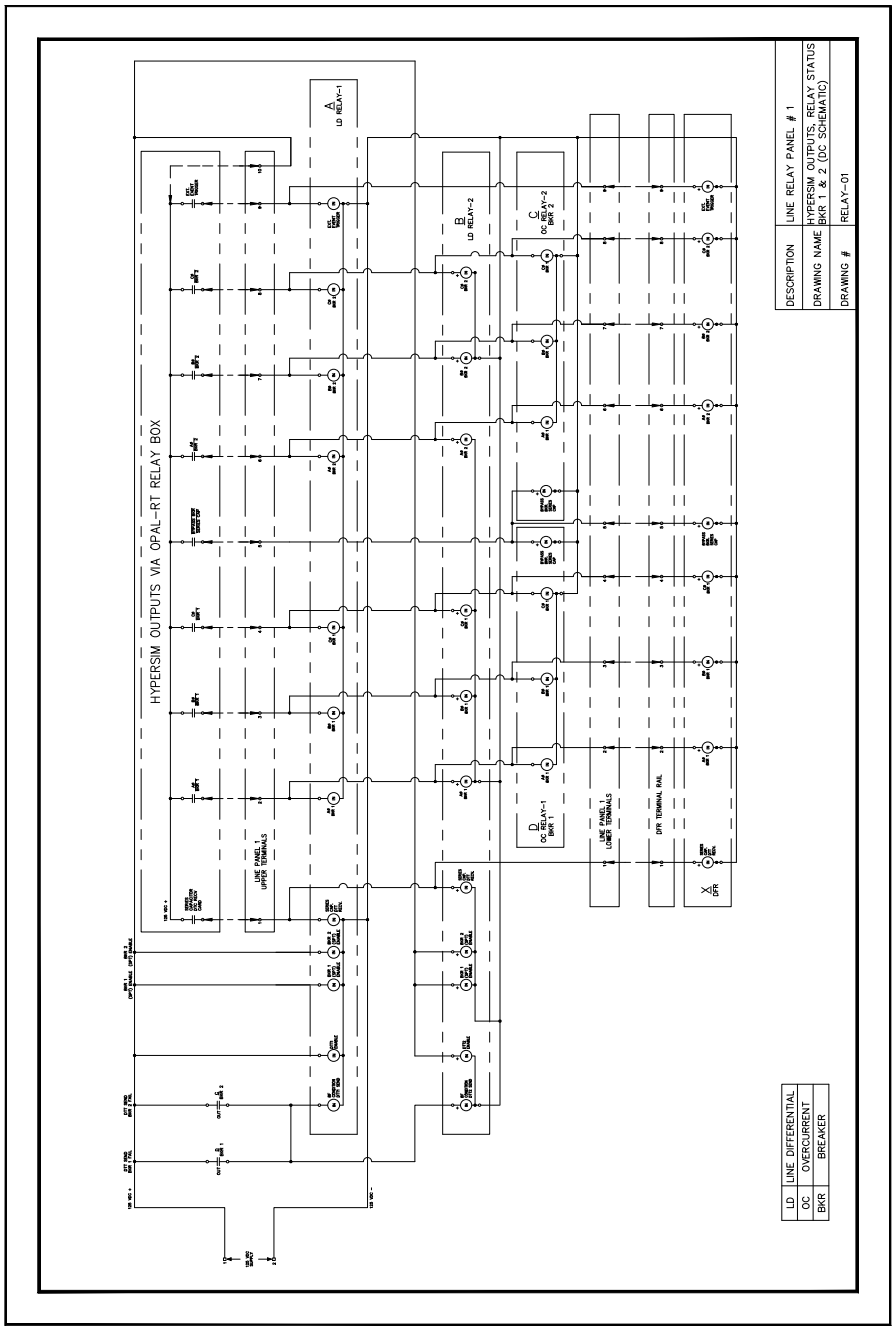

Figure 5.23: Line 1 Relay Inputs from HYPERSIM

Figure 5.24 shows the logic circuit diagram for all the HYPERSIM outputs. This drawing includes logic for status of IPO breakers connected to remote bus of series capacitor line and series capacitor by-pass breaker status. These breakers status was given as inputs to relays in line relay panel-2.

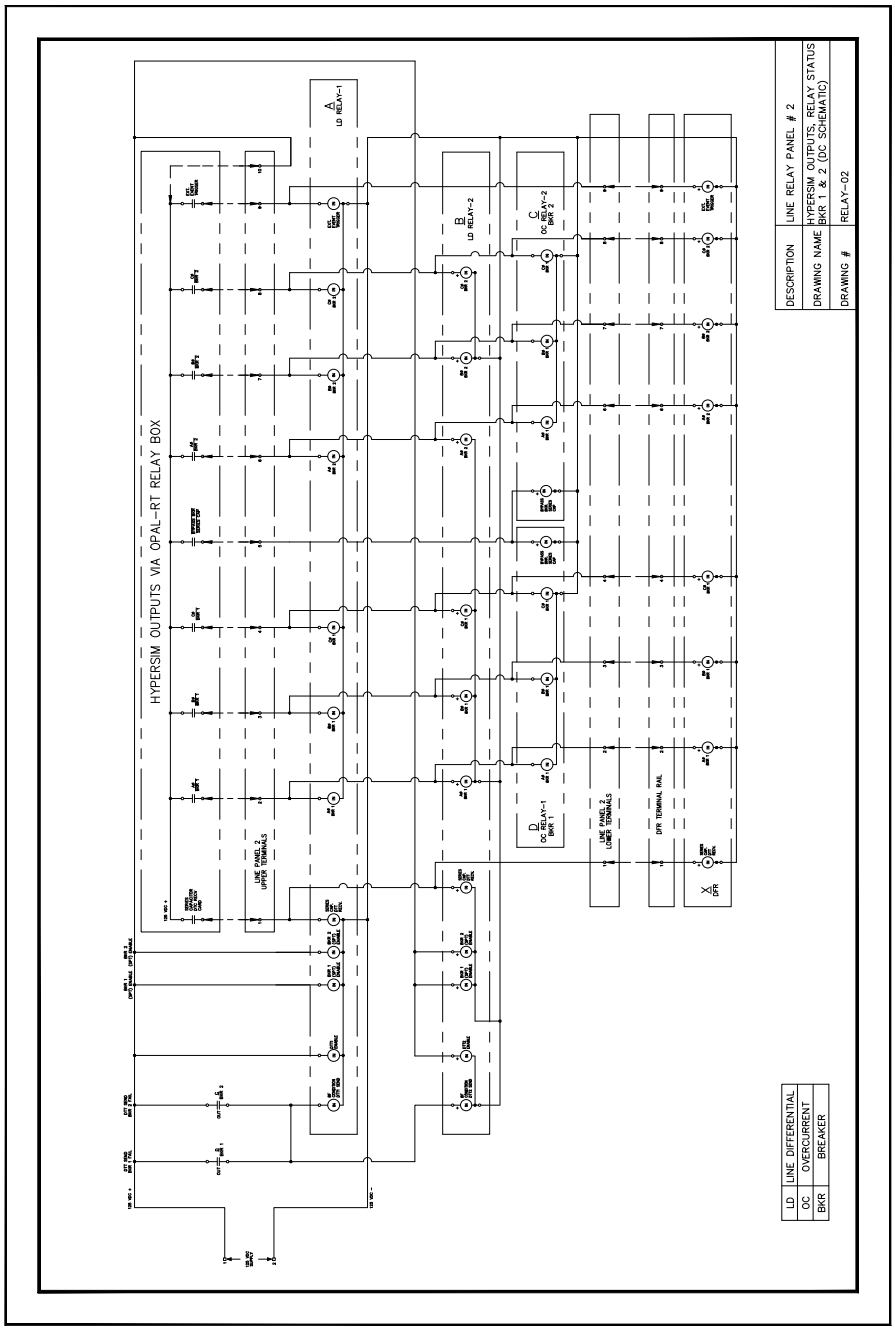

Figure 5.24: Line 2 Relay Inputs from HYPERSIM

Figure 5.25 shows the logic circuit diagram for all the HYPERSIM inputs from line relay panel-1. This drawing includes logic for single pole and three pole trip commands to IPO breakers connected to local bus of series capacitor line. The trip command outputs from line differential relays of line relay panel-1 are fed to the IPO breakers. Also logic for series capacitor by pass breaker is also shown in the drawing. The drawing also includes three pole close command logic circuit, breaker fail trip and pole disagreement trip command logic circuits.

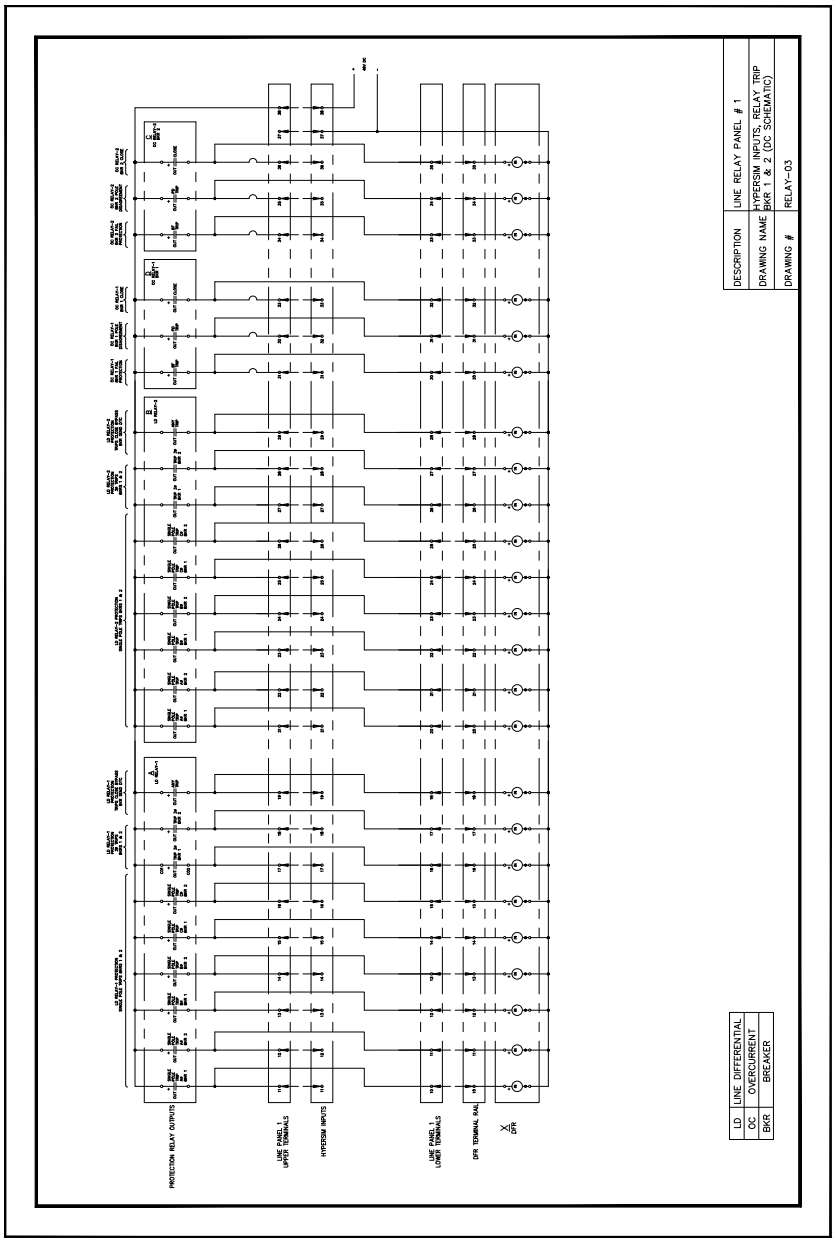

Figure 5.25: Line 1 Relay Outputs to HYPERSIM

Figure 5.26 shows the logic circuit diagram for all the HYPERSIM inputs from line relay panel-2. This drawing includes logic for single pole and three pole trip commands to IPO breakers connected to remote bus of series capacitor line. The trip command outputs from each of the line differential relays of line relay panel-2 are fed to the IPO breakers. Also logic for series capacitor by pass breaker is also shown in the drawing. The drawing also includes three pole close command logic circuit, breaker fail trip and pole disagreement trip command logic circuits.

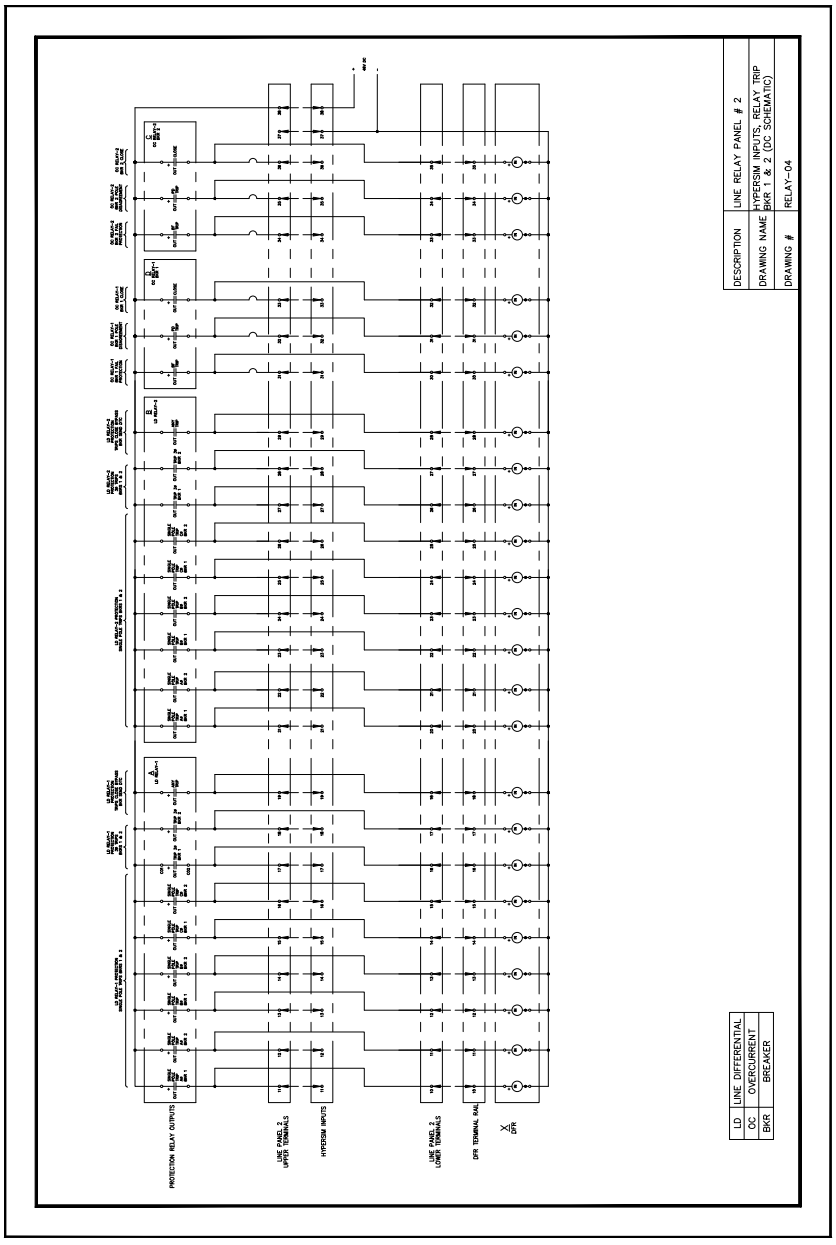

Figure 5.26: Line 2 Relay Outputs to HYPERSIM

Figure 5.27 shows the logic circuit diagram for interface signals from relays in line relay panel-1. This drawing includes close input initiate; breaker fail initiate interface signals for overcurrent relays in line relay panel-1.

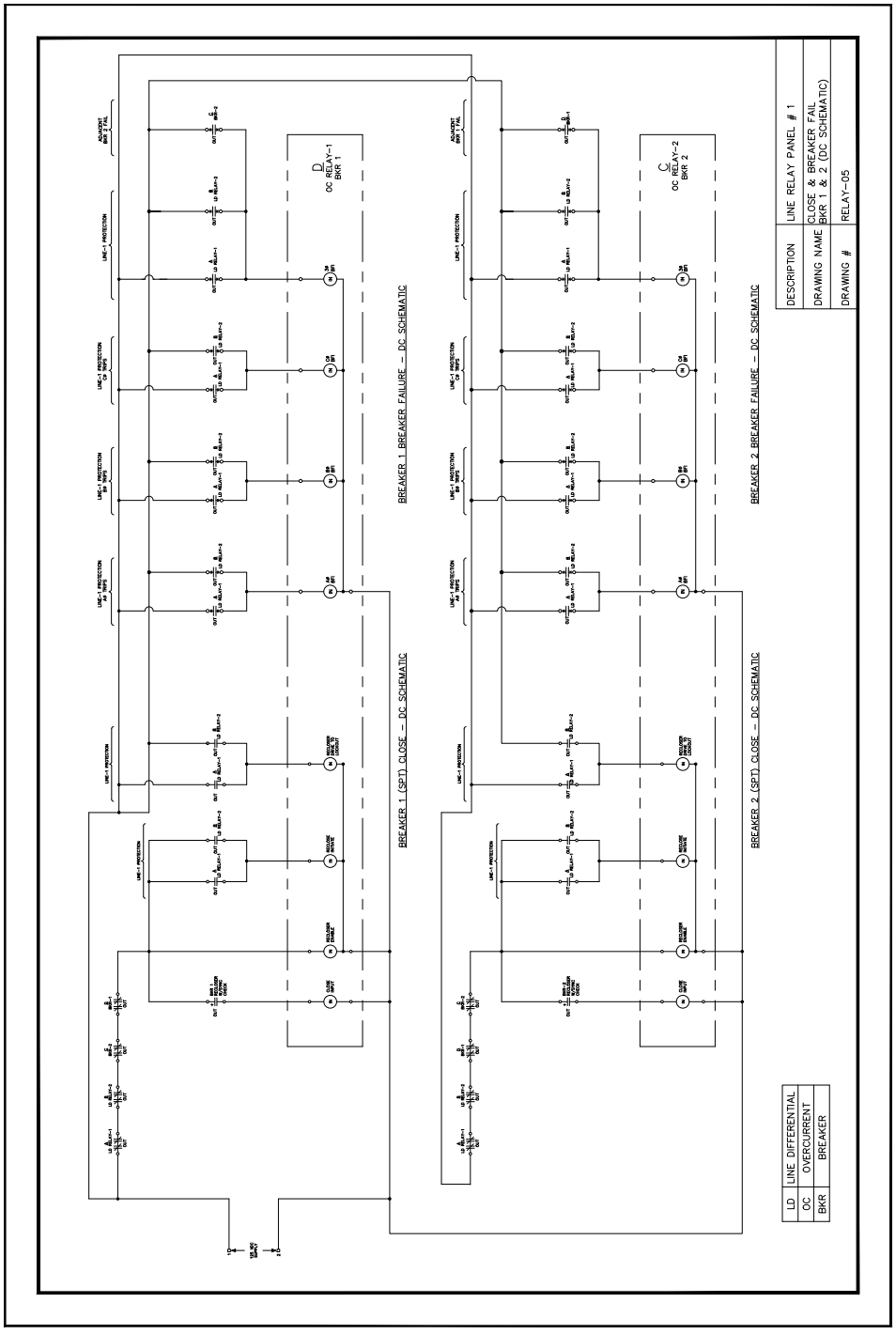

Figure 5.27: Line 1 Brekaer Close and Fail Circuit

Figure 5.28 shows the logic circuit diagram for interface signals from relays in line relay panel-2. This drawing includes close input initiate; breaker fail initiate interface signals for overcurrent relays in line relay panel-2.

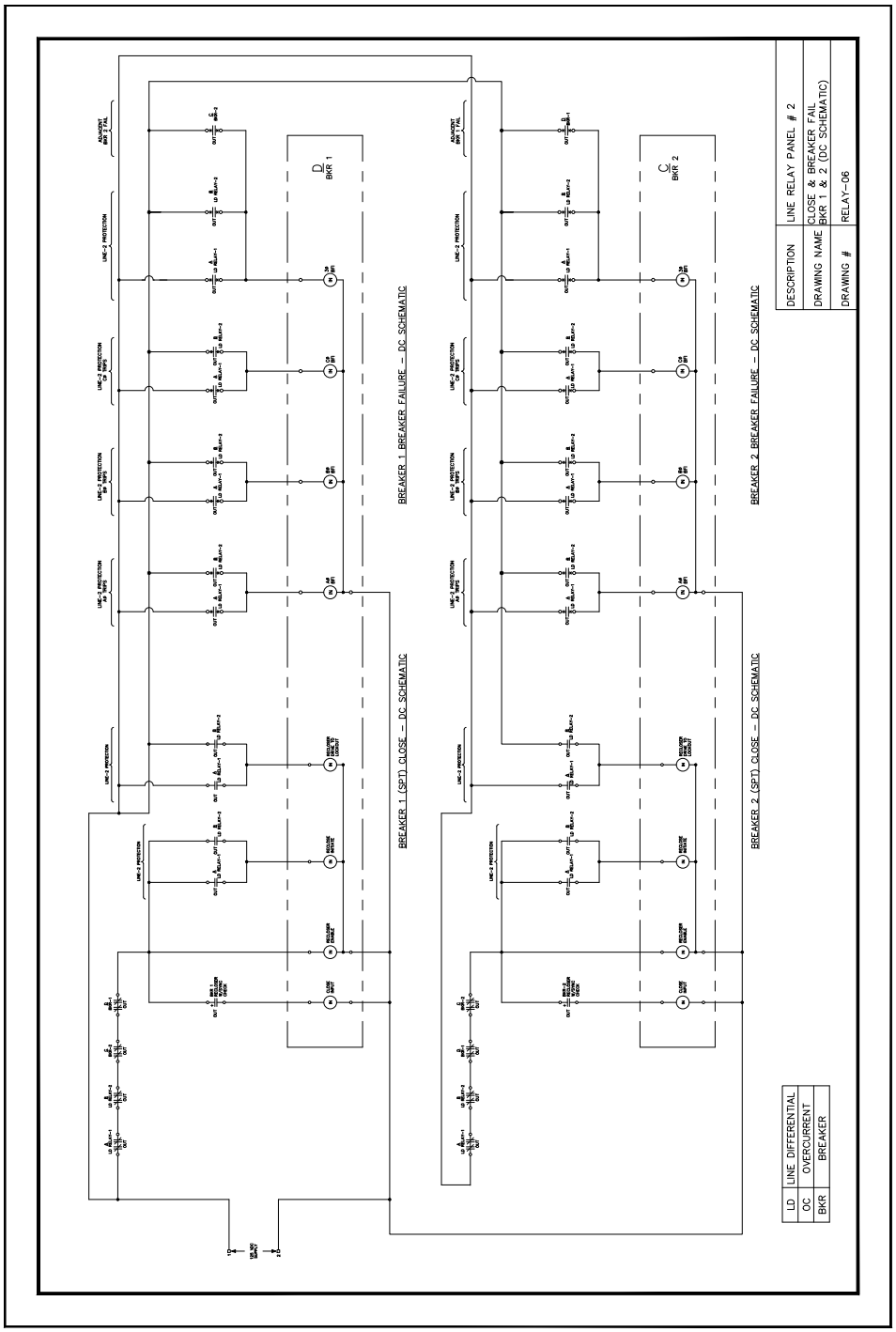

Figure 5.28: Line 2 Brekaer Close and Fail Circuit

Chapter 6

Summary & Future Work

6.1 Summary

This thesis presented a test plan and a test setup to test relays using real time simulator for single pole switching studies. The test plan includes modeling in HYPERSIM software of a test system, which is a portion of a real power network, appropriate for hardware-in-the-loop real time simulation with actual relays. Equipment and transmission lines in the test system are modeled using their parameters. The test setup was designed to show necessary connections between the real-time simulator computer and the protective relays that will operate under a Single Pole Switching (SPS) protection scheme. The input and output signals between the simulator and relays were determined to accommodate test scenarios for SPS operation. The following tasks are completed for this thesis.

- First chapter discusses modeling requirements for relay testing using real time simulators, a historical review of test systems and power system models used for relay testing and outcomes of relay testing using real time simulator, background of single pole switching and historical review on advantages, disadvantages, and challenges with single pole switching.

- The concepts of modeling power system components in HYPERSIM, mathematical equa-

tions representing transmission lines, equivalent circuit representation of transformers and induction motors were discussed in second chapter.

- Transmission line, BC Tran transformers, Induction motor, Fault modelling procedures in HYPERSIM Real-Time Simulator were discussed in third chapter. Also input and output signals between the simulator and relays were determined.

- System data for lines, Voltage Sources with Step-Up Transformers, BC-Tran three winding transformer, Induction motor with Power Transformer, Series capacitor with MOV, Shunt capacitors were shown in fourth chapter.

- The model built for testing relays using HYPERSIM Real-Time simulator was shown, faults close to local end, middle of line and remote end were applied and response of line currents, fault currents and voltages at local end and remote end buses are captured and analyzed. Results of systematic study for identifying worst case scenarios to test relays were also shown. AUTOCAD drawings for relays input and output signals to install and wire relay panels were also shown in fifth chapter.

6.2 Future Work

The following items are possible future work to extend the work presented in this thesis:

- One can consider replacing voltage sources modeled in the test system with generators. Generators with exciters could be modeled to include possible effect of generator dynamics on the performance of an SPS protective relay.

- The test system may include a more detailed modeling of line breakers in order to simulate arc extinguishing and restrike phenomenon when it is opened by relay to replicate actual breaker action.

- Coupling capacitor voltage transformers (CCVT) and current transformers (CT) components may be considered as part of the breaker configuration at the buses where SPS relays are installed to capture the transients of the transformers that might affect the operation of the relays.

- To implement the test plan and test setup developed in this thesis, a comprehensive set of test scenarios needs to be determined to capture the performance of the SPS relays. For example, a test to determine the relay response to an evolving fault scenario can be included to verify how the relay would react when a single-line-to-ground fault evolves into a double-line-ground fault before the single-pole breaker opens for the single-line-ground fault. Other tests may include the bypass breaker open/close conditions, breaker failure conditions, re-closing after single pole trip including restriking, and out of zone/in zone fault combinations.

- The power system model developed and relays input/output signals determined in this work could be implemented to test line differential and overcurrent relays under SPS operation. There might be additional input/output signals for different types of relays to be considered for analyzing the performance of the relays.

Bibliography

[1] Arthur R. Bergen and Vijay Vittal. *Power System Analysis*. Prentice-Hall, New Jersey, 1986, 2000.

[2] Van-Que Do. *User Code Module Tutorial*. Hydro-Quebec, 2005.

[3] Prabha Kundur. *Power System Stability and Control*. Mc-Graw Hill, New York, 1994.

[4] Leander W. Matsch. *Electromagnetic & Electromechanical Machines*. Thomas Y. Crowell Company, Inc, 1972, 1977.

[5] J. Sousa, D. Santos, and M.T. Correia de Barros. Fault arc modeling in emtp. In *IPST'95-International Conference on Power Systems Transients*, Sep 1995.

[6] OPAL-RT Technologies. Hypersim workspace module 2, 2014.

[7] M. Kezunovic and M. McKenna. Real-time digital simulator for protective relay testing. *Computer Applications in Power, IEEE*, 7(3):30–35, July 1994. ISSN 0895-0156. doi: 10.1109/67.294167.

[8] E. Abbasi, H. Seyedi, and K. Strunz. Simulation and analysis of the effect of single-pole auto-reclosing on hv transmission lines switching overvoltages. In *Power Energy Society General Meeting, 2009. PES '09. IEEE*, pages 1–9, July 2009. doi: 10.1109/PES.2009.5275435.

[9] Real time digital simulator. https://en.wikipedia.org/wiki/Real_Time_Digital_Simulator. Accessed: 2016-04-23.

[10] R.J. Marttila, E.P. Dick, D. Fischer, and C.S. Mulkins. Closed-loop testing with the real-time digital power system simulator. In *Digital Power System Simulators, 1995, ICDS '95., First International Conference on*, pages 219–, April 1995. doi: 10.1109/ICDS.1995.492833.

[11] M. Roitman, R.B. Sollero, and J.J. Oliveira. Real time digital simulation: trends on technology and t d applications. In *Power Systems Conference and Exposition, 2004. IEEE PES*, pages 1767–1769 vol.3, Oct 2004. doi: 10.1109/PSCE.2004.1397732.

[12] S.M.C. Wong and M. Allen. Microprocessor relay evaluations using digital model power system. In *Protective Relay Engineers, 2011 64th Annual Conference for*, pages 356–365, April 2011. doi: 10.1109/CPRE.2011.6035637.

[13] P.G. McLaren, G.W. Swift, Z. Zhang, E. Dirks, R.P. Jayasinghe, and I. Fernando. A new positive sequence directional element for numerical distance relays. In *WESCANEX 95. Communications, Power, and Computing. Conference Proceedings., IEEE*, volume 2, pages 334–339 vol.2, May 1995. doi: 10.1109/WESCAN.1995.494051.

[14] P.D. Talbot, Z.Q. Bo, L. Denning, X.F. Shen, Y.F. Qiu, A. Williams, R.H.J. Warren, R. Rhoole, G.C. Weller, and K.J. Mackay. Real-time simulation of critical evolving fault condition on a 500 kv transmission network for testing of high performance protection relays. In *Power Engineering Society Winter Meeting, 2000. IEEE*, volume 3, pages 1923–1927 vol.3, Jan 2000. doi: 10.1109/PESW.2000.847647.

[15] G. Nimmersjo, M.M. Saha, and B. Hillstrom. Protective relay testing using a modern digital real time simulator. In *Power Engineering Society Winter Meeting, 2000. IEEE*, volume 3, pages 1905–1910 vol.3, Jan 2000. doi: 10.1109/PESW.2000.847644.

[16] P.G. McLaren, R. Kuffel, J. Giesbrecht, W. Keerthipala, A. Castro, D. Fedirchuk, S. Innes, K. Mustaphi, and K. Sletten. On site relay transient testing for a series compensation upgrade. *Power Delivery, IEEE Transactions on*, 9(3):1308–1315, Jul 1994. ISSN 0885-8977. doi: 10.1109/61.311157.

[17] C. Gagnon and P. Gravel. Extensive evaluation of high performance protection relays for the hydro-quebec series compensated network. *Power Delivery, IEEE Transactions on*, 9(4): 1799–1811, Oct 1994. ISSN 0885-8977. doi: 10.1109/61.329513.

[18] Chang-Ho Jung, Hyun-Soo Jung, and Jin-O Kim. Dynamic characteristic test of protective relay for double circuit using real time digital simulator (rtds). In *Power System Technology, 2000. Proceedings. PowerCon 2000. International Conference on*, volume 3, pages 1461–1464 vol.3, 2000. doi: 10.1109/ICPST.2000.898184.

[19] B.S. Rigby. Closed-loop testing of an overcurrent relay using a real-time digital simulator. In *AFRICON, 2004. 7th AFRICON Conference in Africa*, volume 2, pages 783–788 Vol.2, Sept 2004. doi: 10.1109/AFRICON.2004.1406791.

[20] S.F. Roekman, M. Al-Tai, S.B. Tennakoon, and A. Perks. Advanced real-time digital simulator for assessing the high performance of numerical distance relays in the indonesian 500 kv transmission line system. In *Universities Power Engineering Conference, 2004. UPEC 2004. 39th International*, volume 2, pages 717–721 vol. 1, Sept 2004.

[21] B.S. Rigby. Automated real-time simulator testing of protection relays. In *Power Engineering Society Conference and Exposition in Africa, 2007. PowerAfrica '07. IEEE*, pages 1–7, July 2007. doi: 10.1109/PESAFR.2007.4498039.

[22] C. W. Taylor, W. A. Mittelstadt, T. N. Lee, J. E. Hardy, H. Glavitsch, G. Stranne, and J. D. Hurley. Single-pole switching for stability and reliability. *Power Systems, IEEE Transactions on*, 1(2):25–36, May 1986. ISSN 0885-8950. doi: 10.1109/TPWRS.1986.4334894.

[23] Single phase tripping and auto reclosing of transmission lines-ieee committee report. *Power Delivery, IEEE Transactions on*, 7(1):182–192, Jan 1992. ISSN 0885-8977. doi: 10.1109/61.108906.

[24] F. Calero and D. Hou. Practical considerations for single-pole-trip line-protection schemes. In *2006 Power Systems Conference: Advanced Metering, Protection, Control, Communication, and Distributed Resources*, pages 299–315, March 2006. doi: 10.1109/PSAMP.2006.285401.

[25] H.R. Nateghi and M. Shahabi. Study of a power system stability considering three-pole and single-pole reclosing in single-pole fault incidence in the network. *Journal of Electrical Engineering*.

[26] Elizabeth Godoy, Alberto Celaya, Hector J. Altuve, Normann Fischer, and Armando Guzman. Tutorial on single-pole tripping and reclosing. 2012.

[27] J. Giesbrecht, D.S. Ouellette, and C.F. Henville. Secondary arc extinction and detection real and simulated. In *Developments in Power System Protection, 2008. DPSP 2008. IET 9th International Conference on*, pages 138–143, March 2008.

[28] Single pole automatic reclosing near 500 kv generation bus through negative sequence current studies. In *Power Engineering and Optimization Conference (PEOCO), 2014 IEEE 8th International*, pages 85–88, March 2014. doi: 10.1109/PEOCO.2014.6814404.

[29] J.J. Trainor and C.E. Parks. Experience with single-pole relaying and reclosing on a large 132-kv system. *American Institute of Electrical Engineers, Transactions of the*, 66(1):405–413, Jan 1947. ISSN 0096-3860. doi: 10.1109/T-AIEE.1947.5059456.

[30] R.Bruce Shipley, H.J. Holley, and D.W. Coleman. Digital analysis of single-pole switching on ehv lines. *Power Apparatus and Systems, IEEE Transactions on*, PAS-87(8):1679–1687, Aug 1968. ISSN 0018-9510. doi: 10.1109/TPAS.1968.292129.

[31] L. Edwards, Jr. Chadwick, J.W., H.A. Riesch, and L.E. Smith. Single-pole switching on tva's paradise-davidson 500-kv line design concepts and staged fault test results. *Power Apparatus and Systems, IEEE Transactions on*, PAS-90(6):2436–2450, Nov 1971. ISSN 0018-9510. doi: 10.1109/TPAS.1971.292855.

[32] C.M.M. Ferreira, J.A.D. Pinto, and F.P.M. Barbosa. Effect of the single and three phase switching in the transient stability of an electric power system using the extended equal area criterion. In *Electrotechnical Conference, 1998. MELECON 98., 9th Mediterranean*, volume 2, pages 950–953 vol.2, May 1998. doi: 10.1109/MELCON.1998.699368.

[33] R. Gutman, S. Kolluri, and A. Kumar. Application of single phase switching on entergy system: three phase unbalance studies. In *Power Engineering Society Summer Meeting, 2001*, volume 2, pages 778–783 vol.2, July 2001. doi: 10.1109/PESS.2001.970148.

[34] K.P. Basu, S. Hamid, and S. Hasan. Application of single-pole auto reclosing of circuit breakers in ehv transmission line with capacitance grounding. In *Transmission and Distribution Conference and Exhibition 2002: Asia Pacific. IEEE/PES*, volume 3, pages 1766–1769 vol.3, Oct 2002. doi: 10.1109/TDC.2002.1177722.

[35] S.J. Balser and P.C. Krause. Single-pole switching - a study of system transients with transposed and intransposed lines. *Power Apparatus and Systems, IEEE Transactions on*, PAS-93 (4):1208–1212, July 1974. ISSN 0018-9510. doi: 10.1109/TPAS.1974.294069.

[36] S.J. Balser, J.R. Eaton, and P.C. Krause. Single-pole switching-a comparison of computer studies with field test results. *Power Apparatus and Systems, IEEE Transactions on*, PAS-93 (1):100–108, Jan 1974. ISSN 0018-9510. doi: 10.1109/TPAS.1974.293920.

[37] B.R. Shperling, A.J. Fakheri, C.H. Shih, and B.J. Ware. Analysis of single phase switching field tests on the aep 765 kv system. *Power Apparatus and Systems, IEEE Transactions on*, PAS-100(4):1729–1735, April 1981. ISSN 0018-9510. doi: 10.1109/TPAS.1981.316510.

[38] K. Ngamsanroaj and S. Premrudeepreechacharn. An analysis of single pole reclosing on 500 kv line in thailand. In *Power Engineering Conference, 2007. IPEC 2007. International*, pages 443–448, Dec 2007.

[39] B.N.K. Marojahan, N. Hariyanto, and M. Nurdin. Characteristics and suppression of secondary arc on 500 kv transmission lines for single pole reclosure purposes. In *Electrical Power, Electronics, Communications, Controls and Informatics Seminar (EECCIS), 2014*, pages 1–7, Aug 2014. doi: 10.1109/EECCIS.2014.7003710.

[40] A.T. Johns, R.K. Aggarwal, and Y.H. Song. Improved techniques for modelling fault arcs an faulted ehv transmission systems. *Generation, Transmission and Distribution, IEE Proceedings-*, 141(2):148–154, Mar 1994. ISSN 1350-2360.

[41] M. Kizilcay, G. Ban, L. Prikler, and P. Handl. Interaction of the secondary arc with the transmission system during single-phase autoreclosure. In *Power Tech Conference Proceedings, 2003 IEEE Bologna*, volume 2, pages 7 pp. Vol.2–, June 2003. doi: 10.1109/PTC.2003.1304294.

[42] K. Ngamsanroaj and S. Premrudeepreechacharn. Investigation of single phase reclosing using arc model on the 500 kv transmission line from mae moh to tha ta ko. In *Power and Energy Engineering Conference, 2009. APPEEC 2009. Asia-Pacific*, pages 1–4, March 2009. doi: 10.1109/APPEEC.2009.4918448.

[43] M. Nurdin, N. Hariyanto, and A. Wijaya. Secondary arc modeling using atpdraw study case tasikmalaya-depok extra high voltage overheadlines. In *Power Engineering and Renewable Energy (ICPERE), 2014 International Conference on*, pages 19–24, Dec 2014. doi: 10.1109/ICPERE.2014.7067228.

[44] PERL. Series capacitor project report. December 2013.

[45] M. Kizilcay and T. Pniok. Digital simulations of fault arcs in power system. pages 55–60, January/February 1991.

[46] Hermann W. Dommel. *EMTP Theory Book*. 1995.

[47] OPAL-RT Technologies. Hypersim testview module 8, 2014.

[48] Nagendrakumar Beeravolu. Pattern recognition of power systems voltage stability using real time simulations, December 2010.

[49] M. Goulkhah and A.M. Gole. Practical application of waveform relaxation method for testing remote protective relays. In *Industrial Technology (ICIT), 2015 IEEE International Conference on*, pages 1381–1386, March 2015. doi: 10.1109/ICIT.2015.7125290.

Vita

The author was born in 1985, in India. He completed his bachelors of technology degree in Electrical and Electronics Engineering from JNTU, Hyderabad India in 2006 with distinction. He finished his Masters in Electrical Engineering from the University of New Orleans in May 2016 with a cumulative GPA of 4.0. He worked as an Engineer in ABG Shipyard, India and is working as a Research Assistant under Prof. Dr. Parviz Rastgoufard. His areas of interests are real time simulation studies, real time simulation modeling and relay protection and testing using real-time simulator.